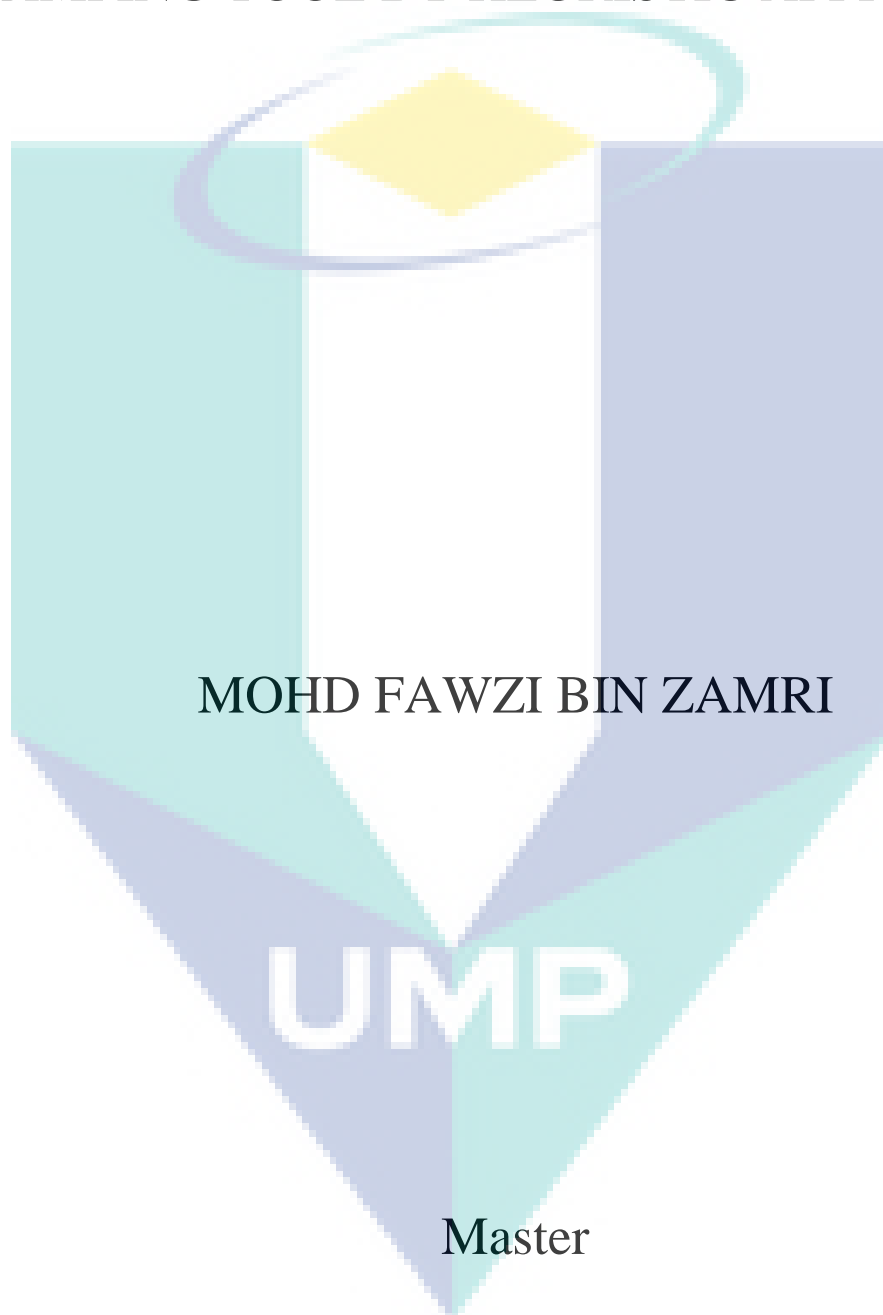


DESIGN OF COOLING CHANNEL IN HOT STAMPING TOOL BY HEURISTIC APPROACH



UNIVERSITI MALAYSIA PAHANG

UNIVERSITI MALAYSIA PAHANG

DECLARATION OF THESIS AND COPYRIGHT

Author's Full Name : MOHD FAWZI BIN ZAMRI

Date of Birth : 02 SEPTEMBER 1989

Title : DESIGN OF COOLING CHANNEL IN HOT STAMPING
TOOL BY HEURISTIC APPROACH

Academic Session : SEMESTER 2 2016/2017

I declare that this thesis is classified as:

- ☐ **CONFIDENTIAL** (Contains confidential information under the Official Secret Act 1997)*
- ☐ **RESTRICTED** (Contains restricted information as specified by the organization where research was done)*
- ☒ **OPEN ACCESS** I agree that my thesis to be published as online open access (Full Text)

I acknowledge that Universiti Malaysia Pahang reserves the following rights:

1. The Thesis is the Property of Universiti Malaysia Pahang
2. The Library of Universiti Malaysia Pahang has the right to make copies of the thesis for the purpose of research only.
3. The Library has the right to make copies of the thesis for academic exchange.

Certified by:

(Student's Signature)

(Supervisor's Signature)

890902-06-5725

New IC/Passport Number
Date:

ASSOC. PROF. DR. AHMAD
RAZLAN BIN YUSOFF

Name of Supervisor
Date:

NOTE : * If the thesis is CONFIDENTIAL or RESTRICTED, please attach a thesis declaration letter.

SUPERVISOR'S DECLARATION

I hereby declare that I have checked this thesis and in my opinion, this thesis is adequate in terms of scope and quality for the award of the degree of Master of Engineering in Manufacturing.

(Supervisor's Signature)

Full Name : ASSOC. PROF. DR AHMAD RAZLAN BIN YUSOFF

Position : SENIOR LECTURER

Date :

STUDENT'S DECLARATION

I hereby declare that the work in this thesis is based on my original work except for quotations and citations which have been duly acknowledged. I also declare that it has not been previously or concurrently submitted for any other degree at Universiti Malaysia Pahang or any other institutions.

(Student's Signature)

Full Name : MOHD FAWZI BIN ZAMRI

ID Number : MMF13002

Date :

DESIGN OF COOLING CHANNEL IN HOT STAMPING TOOL BY HEURISTIC
APPROACH

The logo of the University of Malaysia Pahang (UMP) is a large, stylized shield. The shield is divided into four quadrants: top-left is light blue, top-right is light purple, bottom-left is light blue, and bottom-right is light purple. In the center of the shield is a white vertical rectangle. Above the shield, there is a yellow diamond shape with a light blue oval ring around it.

MOHD FAWZI BIN ZAMRI

Thesis submitted in fulfillment of the requirements
for the award of the degree of
Master of Engineering (Manufacturing)

UMP

Faculty of Manufacturing Engineering
UNIVERSITI MALAYSIA PAHANG

2017

ACKNOWLEDGEMENTS

First of all, thanks to Allah the Almighty for giving me the strength to complete my project successfully. I would like to express my sincere gratitude to my supervisor Assoc. Prof Madya Dr Ahmad Razlan Yusoff for his ideas, invaluable guidance, continuous encouragement and constant support in making this project possible. My deep thanks go to my dearest family, especially to my father Zamri Bin Marzuki and mother, Fauziah Binti Masri, who are always support and pray for my success throughout this project. Their support provides me the spirit and strength that I require to endure throughout the period of my study. I would like to thank the lecturers and technicians at Faculty of Manufacturing Engineering and other related faculties for their valuable comments and constructive criticisms. Besides that, I would like to thank to UMP, this work were funded by Internal Grant, RDU 130343 Development of Hot Stamping Die for Ultra High Strength Steels in Automotive Component Application and Postgrad Research Scheme (PGRS). Finally, I would also like to thank my fellow colleagues for being there for me through thick and thin.

ABSTRAK

Disebabkan permintaan untuk mengurangkan pelepasan gas, penjimatan tenaga, dan pengeluaran kenderaan yang lebih selamat, pembangunan bahan ultra kekuatan tinggi keluli (UHSS) adalah bukan perkara yang remeh. Untuk mengukuhkan bahan UHSS seperti keluli boron, ia diperlukan untuk menjalani beberapa proses iaitu pemanasan melalui cap panas pada suhu dan masa tertentu serta penyejukan melalui pelindapkejutan. Dalam proses cap panas, die yang sama digunakan seperti dalam proses cap sejuk, tetapi dengan saluran penyejukan tambahan. Sistem saluran penyejukan disepadukan ke dalam reka bentuk die untuk mengawal kadar pemindahan haba untuk proses kosong panas pelindapkejutan. Semasa proses pelindapkejutan, reka bentuk mati berkesan menyumbang ke arah pencapaian kadar pemindahan haba yang optimum dan pengedaran suhu homogen pada kekosongan panas. Dalam kajian ini, parameter reka bentuk saluran penyejukan iaitu garis pusat saluran pendinginan (CA), padang antara saluran penyejukan (CB), jarak saluran penyejukan ke permukaan alat (CC), dan jarak saluran penyejuk ke alat dinding (CD) dioptimumkan untuk alat rata dan U-bentuk menggunakan kaedah heuristik. Kaedah heuristik digabungkan dengan analisis haba dan statik analisis unsur terhingga (FEA) melalui ANSYS untuk menentukan reka bentuk optimum penyejukan penyejukan panas. Analisis statik dilakukan untuk memastikan alat tersebut mampu menahan tekanan yang dikenakan, sementara analisis haba dilakukan untuk memastikan pengedaran suhu homogen. Setiap parameter saluran penyejukan dioptimumkan dan ditanda aras dengan kaedah tradisional Taguchi. Kemudian, percubaan proses cap panas dilakukan untuk mendapatkan pengedaran suhu produk dan alat kosong. Seterusnya, hasil simulasi dibandingkan dengan kerja eksperimen untuk tujuan pengesahan. Hasil pengedaran suhu antara FEA dan eksperimen adalah mendapatkan ralat kurang daripada 20 %. Reka bentuk optimum alat setem panas dengan pemindahan haba yang tinggi dan tegasan von Mises yang lebih rendah (VMS), parameter berikut (sebelum ini ditakrifkan sebagai CA, CB, CC, CD mm) diperlukan (8,8,10) mm untuk alat rata, (8,8,8,10) mm untuk alat U-bentuk atas dan (8,8,8,8) mm untuk alat U-bentuk yang lebih rendah. Juga jelas bahawa corak pengedaran suhu model FEA bersetuju dengan keputusan percubaan. Berdasarkan alat bentuk rata, ralat peratusan purata untuk taburan haba kosong ialah 1.83 % dan untuk alat itu ialah 2.67%. Bagi alat U-shape, ralat peratusan purata bagi alat atas, alat bawah dan pengagihan haba kosong masing-masing 16.65 % 17.95 % dan 7.92 %. Kekuatan tegangan dan nilai kekerasan produk kosong (sampel rata dan U berbentuk) diukur menjadi kira-kira 1200 MPa dan 600 HV, masing-masing. Kesimpulannya, berdasarkan parameter yang dioptimumkan dalam kajian ini, jelaslah kekuatan tegangan yang tinggi dengan nilai kekerasan yang tinggi dapat dihasilkan dari kaedah heuristik.

ABSTRACT

Owing to the demand for reducing gas emissions, energy savings, and the production of safer vehicles, the development of Ultra High Strength Steel (UHSS) materials is non-trivial. To strengthen a UHSS material such as boron steel, it is required to undergo a number of processes namely, heating it via hot stamping at a certain temperature and time as well as cooling it through quenching. In the hot stamping process, a similar die is used as in the cold stamping process, but with additional cooling channels. The cooling channel systems are integrated into the die design to control the heat transfer rate for quenching process of hot blanks. During quenching process, an effective die design contributes towards the achievement of the optimum heat transfer rate and homogeneous temperature distribution on hot blanks. In this study, the parameters of the cooling channel design i.e. the diameter of cooling channel (C_A), the pitch between cooling channel (C_B), the cooling channel distance to tool surface (C_C), and the cooling channel distance to wall tool (C_D) are optimised for a flat and U-shape tool using heuristic method. The heuristic method is coupled with the thermal and static analysis of finite element analysis (FEA) via ANSYS to determine the optimum design of hot stamping cooling channels. The static analysis are performed to ensure that the tool is able to withstand the applied pressure, whilst the thermal analysis was carried out to ensure homogeneous temperature distribution. Each parameter of the cooling channels optimised and benchmarked with traditional Taguchi method. Then, hot stamping process experiment is conducted to get the temperature distribution of the blank product and tool. Next, the simulation results were compared with experimental works for validation purpose. The result of the temperature distribution between FEA and experiment expected error less than 20 %. It is found that the optimum design of the hot stamping tool with a high heat transfer and lower von Mises stress (VMS), the following parameters (previously defined as C_A , C_B , C_C , C_D in mm) are required (8,8,10) mm for the flat tool, (8,8,8,10) mm for the upper U-shape tool and (8,8,8,8) mm for the lower U-shape tool, respectively. It is also evident that the pattern of the temperature distribution of the FEA model agrees the experimental results. Based on the flat shape tool, the average percentage error for the blank heat distribution is 1.83 % and for the tool is 2.67 %. As for the U-shape tool, the average percentage error for the upper tool, lower tool, and the blank heat distribution are 16.65 % 17.95 % and 7.92 %, respectively. The tensile strength and the hardness value of the blank products (flat and U-shaped samples) are measured to be approximately 1200 MPa and 600 HV, respectively. In conclusion, based on the aforementioned optimised parameters in the study, it is apparent that a high tensile strength with high value of hardness product could be produced from the heuristic method.

TABLE OF CONTENT

DECLARATION

TITLE PAGE

ACKNOWLEDGEMENTS **ii**

ABSTRAK **iii**

ABSTRACT **iv**

TABLE OF CONTENT **v**

LIST OF TABLES **ix**

LIST OF FIGURES **xi**

LIST OF SYMBOLS **xiv**

LIST OF ABBREVIATIONS **xv**

CHAPTER 1 INTRODUCTION **1**

1.1 Research Background 1

1.2 Problem Statement 5

1.3 Aim and Objectives 6

1.4 Research Scope 7

1.5 Thesis Organisation 8

CHAPTER 2 LITERATURE REVIEW **9**

2.1 Introduction 9

2.2 Forming of Boron Steel 9

2.3 Hot Stamping Process 12

2.3.1 Sheet Metal Forming 13

2.3.2	Heating Method	15
2.3.3	Heat Transfer Mechanism	17
2.4	Operation in Hot Stamping	21
2.4.1	Forming process	22
2.4.2	Punching	24
2.5	Hot Stamping Die	26
2.5.1	Die Design	26
2.5.2	Tool Construction	26
2.5.3	Cooling channel system	27
2.5.4	Type of cooling channel	29
2.6	Die Design Optimization	30
2.6.1	Heuristic Method	30
2.6.2	Taguchi Method	32
2.7	Summary	33
CHAPTER 3 METHODOLOGY		35
3.1	Introduction	35
3.2	Material and Sample Preparations	35
3.2.1	Flat Samples	37
3.2.2	U-shape samples	38
3.2.3	U-shape die	40
3.3	Cooling Channel Design for Hot Stamping Tool	41
3.4	Finite Element Analysis	45
3.4.1	Material Data	47
3.4.2	Geometric Modelling	47
3.4.3	Define Constraints	48

3.4.4	Meshing	49
3.4.5	Thermal and Static Analysis	51
3.5	Cooling Channel Design Analysis	54
3.5.1	Heuristic Method	55
3.5.2	Taguchi Method	56
3.6	Hot stamping of 22MnB5 steel	58
3.6.1	Flow rate experimental	59
3.6.2	Heat transfer experiment	60
3.6.3	Tensile Test Measurement by Universal Tensile Machine	64
3.6.4	Hardness Measurement by Vickers Microhardness Machine	64
3.7	Summary	65
CHAPTER 4 RESULTS AND DISCUSSION		66
4.1	Introduction	66
4.2	Finite Element Analysis	66
4.2.1	Meshing	66
4.2.2	Thermal and Static Analysis for flat and U-shaped	69
4.3	Design Optimization	72
4.3.1	Heuristic Method for Flat Sample	72
4.3.2	Heuristic Method for U-Shape Sample	77
4.3.3	Taguchi Method	83
4.3.4	Heuristic and Taguchi Method Comparison	86
4.4	Experiment Validation of Hot Stamped 22MnB5 Steel	88
4.4.1	Validation of FEA Thermal Analysis with Experiment for Flat Tool	88
4.4.2	Validation of FEA Thermal Analysis with Experiment for U-shaped tool	88

4.4.3	Experimental Analysis of Hot Stamping for Flat shaped tool	89
4.4.4	Experimental Analysis of Hot Stamping for U-shaped tool	93
4.5	Summary	94
CHAPTER 5 CONCLUSION		96
5.1	Conclusion	96
5.2	Recommendations	98
REFERENCES		99
APPENDIX A1 G-CODE FOR CUTTING Flat Samples		105
APPENDIX A2 CALCULATION FOR HEAT TRANSFER COEFFICIENT		106
APPENDIX A3 CALCULATION OF HEAT TRANSFER RATE FOR SIMULATION 5 U-SHAPE LOWER TOOL		107
APPENDIX B1 INTERNATIONAL MANUFACTURING ENGINEERING CONFERENCE, ADVANCED MATERIALS RESEARCH VOL. 903 (2014) PP 163-168		108
APPENDIX B2 ADVANCES IN MATERIALS AND PROCESSING TECHNOLOGIES, 2015 VOL. 1, NOS. 1–2, 27–35		109
APPENDIX B3 JOINT CONFERENCE iMEC & APCOMS 2015		110

LIST OF TABLES

Table 1.1	Mechanical and thermal properties of high strength steels	3
Table 2.1	Chemical composition based on weight percentage of boron steel and mechanical properties of boron steel before and after quenching	10
Table 2.2	Temperature dependent properties of boron steel	11
Table 2.3	Value of contact pressure and HTC Standard deviation	20
Table 2.4	Conditions of warm and hot punching process	25
Table 3.1	Mechanical properties of 22MnB5 and SKD61 steel at room temperature	37
Table 3.2	Comparison on blank diameter, stroke of punch (SOP) and schematic diagram of U-shape samples used in previous works and current study	39
Table 3.3	Boundary condition for analysis	49
Table 3.4	Heuristic approach for cooling channel parameter for flat and U-shape	55
Table 3.5	Factor and Level Description for flat shape cooling channel parameter	57
Table 3.6	L9 Test matrix for Flat shape cooling channel parameters	57
Table 3.7	Mechanical Press, OCP 80 specification	58
Table 3.8	Mini Hydraulis Press machine specification	58
Table 3.9	Water flow rate for hot stamping process experiment	59
Table 3.10	Factor and level description of hot stamping process for Taguchi method	60
Table 3.11	L9 Test Matrix hot stamping process for flat shape	61
Table 3.12	Universal Tensile Machine Specification	64
Table 3.13	Wilson Vickers 402 MVD specifications	65
Table 4.1	Meshing results for coarse, medium and fine meshing for flat tool	67
Table 4.2	Meshing results for coarse, medium and fine meshing for U-shape tool	68
Table 4.3	Cooling channel design performance for parameter (C_A) for flat tool	73
Table 4.4	Cooling channel design performance for parameter (C_B) for flat tool	73
Table 4.5	Cooling channel design performance for parameter (C_C) for flat tool	74
Table 4.6	Optimum cooling channel design for flat tool	75

Table 4.7	Effect of cooling channel diameter (C_A) on heat transfer rate and von Mises stress	78
Table 4.8	Effect of pitch between cooling channels (C_B) heat transfer rate and von Mises stress	78
Table 4.9	Effect of distance between cooling channel to tool surfaces (C_C) heat transfer rate and von Mises stress	79
Table 4.10	Effect of the distance cooling channels to wall tool (C_D) heat transfer rate and von Mises stress	80
Table 4.11	Optimum cooling channel design for U-shape tool	80
Table 4.12	Result of Cooling rate and VMS from the Taguchi method for flat tool	83
Table 4.13	Average main effect for cooling rate and VMS for taguchi method of flat tool.	84
Table 4.14	Respond value and S/N ratio for flat tool	86
Table 4.15	Value of tensile strength and hardness	90
Table 4.16	Average main effect for tensile strength and hardness	90
Table 4.17	S/N ratio analysis	92
Table 4.18	Result of responding value from Taguchi method for flat tool experiment	93
Table 4.19	Summarise result tensile strength and hardness for U-shape	94

UMP

LIST OF FIGURES

Figure 1.1	The elongation versus strength of different steel material	2
Figure 1.2	Hot stamped parts in typical middle class car	2
Figure 1.3	Mechanical properties of 22MnB5 as delivery and hot stamped	3
Figure 1.4	Basic Hot Stamping process chain	4
Figure 2.1	Temperature, time and transformation diagram of boron steel at different cooling rate	11
Figure 2.2	Direct method of hot stamping	12
Figure 2.3	Indirect method hot stamping	13
Figure 2.4	V-bending operation	14
Figure 2.5	L-Bending process	14
Figure 2.6	U-Bending Process	15
Figure 2.7	Types of heating system (a) Roller hearth furnace, (b) Induction heating and (c) Resistance heating	16
Figure 2.8	Temperature distribution on punching load as a function heating temperature at shearing zone	17
Figure 2.9	Thermal contact resistance with (a) ideal (perfect) thermal contact, and (b) actual (imperfect) thermal contact	18
Figure 2.10	Heat transfer coefficient experiment apparatus	19
Figure 2.11	Heat transfer coefficient as a function of the contact pressure for different tool temperatures	20
Figure 2.12	Typical Forming Limit Diagram	22
Figure 2.13	Sample B-Pillar with tools	23
Figure 2.14	Geometries of die and test piece for (a) V-bending and, (b) U-shape	23
Figure 2.15	Relationship between amount of springback after V-bending and temperature of bending zone (a) relationship between amount of springback high-strength steel after V-bending and temperature of flange (b)	24
Figure 2.16	Warm and hot punching process of UHSS sheet using resistance heating	25
Figure 2.17	Relationship between maximum punching load and heating temperature	25
Figure 2.18	Tool design for the hot stamping process	28
Figure 2.19	Schematic exposition of the quenching tool with integrated heating cartridges	28
Figure 2.20	Schematic of a test hot stamping tool	28
Figure 2.21	The constraints for optimizing cooling channel	29

Figure 2.22	Cooling channel configuration (a) parallel cooling channel, and (b) serial cooling channel	30
Figure 2.23	Experiment steps for Heuristic method	31
Figure 3.1	Research project flow chart	36
Figure 3.2	Flat sample, E8M04	37
Figure 3.3	Process flow for flat sample fabrication	38
Figure 3.4	Process flow for U-shape samples fabrication	39
Figure 3.5	Die design during compression	41
Figure 3.6	U-shape die design	41
Figure 3.7	Hot stamping flat shape tool design	42
Figure 3.8	Hot stamping U-shape shape tool design	43
Figure 3.9	Flat hot stamping tool with cooling channel parameter	44
Figure 3.10	U-shape hot stamping tool with cooling channel parameter	44
Figure 3.11	Flow chart of meshing in FEA of hot stamping	46
Figure 3.12	Toolbox of geometric modelling in ANSYS simulation software	47
Figure 3.13	Flat hot stamping tool import on Ansys software	48
Figure 3.14	U-shape hot stamping tool import on Ansys software	48
Figure 3.15	Thermal contact conductance between blank and die	50
Figure 3.16	Setting interface of thermal and static analysis	51
Figure 3.17	Thermal distribution in the hot stamping tool, (a) heat transfer distribution along 10 s, (b) close-up scale for heat transfer distribution	53
Figure 3.18	Sequence for cooling channel design analysis	54
Figure 3.19	Cooling channel optimization steps using Heuristic method	56
Figure 3.20	Schematic of experimental setup for hot stamping tool	61
Figure 3.21	Hot stamping process flow for (a) Flat shape; (b) U-shape sample	62
Figure 3.22	Thermocouple location for (a) flat shaped tool, (b) u-shaped tool	63
Figure 4.1	Flat shape tool meshing structure at (a) Coarse; (b) Medium and (c) Fine, mesh size at FEA simulation	67
Figure 4.2	U-shaped tool meshing structure at (a) Coarse; (b) Medium and (c) Fine, mesh size at FEA simulation	68
Figure 4.3	Local meshing control for hot stamping tool (a) Mapped mesh (b) Mesh quality criteria chart of mapped mesh.	69
Figure 4.4	Local meshing control for hot stamping tool (a) Refined mesh (b) Mesh quality criteria chart of refined mesh.	69

Figure 4.5	Steady state condition for hot stamping simulation of a) flat sample, b) U-shape sample	70
Figure 4.6	Transient thermal with 10 s quenching time for hot stamping simulation a) flat sample, b) U-shape sample	71
Figure 4.7	Von Mises stress distribution based on static stress analysis on; (a) flat tool, (b) upper U-shape tool and (c) lower U-shape tool	72
Figure 4.8	Flat tool design with optimum cooling channel parameter	75
Figure 4.9	Blank and Tool Condition of flat tool of thermal distribution for holding time for flat tool at (a) 0 s, (b) 4 s, (c) 8 s and (d) 10 s	77
Figure 4.10	U-shape tool design with optimum cooling channel parameter	81
Figure 4.11	Blank and Tool Condition of U-shape tool of thermal distribution for holding time for flat tool at (a) 0 s, (b) 4 s, (c) 8 s and (d) 10 s	82
Figure 4.12	Main effect plot for heat transfer rate of flat tool (a) Diameter of cooling channel (b) Pitch between cooling channel (c) Cooling channel distance to tool surface.	84
Figure 4.13	Main effect plot for maximum von Mises stress (VMS) of flat tool (a) Diameter of cooling channel (b) Pitch between cooling channel (c) Cooling channel distance to tool surface.	85
Figure 4.14	Temperature distribution for cooling channel design of flat tool between heuristic and taguchi method	87
Figure 4.15	Cooling channel design performance for flat shape tool based on heuristic versus taguchi method.	87
Figure 4.16	Comparison of heat transfer distribution between FEA and experiment for flat tool	88
Figure 4.17	Comparison of heat transfer distribution between FEA and experiment for U-shape tool	89
Figure 4.18	Main effects plot for tensile strength of flat tool (a) thickness (b) temperature (c) heating time	91
Figure 4.19	Main effects plot for hardness of flat tool (a) thickness (b) temperature (c) heating time	92
Figure 4.20	Locations on stamped sample for tensile specimen and hardness test	94

LIST OF SYMBOLS

MPa	Mega Pascal
°C/s	Degree Celsius per Second
min	Minutes
s	Second
W/m.K	Watt per Meter Kelvin
mm	Milimeter
°C	Celsius
E	Elastic of Modulus
k	Thermal Conductivity
C_p	Specific Heat
%	Percentage
t	Thickness
B	Bending Length
P	Force
L	Length
Re	Reynolds Number
ρ	Density
μ	Absolute viscosity
V	Velocity
D	Distance
q	heat transfer
h	Heat Transfer Coefficient
A	Heat Transfer Area
T_f	Surrounding fluid temperature
T_s	Surface temperature

UMP

LIST OF ABBREVIATIONS

UHSS	Ultra-High Strength Steel
HSS	High Strength Steel
AHSS	Advance High Strength Steel
FEA	Finite Element Analysis
C_A	Diameter of Cooling Channel
C_B	Pitch Between Cooling Channel
C_C	Distance Cooling Channel To Tool Surface
C_D	Distance Cooling Channel To Wall Tool
HTC	Heat Transfer Coefficient
FLD	Forming Limit Diagram
DOE	Design of Experiment
VMS	Von Mises Stress
OA	Orthogonal Array

UMP

CHAPTER 1

INTRODUCTION

1.1 Research Background

The development of ultra-high strength steel (UHSS) material has received much attention due to the demand for the reduction in gas emissions, energy savings and the production of safer vehicles. UHSS has higher tensile strength than mild steel and a weight ratio that exceeds aluminum alloy (Karbasiyan & Tekkaya, 2010). The statement suggests that UHSS is a promising material that can be used in the production of vehicles. However, steel formability decreases with increasing strength, as shown in Figure 1.1. In cold stamping, the following problems often occur for high strength steels (HSS), advanced high strength steels (AHSS) and UHSS such as poor formability, forming accuracy and greater spring back problem. Equipment with high pressure is often required in manufacturing the UHSS, however, at times it is difficult or even impossible to shape it using such technique (IISI, 2009).

The traditional cold stamping method has become unsuitable for UHSS forming due to the formability of the material. Hence, to overcome this technological barrier of high-strength steel forming, sheet stamping industries are actively developing hot stamping technologies (Turetta, 2008). Hot stamping is a new forming method as it can significantly improve the formability of high strength steel. In addition to high strength and dimensional accuracy of steel sheet formed, it can also avoid cold stamping spring-back problem for high-strength steel and achieve the purpose of weight reduction (Seok & Koc, 2008; Sever et al., 2012 and Thanadngarn et al., 2013). Much effort was being put into the development of lightweight components and structures in automotive applications. Figure 1.2 shows the components of lightweight vehicle that utilises UHSS. The applied hot stamped parts in the automotive industry are chassis components, for instance A-pillar, B-pillar, bumper, roof rail, rocker rail, and tunnel.

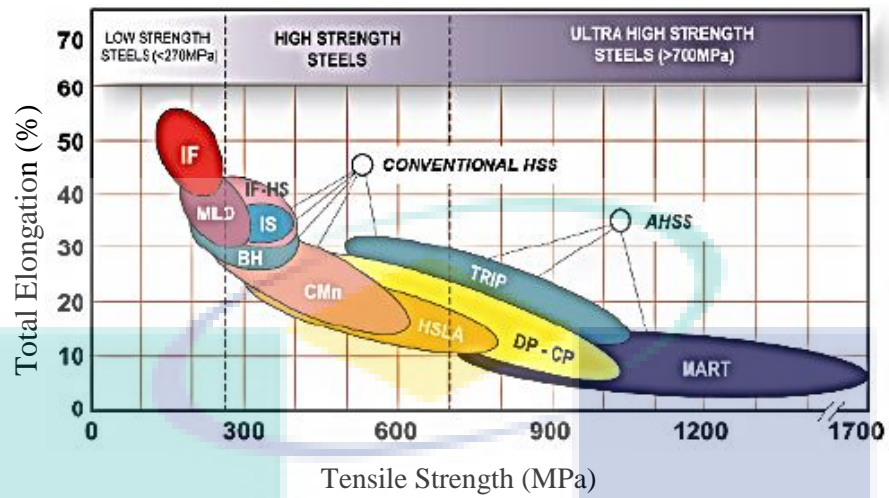


Figure 1.1 The elongation versus strength of different steel material
Source: IISI (2009)

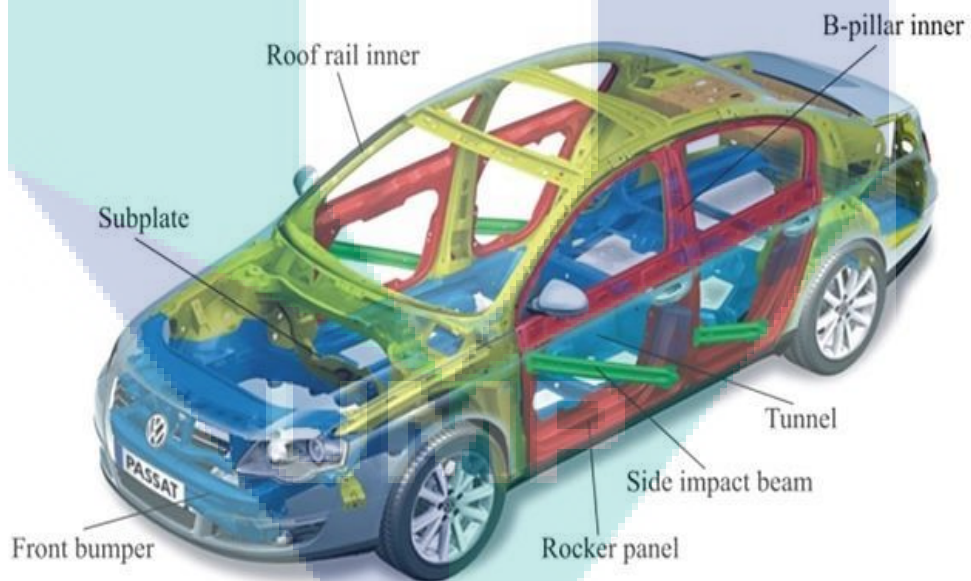


Figure 1.2 Hot stamped parts in typical middle class car
Source: Naderi (2007)

As of today, only three steel grades have exhibited the capacity of reaching a fully martensite microstructure at the end of a quenching process performed with cooled dies, all of them being boron alloys: 22MnB5, 27MnCrB5, 37MnB4. The mechanical properties before and after quenching of these are visible in Table 1.1. In this work the attention is focused on the 22MnB5 alloy which is one of the most widely used in hot forming operations. Figure 1.3 shows the material has a tensile strength of 600 MPa approximately at the delivery state, as the tensile strength can be increased up to 1500 MPa. Higher tensile can be achieved by a rapid cooling of hot stamping tool at least at the rate of 27 °C/s (Merklein & Lechler, 2008). Before forming process, the initial sheet of 22MnB5 that consists of ferritic-perlitic microstructure must be austenitized in order to achieve a ductility. Martensite transformation occurred when the austenite cools fast enough during the process. This microstructure with martensite properties provides hardness for the final product.

Table 1.1 Mechanical and thermal properties of high strength steels

Material	Martensite start temperature (°C)	Critical cooling rate (°C/s)	Yield Stress (MPa)		Tensile strength (MPa)	
			As delivered	Hot stamped	As delivered	Hot stamped
20MnB5	450	30	505	967	637	1354
22MnB5	410	27	457	1010	608	1478
37MnB4	350	14	580	1378	810	2040

Source: Karbasian & Tekkaya (2010)

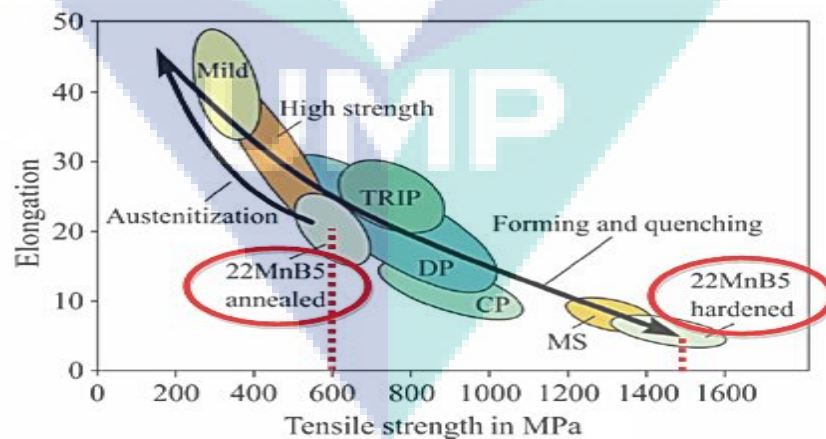


Figure 1.3 Mechanical properties of 22MnB5 as delivery and hot stamped

Source: Karbasian & Tekkaya (2010)

The hot stamping also named as press hardening process, which is a combination of three phases: heating blank, part forming and part quenching (So et al., 2012). In the process, UHSS blank is cut into the rough shape. The blank is heated to the required temperature (850 – 900 °C) for 5-10 min inside the furnace. Then, the blank must be transferred quickly to the press to avoid the part is cooled before forming. Subsequently, the blank is formed and cooled simultaneously by the water-cooled die for 5 - 10 s. Due to the contact between the hot blank and the cool tool, the blank is cooled in the closed tool (Karbasian & Tekkaya, 2010). Besides that, hot stamping exists in two different types of methods which are the direct and indirect method, as shown in Figure 1.4. For indirect hot stamping method, before the blank is heated inside the furnace, it has to undergo cold pre-forming process. This process is done once after the blank is cut. In this project, indirect method is chosen due to the in capability to install the heating element inside the hot stamping tool.

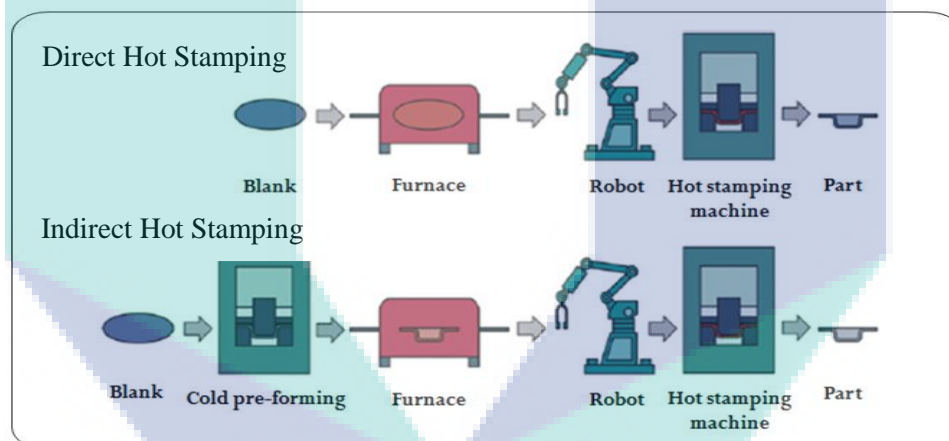


Figure 1.4 Basic Hot Stamping process chain

Source: Karbasian & Tekkaya (2010)

The quenching operation during the hot stamping process does not only influence the economy of the process but also the final properties of the component. The objective of the cooling channel design is to quench the hot part effectively and to achieve a cooling rate of at least 27 °C/s whilst martensite forms. The die cooling system is economical if a fluid coolant, such as water, is used, which flows through cooling ducts around the contours of the component. The heat flow in the formed component is dependent on the heat transfer from the component to the tool, the heat conductivity within the tool, and the heat transfer from the tool to the coolant. For an optimum heat transfer between component and tool, the contact surface should not

exhibit a scale or a gap. The heat conductivity within the tool can be considerably influenced by the choice of the tool material.

Another important factor with respect to heat drain is the design of the cooling ducts, which is defined by the size, location, and distribution of the cooling ducts. The cooling holes can be drilled in the forming tool. For this method, the machining restrictions should be considered in the design of the hole position (Steinbeiss et al., 2007). Therefore, an optimal design of the cooling system as to heat transfer is not possible. Another alternative is to provide the cooling holes as pipes in the casting mold of the tool. The unrestricted design of the cooling system is the advantage of this method. Alternatively, the tools can be manufactured using the lasered blank segments, which are screwed and form the tool surface with integrated cooling holes. This method is very cost-effective, but the lamellar design can have adverse effects on the part surface and the heat transfer within the tool (Karbasiyan & Tekkaya, 2010).

1.2 Problem Statement

Hot stamping process involves rapid cooling of the blank inside of the tools, this requires the cooling system to be integrated into the tools in order to control the cooling rate. The tool must be designed to cool efficiently in order to achieve maximum cooling rate and homogeneous temperature distribution of the hot stamped part. Current practice in local industry, Miyazu (M) Sdn. Bhd, the mean for holding time during quenching is 12 s and it takes about 25 to 30 s to completely produce one single part with an estimation cooling rate is 27 °C/s. The fluid used for coolants is water or chilled water with a thermal conductivity of approximately 0.5 W/m.K. The side beam hot forming die is segmented into 12 blocks due to the cooling channel drilling process capability with a limitation of 400 mm in length. The diameter of the cooling channel ranging from 6 mm to 12 mm, whilst its pitch is 10 mm, and the distance to the loading surface is between 8 mm to 15 mm (Hafizuddin, 2014). Lundström, (2012) at Proton (M) Sdn. Bhd training of hot stamping, suggests that the diameter of the cooling channel should be either 6 mm or 8 mm, whilst the small distance between coolant lines is 6 mm and the small distance from coolant line to die surface is between 6 mm to 8 mm. From statement, the best cooling channel parameter for hot stamping process is not fixed. Hence, from this research, the suitable parameters for cooling channel need to be obtained.

In die design concept development, the effect of heat transfer and material deformation, die clearance, cooling channel design and die material must be considered. In the same time, it must fulfill the required process system in terms of heating temperature to stamping process, transmitting time, the rate controlling of hot and heating furnace. Dealing with UHSS properties in hot forming the process requires the tool to cool down the blank rapidly, a cooling system must be integrated into the tool. This cooling system must be capable of lowering the tool temperature to accelerate the blank cooling rate as well as sinking away the heat to the cooling fluid as fast as possible (Karbasian & Tekkaya, 2010 and Altan & Tekkaya, 2012). Therefore the objective of the study is examined the heat distribution and the strength of the material of the die as a function of temperature in improving the rapid cooling process of quenching and optimization of cooling channel die design. In this case, apart from the material of the die, crucial factors to be considered are the design of the cooling channel including the size, location and distribution temperature (Zhong-de et al., 2010; Kumar et al., 2011 and Liu et al., 2013). Besides that, instead of having tool with higher cooling rate, hot stamping with strong structure also needed. Thus, thermal and static analysis need to be combined as to obtain the best hot stamping cooling channel. In this research, heuristic method is used to optimize the cooling channel design coupled with finite element analysis (FEA) of static and thermal analysis. This aforementioned parameters were evaluated in terms of both simulation and physical experimental works.

1.3 Aim and Objectives

The research aims to design and develop cooling channel design by means of a heuristic method in hot stamping tool. In order to achieve the goal of this project, specific objectives were constructed as follow:

- i) To develop an optimized cooling channel design for hot stamping tool using heuristic method coupled with finite element analysis (FEA) for maximum mechanical properties of boron steel.
- ii) To simulate thermal distribution in cooling channel of flat and U-shape tools using FEA.
- iii) To analyse the hardness and tensile strength of hot stamping product for both flat and U-shaped boron steel.

1.4 Research Scope

- i) In designing the cooling channel for the hot stamping tool, four parameters were used, such as the diameter of cooling channel (C_A), the pitch between cooling channel (C_B), the distance of the cooling channel to the tool surface (C_C) and the distance of the cooling channel to wall tool (C_D). The parameters selected for (C_A) are 6 mm, 8 mm, and 12 mm, and for (C_B), (C_C) and (C_D) are 6 mm, 8 mm and 10 mm, respectively. The parameters were analysed based on both the thermal and static analysis. Based on the output result from the analysis, the cooling channel design was optimised by using heuristic method. As for the flat tool, three parameters were used viz. (C_A), (C_B), and (C_C) and were validated by means of the Taguchi method. For the U-shaped tool, the parameter used were (C_A), (C_B), (C_C), and (C_D). Then, the optimum parameters obtained from the FEA simulation results were selected, and used to fabricate the flat shaped and U-shaped hot stamping tools.
- ii) The fabricated tools were then used to run a hot stamping process. For the flat tool experiment, the pressure was fixed, due to the capacity of the mini hydraulic press machine in Faculty of Manufacturing Engineering (FKP). Other examined variables were the thickness of the material (1.8 mm, 2.0 mm and 3.0 mm), the heating temperature (800 °C, 850 °C and 900 °C) and the heating time (4 s, 6 s, and 8 s). The results of the temperature distribution from the experiment was validated with the results from FEA simulations. While for the U-shaped tool experiment, the hot stamping process parameters was taken based on the best parameter obtained from the flat shape experiment. Again, the temperature distribution obtained from the FEA simulation results was validated with the experimental data. The experimentally measured temperature distribution was attained via a K-type thermocouple placed inside the hot stamping tool.
- iii) The shape of hot stamping tool used was a flat and U-shaped tool. Then, the cooling channel was intergrated into the tool. The material used in this project was 22MnB5 for boron steel and SKD61 for hot stamping tool material. The tool material utilised was SKD61 due to its cost effectiveness as well as its ease of procurement, instead of HTCS 150. The mechanical properties (tensile

strength and hardness test) of the blanks produced from the stamping process (i.e. flat and U-shaped blanks) were examined. As for the tensile test, the equipment used was Universal Testing Machine Instron 3369, whilst the Wilson Vickers 402 MVD was used to measure the hardness.

1.5 Thesis Organisation

This thesis is arranged and discussed as follows:

Chapter 2: Literature Review of Hot Stamping Process – This chapter elaborates on the technology of high strength steel materials as well as a comprehensive review on past research works.

Chapter 3: Methodology – Chapter 3 presents the methodology employed in this study for the fabrication of the hot stamping tool for flat and U-shaped with different cooling channel parameters. The FEA simulation for the tools are analysed by means of thermal and static analysis. Once the results from the simulations were obtained, a heuristic method is used to further optimise the results. As for the flat tool, the Taguchi method was used. This was followed by experimental works performed to validate the simulation results, and the mechanical properties of the product will be determined via the tensile and hardness test that will be further discussed in Chapter 4.

Chapter 4: Results and Discussion – Chapter 4 presents the analysis required for the improvement of hot stamping tool i.e. heuristic method optimisation where the cooling parameter are optimised by taking into account low static stress and high cooling rate of the tool. Next, the experiment is conducted to obtain an improved blank product. The three factor with three levels of the hot stamping experiment is used, i.e. the thickness of the material, the heating temperature and the heating time. The best parameters from the experiment will be validated against the temperature distribution of the FEA. Lastly, the strength and the hardness of the product will be examined.

Chapter 5: Conclusion – Summarised all the research finding to fulfill the predetermine objectives.

CHAPTER 2

LITERATURE REVIEW

2.1 Introduction

A review of previous research efforts related to the boron steel material, hot stamping process, hot stamping die and design of experiment are presented in this chapter. The review begins with the properties of the boron steel material, followed by the type of hot stamping process which includes the cold stamping die, heating method transfer time and heat transfer coefficient. Then, die material and cooling channel design of the hot stamping die is discussed. Finally, at the end of this chapter, the overview of the design of experiment including heuristic and Taguchi method were described.

2.2 Forming of Boron Steel

Boron Steel is one type of low carbon martensitic steel. This form of metal achieves UHSS grade only after the austenitization process (Srithananan et al., 2016). In its initial form, the strength of boron steel is 600 MPa and the final formation after hot press forming is about 1500 MPa (Naderi, 2007). The main purpose of using this material is the ability to achieve complex geometry with good hot formability and the absence of the "springback" effect. Furthermore, it is desirable owing to its uniform mechanical properties as well as its exceptional fatigue strength (Dhillon, 2002).

In general, boron steel is classified as a low alloyed steel and it is well-known for its capability to be hardened through heat treatment to alter its mechanical properties as well increasing its hardness. Typically boron steel contains a number of alloying element Carbon (*C*), Mangan (*Mn*), Phosphorus (*P*), Sulphur (*S*), Silicon (*Si*), Aluminum (*Al*), Titanium (*Ti*) and Boron (*B*), as shown in Table 2.1. Among these

elements, boron is the most significant element that greatly improves the hardenability of Boron Manganese Steel while the presence of carbon determined its hardness (López-Chipresa et al., 2008).

Table 2.1 Chemical composition based on weight percentage of boron steel and mechanical properties of boron steel before and after quenching

Alloy Element								
	C	Mn	P	S	Si	Al	Ti	B
22MnB5	0.200-0.250	1.100-1.400	≤ 0.025	≤0.008	0.150-0.350	≥ 0.015	0.020-0.050	0.002-0.005
Mechanical Properties								
	Yield Strength (MPa)		Ultimate Strength (MPa)		Elongation (%)			
As delivered	400		600		25			
After die quench*	1200		1500		5			

*According to best practice

Source: Karbasian and Tekkaya (2010)

An annealed boron steel has a mixture of ferrite and pearlite phase microstructure with an ultimate strength of 600 MPa. Heating boron steel, causes the microstructure to gradually transform into austenitic phase at 830 °C until it is fully transformed at a temperature of approximately 900 - 930 °C (Karbasian & Tekkaya, 2010). As the austenitic is quenched or cooled down rapidly, the austenitic phase is transformed to martensitic or bainite phase or a mixture of both phases depending on its cooling rate (Figure 2.1). In order to achieve the final part strength of 1500 MPa, the austenitic phase must be fully transformed to the martensitic phase where it must be cool down at a rate of at least 27 °C/s (Zhang et al., 2014). During quenching, the austenitic phase is gradually transformed into martensitic phase starting at a temperature of approximately at 400 – 450 °C until it is fully transformed at 200 – 250 °C (Figure 2.1). This metallurgical transformation significantly alters the final mechanical properties of the boron steel especially its strength, hardness and the percentage of elongation as shown in Table 2.1.

Since boron steel exhibits a broad range of temperature as well as different microstructures phase during processing, the material temperature dependent properties should be taken into account. According to Shapiro, (2009), thermal property of the boron steel such as elastic modulus, E , thermal conductivity, k and specific heat C_p are likely to vary with the change of the material microstructure from austenitic phase (at 400 – 1000 °C) to martensitic phase (at temperature less than 400 °C) as shown in Table 2.2.

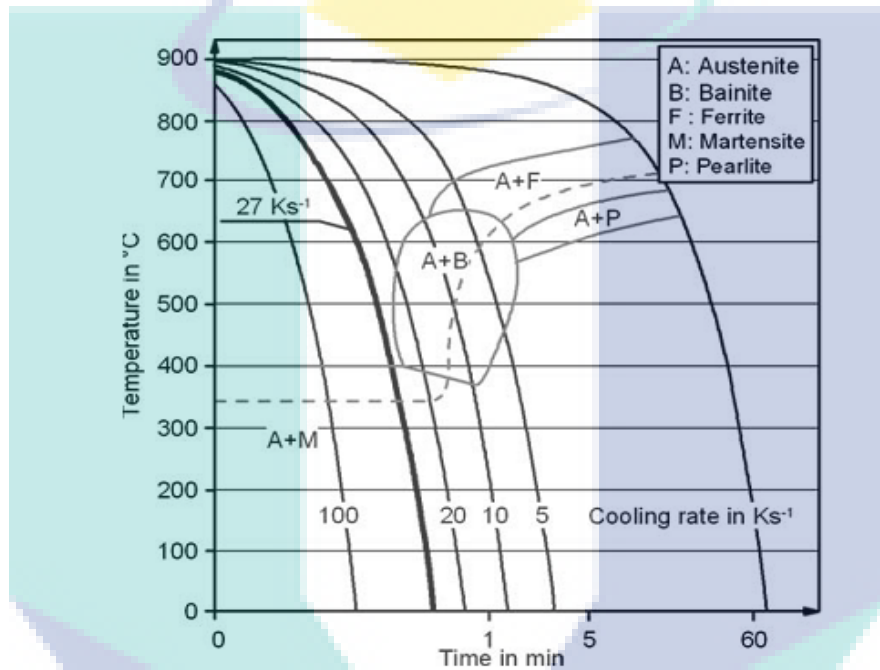


Figure 2.1 Temperature, time and transformation diagram of boron steel at different cooling rate

Source: Karbasian & Tekkaya (2010)

Table 2.2 Temperature dependent properties of boron steel

	Temperature (°C)										
	20	100	200	300	400	500	600	700	800	900	1000
E (GPa)	212	207	199	193	166	158	150	142	134	126	118
k (W/m °C)	30.7	31.1	30	27.5	21.7		23.6		25.6		27.6
C_p (J/kgK)	444	487	520	544	561	573	581	586	590	596	603

Source: Shapiro (2009)

2.3 Hot Stamping Process

Saab Automobile AB is the first vehicle manufacturer implement hardened boron steel (UHSS) in 1984 for Saab 9000 (Iron & Institute, 2002). There are two different methods of hot forming process namely the direct and indirect method. The direct hot stamping process is shown in Figure 2.2. It begins with a blank sheet metal that is fully austenitized inside a hot furnace at around 900 °C at a certain period. Then, the heated blank is transferred to a forming tool by a transfer unit i.e. robotic arm. Even with lower punch force, any complex shape can be obtained. This is because at high temperature steel exhibits excellent ductility properties. After being stamped, a specific coolant depending on the heat properties and thicknesses of steels are used to cool down the blank sheet in a closed die. Finally, a complete martensitic transformation product was achieved (Lee et al., 2009).

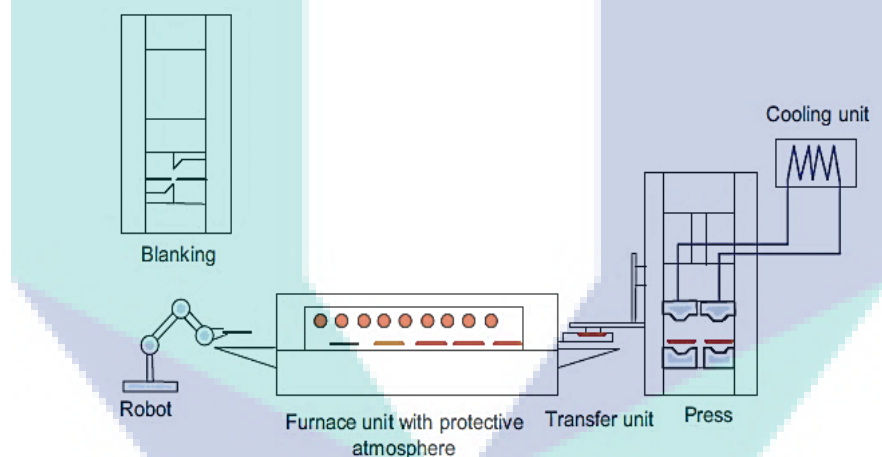


Figure 2.2 Direct method of hot stamping

Source: Lee et al., (2009)

On the other hand, Figure 2.3 shows the other method namely the indirect hot press forming (IHPF) that includes the conventional cold forming procedure prior to the austenitizing process. It begins by providing a part to be pre-form, drawn, unheated, to approximately 90 % to 95 % of its final shape in a cold die, followed by a partial trimming operation, depending on edge tolerance. Then, it is heated continuously in a furnace and quenched in the die. The reason for the additional step is to extend the forming limits for very complex shapes by hot forming and quenching the cold- formed parts.

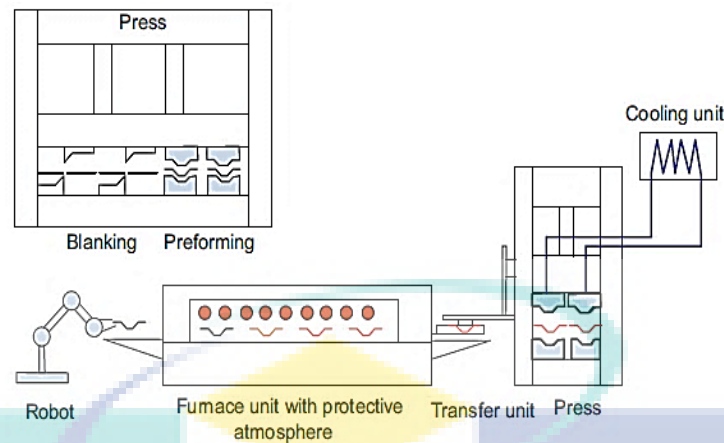


Figure 2.3 Indirect method hot stamping

Source: Lee et al., (2009)

The usage of nearly complete cold pre-formed part which focused to quenching and calibration operation in the press after austenization is namely as indirect hot stamping process (Merklein & Lechler, 2008). An increasing of tensile strength up to 1500 MPa is due to full martensite transformation in the material (Karbasian & Tekkaya, 2010). Indirect process provides a part to be drawn, unheated to approximately 90 % and 95 % of its final shape in a conventional die, followed by a partial trimming operation depending on edge tolerance which difference from direct process. Then, the pre-forms are heated in continuous furnace and quenched in the die.

The additional step is added to extend the forming limits for the complex shapes by hot forming and quenching of the cold formed parts (Naganathan, 2010). Basically, product designs in indirect hot stamping started with pre-cold forming die design before continue with hot stamping process. The applied hot stamped parts in the automotive industry are chassis components, like A-pillar, B-pillar, bumper, roof rail, rocker rail and tunnel (Figure 1.2).

2.3.1 Sheet Metal Forming

One of the most common processes for sheet metal forming is bending. It is used not only to form pieces such as V, L, or U profiles (Figure 2.4, 2.5 and 2.6), but also to improve the stiffness of a piece by increasing its moment of inertia (Hu et al., 2002). Bending consists of uniformly straining flat sheets or strips of metal around a linear axis. However, it also may be used to bend tubes, drawn profiles, bars and wire.

V-bending is performed when single bending axis is produced in the same operation (Lempco, 2000). In v-bending, the cutting clearance between the punch and die is constant (equal to the thickness of sheet blank). The thickness of the sheet ranges from approximately 0.5 mm to 25 mm. Figure 2.4 shows an example of v-bending where t is the thickness of material, P is the bending force, B is the bending length and L is the die shoulder width.

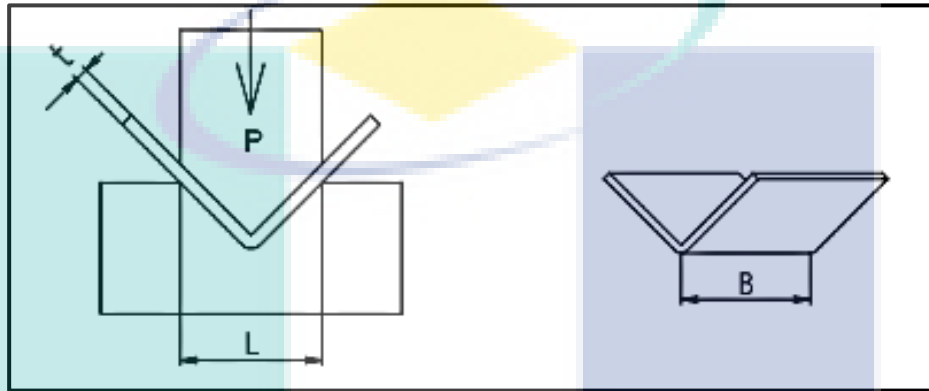


Figure 2.4 V-bending operation

Source: Misumi (2015)

Wiping die bending is also known as flanging. One edge of the sheet is bent to 90° while the other end is restrained by the force of blank holder and pad (Lempco, 2004). The flange length can be easily changed and the bend angle can be controlled by the stroke position of the punch. Figure 2.5 shows of L-bending process, where t is thickness of material, P is the bending force, and B is the bending length.

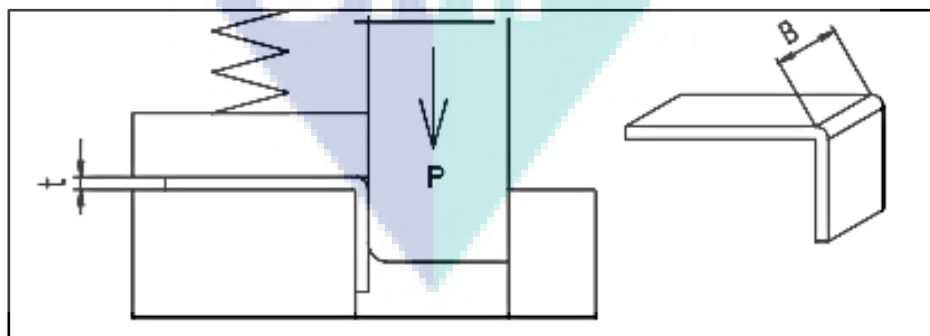


Figure 2.5 L-Bending process

Source: Misumi (2015)

U-bending is performed when two parallel bending axes are produced in the same operation (Bar-Meir, 2009). Then, a backing pad is used to force the sheet contacting with the punch bottom. It requires about 10 % of the bending force for the pad to press the sheet contacting the punch (Boljanovic & Paquin, 2006). Figure 2.6 shows an example of u-bending. This shape is taken as the basis for the bending force for pad-pressed bending. In the case of u-bending, since the bending line (B) is present at two locations, the bending force is made by doubling the value of the bending line length (B) (Misumi, 2015). In this project, u-bending was applied in hot stamping process for designing the cooling channel.

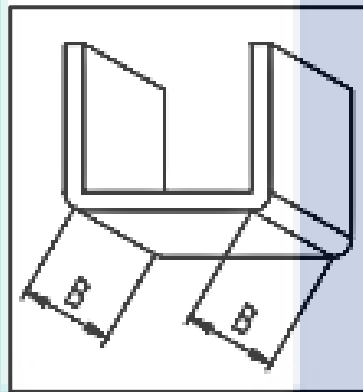


Figure 2.6 U-Bending Process

Source: Misumi (2015)

2.3.2 Heating Method

In the hot stamping process, the blank is heated using different thermal phenomena: radiation inside furnace, induction, and electrical resistance (Figure 2.7). Depending on the purpose either production or for research, the heating method would be different. In the case of mass production, radiation inside furnace is widely used and has proven its capability of heating the blank sheet. While in research environments, all the three heating method could be employed depending on the suitability and adaptability of the method to the experimental apparatus (Karbasiyan & Tekkaya, 2010).

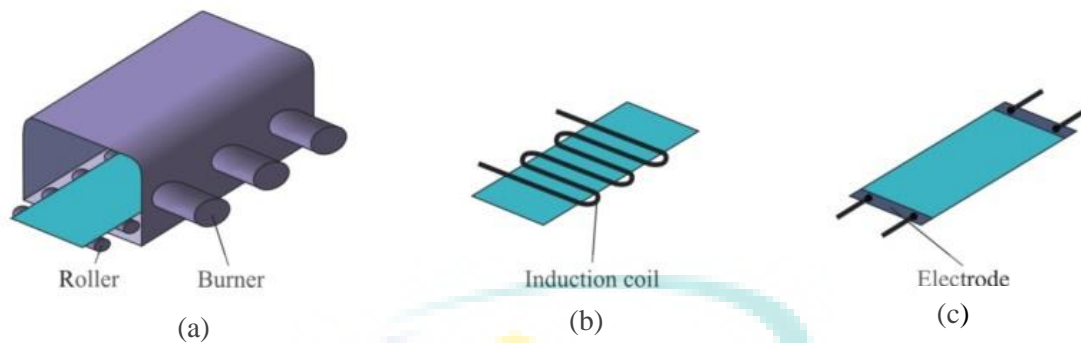


Figure 2.7 Types of heating system (a) Roller hearth furnace, (b) Induction heating and (c) Resistance heating

Source: Karbasian & Tekkaya (2010).

In the radiation inside furnace method, the most common types of furnace used are the roller hearth furnace. In this method, the pre-cut blank is continuously fed into the furnace by a conveyor passing through the heating chamber where the radiation from the combustion of petroleum gas along the heating chamber will raise up the blank temperature (Karbasian & Tekkaya, 2010). Compared with the radiation inside the furnace method, the other two methods use electrical energy to heat-up the blank to the austenization temperature. The principle of induction heating is an electrical conductor material inducing a current whenever it passes through a magnetic field. This induced current or so called eddy current will flow inside the conductor material causing a rise in temperature of the material. A study conducted by Kollack et al., (2009) analysed the capability of induction heating to heat-up a blank to the austenization temperature was done using a custom made induction furnace.

While in the resistance heating method, the blank sheet offer some resistance as current passes through it causing the temperature of the blank sheet to rise-up. Using this method, a homogenous temperature distribution on the blank sheet with symmetrical shape can be achieved by properly positioning the electrode (Kollack et al., 2009). However, for the irregular blank shape, homogenous temperature is very difficult to achieve due to inconsistency distance between the positive and negative terminal. Although this method has a limitation on heating a sheet with irregular shape and wide surface area, but for spot heating or localize heating this method is the best. In a study Mori et al., (2012) punched a small hole on a hardened boron steel part. The cutting operation was done at different temperatures ranging from room temperature to 800 °C. Heating of a small area on the hardened part was done using a pair of

rectangular electrode integrated inside the cutting tool, as shown in Figure 2.8. Results from the experiment indicate that with proper selection of input energy, resistance heating is capable of rising the sheet temperature up to 800 °C in less than 3 s. In this study, normal furnace was used, where the product was heated inside the furnace. The product was manually transfer to the hot stamping tool for quenching process.

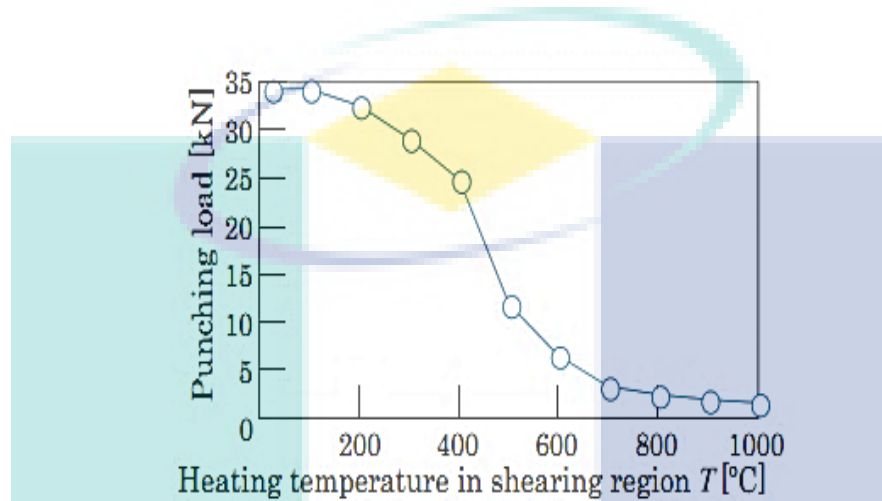


Figure 2.8 Temperature distribution on punching load as a function of heating temperature at shearing zone

Source: Mori et al. (2012).

2.3.3 Heat Transfer Mechanism

Heat is defined as a form of energy that can be transferred from one system to another as a result of temperature difference (Abdul Hay et al., 2010). A thermodynamic analysis is concerned with the amount of heat transfer as a system undergoes a process from one equilibrium to another. Heat transfers are the determination of the rates of such energy transfers. The transfer of energy as heat is always from the higher-temperature medium to the lower-temperature one, and heat transfer stops when the two mediums reach the same temperature (Cengal & Ghajar, 2011).

(i) Thermal Contact Resistant

Thermal contact resistant is an interface offers some resistance to heat transfer and this resistance per unit interface area. When two such surfaces are passed against each other, the peaks form good material contact but the valleys form voids filled with air. As a result, an interface contains numerous air gaps of varying sizes that act as

insulation because of the low thermal conductivity of air (Cengal & Ghajar, 2011). There are several factors that lead to the factor dependency of heat transfer. These factors are surface condition, contact pressure, tool temperature and flow type.

(ii) Surface condition

In the analysis of heat conduction through multilayer solids, it is assumed that "perfect contact" exist at the interface of two layers, and thus no temperature drop occurs at the interface. This would be the case when the surfaces are perfectly smooth, and produce a perfect contact at each point (Cengal & Ghajar, 2011). In Figure 2.9, it shows the temperature distribution and heat flow lines along two solid plates pressed against each other for the case of perfect and imperfect contact.

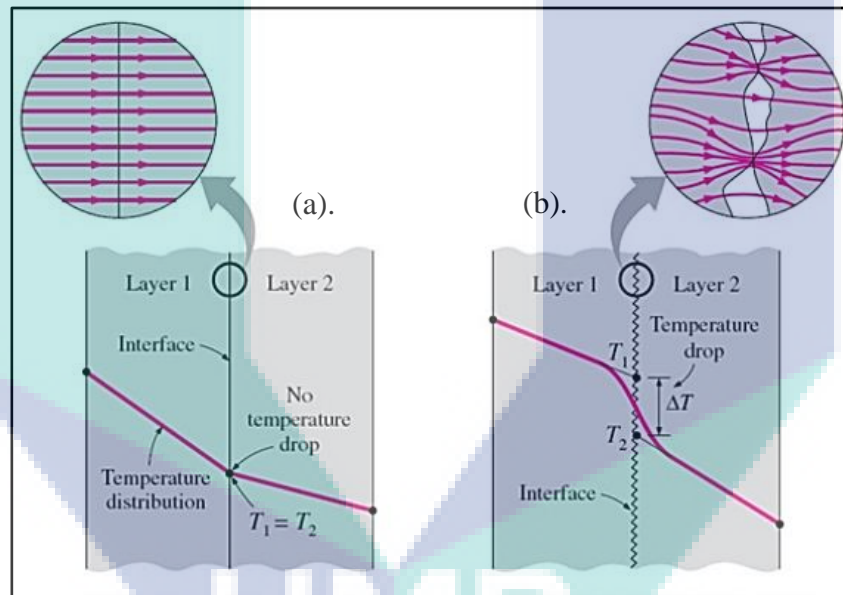


Figure 2.9 Thermal contact resistance with (a) ideal (perfect) thermal contact, and (b) actual (imperfect) thermal contact

Source: Cengal & Ghajar, (2011)

(iii) Contact Pressure and Tool Temperature

Based on an experiment performed by (Bosetti et al., 2010), study had identified the heat transfer coefficient (HTC) in hot stamping of boron steel sheets under conditions very close to the industry. In order to identify HTC at the blank-dies interface, pressure were applied. In the experiment, the testing procedure consists of the compression of the metal blank between two flat dies at imposed value of applied pressure, without large-scale sheet deformation. Based on Figure 2.10, the quenching

device mainly consists of two 10 mm exchangeable water cooled contact plates. Thermocouple equipped specimens (58 x 160) mm² are manually placed on four spring seated pins after undergoing a previous homogeneous austenitization at a temperature of 900 °C in a furnace under atmospheric conditions. By using a set-point testing software, the specimens can be loaded during quenching with a defined nominal contact pressure up to 40 MPa. During the test, the temperatures of the blank and of both contact plates are recorded by using integrated Ni/Cr-Ni-thermocouples (Merklein & Lechler, 2008).

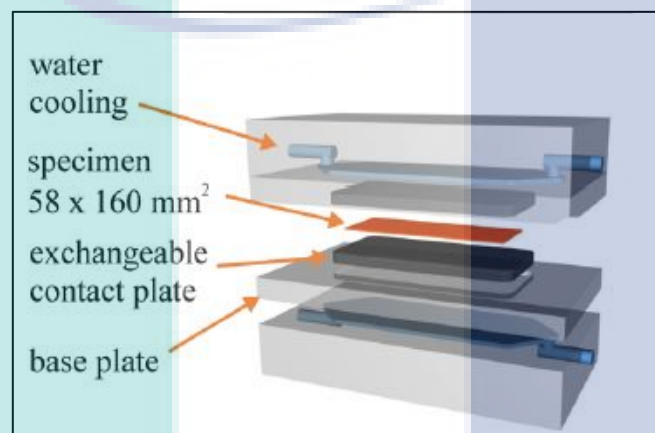


Figure 2.10 Heat transfer coefficient experiment apparatus
Source: Bosetti et al. (2010).

Based on the result in Table 2.3 heat transfer increases with increase in pressure and at the same time the standard deviation also increases. Figure 2.11 shows that the contact pressure is directly proportional with the heat transfer coefficient, where when the contact pressure increase, the heat transfer coefficient also increase. Besides that, the temperature of the tool is also directly proportional with the heat transfer coefficient. When the temperature of tool increases, the heat transfer coefficient also increases.

Table 2.3 Value of contact pressure and HTC Standard deviation

Contact pressure (MPa)	HTC (W/m ² K)	Standard deviation (W/m ² K)
0	1231	82
5	1484	27
10	2025	37
20	2395	69
30	3065	117
40	3308	159

Source: Bosetti et al. (2010)

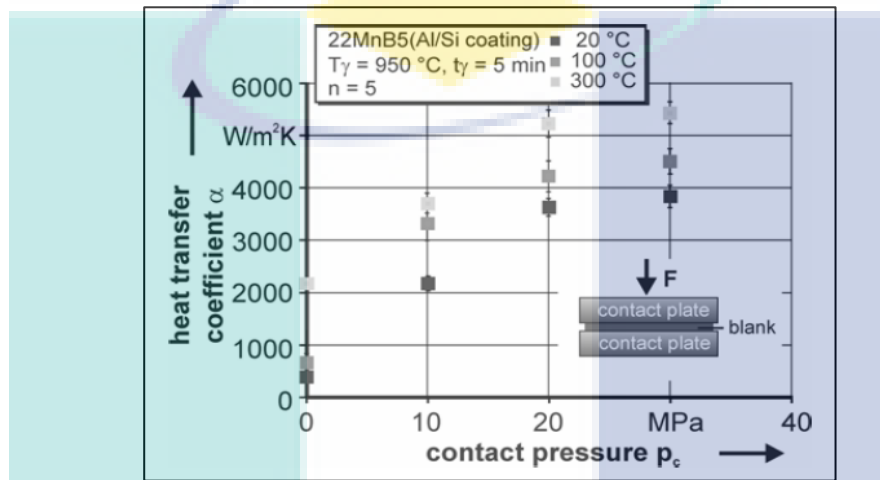


Figure 2.11 Heat transfer coefficient as a function of the contact pressure for different tool temperatures

Source: Merklein & Lechler. (2006).

(iv) Fluid Flow type

Fluid flow can be either laminar or turbulent. The highly ordered fluid motion characterized by smooth layers of fluid is called laminar. Moreover, the highly disordered fluid motion that typically occurs at high velocities and is characterized by velocity fluctuations is called turbulent. The factor that determines which type of flow is present is the ratio of inertia forces to viscous forces within the fluid, expressed by the non-dimensional Reynolds Number, Re (Holman, 2009).

$$R = \rho v D / \mu \quad 2.1$$

Where, ρ is the water density, and μ is the absolute viscosity. While, v and D are a fluid characteristic velocity and distance. For example, for fluid flowing in a pipe, v could be the average fluid velocity, and D would be the pipe diameter. Typically, viscous stresses within a fluid tend to stabilize and organize the flow, whereas excessive

fluid inertia tends to disrupt organized flow leading to chaotic turbulent behaviour (Cengal & Ghajar, 2011).

Fluid flows can be considered as laminar for Reynolds Numbers when it up to 2000. Beyond Reynolds Number of 4000, the flow is completely turbulent. Between 2000 and 4000, the flow is in transition between laminar and turbulent, and it is possible to find sub-regions of both flow types within a given flow field (Incropera et al., 2002). In this project, turbulent flow will be applied for highest heat convection.

(v) Convection Heat Coefficient

Newton's law of cooling states that the heat transfer rate leaving a surface at temperature T_s into a surrounding fluid at temperature T_f is given by the Equation 2.2.

$$\dot{Q}_{convection} = hA [T_f - T_s] \quad 2.2$$

Where the heat transfer coefficient h has the units of $W/m^2.K$ or $Btu/s.in^2.F$. The coefficient h is not a thermodynamic property. It is a simplified correlation to the fluid state and the flow conditions and hence it is often called a flow property (Cengal & Ghajar, 2011). In this project, the equation above is used to simulated the thermal analysis.

2.4 Operation in Hot Stamping

In hot stamping, two major operations are involve in the process, i.e. forming and cutting. Forming is a process of shaping the material into the desired shape (Banabic, 2010). In forming process, the major parameter that needs to be considered are the behavior of material itself and springback. The behaviour of material can be predicted by using the forming limit diagram (FLD) to show whether it fail or not. While springback is metal tends to return to its original shape or contour after undergoing a forming operation (Kim et al., 2009). On the other hand, cutting processes is a piece of sheet metal is separated by applying a great enough force causing the material to fail. The most common cutting processes are performed by applying a shearing force.

2.4.1 Forming process

Forming process is where a flat blank sheet metal is plastically deformed or drawn into a specific shape punch and die. Majority of sheet metal parts are formed using this process. In the past, conventional cold forming process was used to form sheet metal, but nowadays hot forming process is used. The advantages as compared to the conventional cold forming process, of hot forming are as follows (Zhang et al., 2010).

- a) The thickness of part can be reduced and the weight of car body can be lightened. In the meantime, the passive safety can be enhanced.
- b) The tonnage of the pressing machine used in the hot forming is much lower than that in the cold forming.
- c) The amount of the springback in the hot forming is low. So the high dimensional accuracy and high strength parts can be obtained.

(i) Forming limit diagram

The forming limit diagram is used in sheet metal forming for predicting the forming behaviour of sheet metal (Cui et al., 2015). The diagram attempts to provide a graphical description of material failure tests. In order to determine whether a given region has failed, a mechanical test is performed, as shown in Figure 2.12.

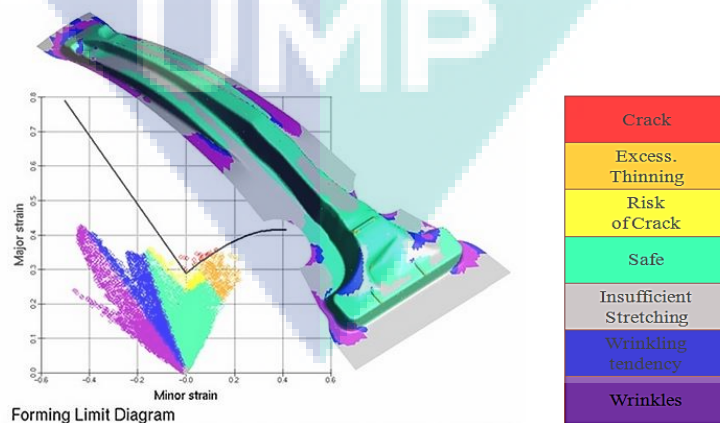


Figure 2.12 Typical Forming Limit Diagram

Source: Skrikerud et al. (2010).

Based on the simulation that conducted by Skrikerud et al., (2010), study had taken a B-Pillar, for geometry and tools, as shown by Figure 2.13. The initial blank temperature assumed is 800 °C and tool surface temperature is 200 °C. The study had made a comparison between hot forming and cold forming process. By using a software to simulate the part, study had shown that the given part clearly fails if it was stamped at room temperature.

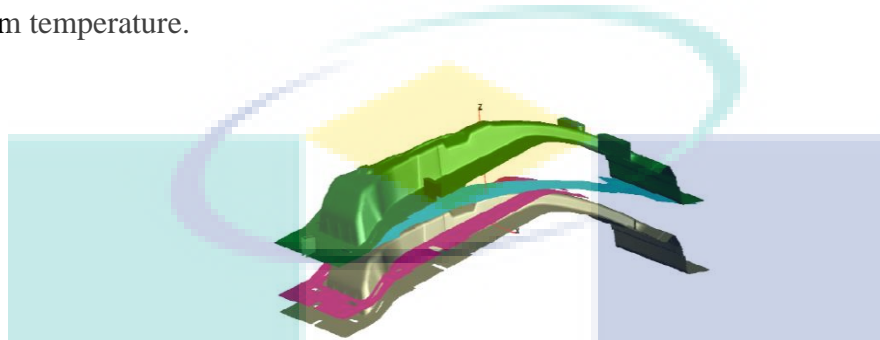


Figure 2.13 Sample B-Pillar with tools

Source: Skrikerud et al. (2010).

(ii) Springback

A research was conducted on the springback of high-strength steel after hot and warm sheet forming. Yanagimoto et al., (2005), performed an experiment on the warm and hot bendings of high-strength steel sheets. Experiment shows that the springback of hot steels is reduced when the temperature of steel is beyond the recrystallization temperature of austenite. In order to proceed to the experimental stage, they had to judiciously control the temperature. Two different positions are selected; plastically deforming zone (position A) and flange (position B) see Figure 2.14.

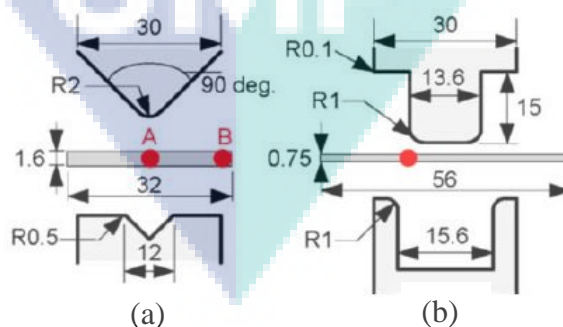


Figure 2.14 Geometries of die and test piece for (a) V-bending and, (b) U-shape

Source: Yanagimoto et al. (2005).

In Figure 2.15, it shows that when the temperature is higher than 750 K, the amount of springback decreases markedly (Figure 2.15a). Springback effect may be reduced when the temperature of plastically deformation zone is less than the recrystallization temperature of austenite (Yanagimoto et al., 2005). Besides that, when the flange temperature is higher than 1000 K, the springback is decreased (Figure 2.15b). It is clear that springback could be significantly decreased when the temperature of the bending zone is in the warm forming range which is equal to 750 K.

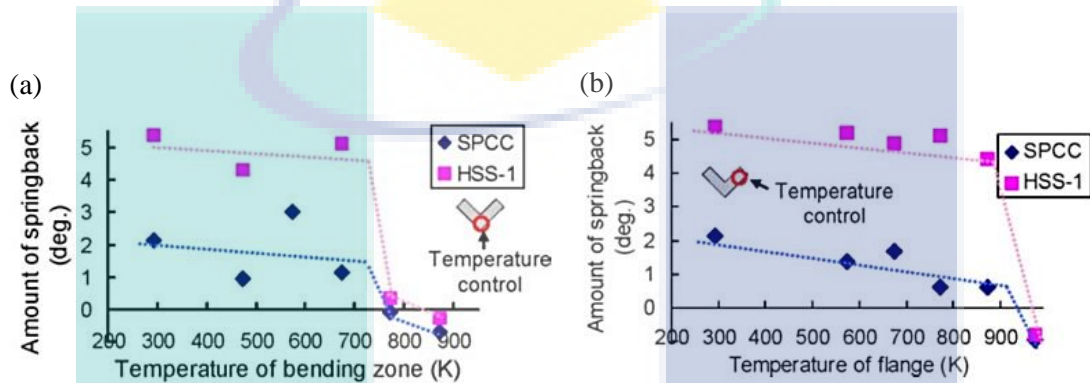


Figure 2.15 Relationship between amount of springback after V-bending and temperature of bending zone (a) relationship between amount of springback high-strength steel after V-bending and temperature of flange (b)

Source: Yanagimoto et al., (2005).

2.4.2 Punching

Based on research carried out by Mori et al., (2005), a warm and hot punching process using resistance heating was developed to reduce the punching load of UHSS sheets. The shearing load is reduced by heating the sheets. In the experiment the (UHSS) sheet SPFC980 having a thickness of 2.0 mm was punched at elevated temperatures. To prevent the temperature decrease and oxidation, the resistance heating was applied to the warm and hot punching as shown in Figure 2.16. The length and width of the sheet are 130 mm and 50 mm, and only 5 mm of each edge of the length is in contact with the electrode. The punch having 10 mm in diameter is made of SKH51 and is coated with TiCN. A pressure of 8 MPa was applied by the sheet holder to obtain sufficient contact between the sheet and electrode for the electrifying. The conditions of the warm and hot punching are shown in Table 2.4.

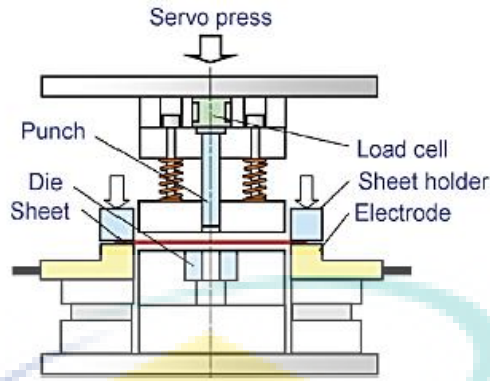


Figure 2.16 Warm and hot punching process of UHSS sheet using resistance heating
Source: Mori et al. (2008).

Table 2.4 Conditions of warm and hot punching process

Parameters	Value
Heating Temperature, T ($^{\circ}\text{C}$)	650, 700, 830, 970, 1070
Clearance Ratio, c (%)	5, 10, 15
Punching Speed (mm/s)	150

The relationship between the maximum punching load and the heating temperature is shown in Figure 2.17. From the graph, it is apparent that the higher the heating temperature, the lesser the punching load can be given into the (UHSS) sheets. The punching load slightly increases if the heating temperature is below 650°C . Hence, warm and hot shearing process is effective for the (UHSS) sheets. Furthermore, the advantages of this process are the decrease in shearing loads and also the improvement in the quality of sheared edge (Mori et al., 2008).

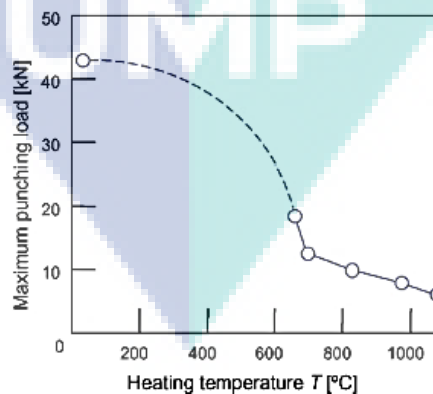


Figure 2.17 Relationship between maximum punching load and heating temperature
Source: Mori et al. (2008).

2.5 Hot Stamping Die

One of the essential equipment in stamping production is stamping die. The important terms need to be considered in die design are quality, productivity and production cost of stamping. The stamping die classified by four characteristic. First, the stamping process i.e blanking dies, bending dies, drawing dies, and forming dies. There is also the characterisation by the combination of processes such as single process mode, composite mold, and continuous mold. Die are also characterised by its orientation mode and the way of guide pin or position (Hu et al., 2013).

The selection of die material is not only focused on the durability of the die but also its ability to withstand shock load and continuous work. The selection of the die material depends on the type of the die and its operating condition i.e. high strength, hardness, wearing resistance, impact resistance and fatigue resistance. Apart from the aforementioned criteria die material selection relies also on the type of blank and production. The processing performance should also be considered which includes machinability, good hardenability, and low heat treatment deformation. Finally, the material should also meet the economical requirement (Hu et al., 2013).

2.5.1 Die Design

In the die design concept development, the effect of heat transfer and material deformation, die clearance, cooling channel design and die material must be considered (Hoffmann et al., 2007). Furthermore, it must also fulfill the required process system in terms of temperature heating to stamping process, transmitting time, the rate controlling of hot forming and heating furnace. Some of the issues that are faced in dealing with UHSS in hot forming are no uniform distribution thickness, wrinkling, cracking and failure to complete fully quenching (Naganathan & Penter, 2012).

2.5.2 Tool Construction

In general, the tool used in hot stamping process is the same with normal stamping process except for the additional cooling system that is machined inside the tool. The objective of the cooling ducts design is to quench the hot part effectively and to achieve a cooling rate of at least 27 °C/s whilst martensite forms (Karbasian & Tekkaya, 2010). To ensure good characteristics of the drawn part, the whole main tool

for instance punch, die and blank holder, are required to be designed to cool sufficiently (Merklein & Lechler, 2006). These main tools are connected to a chiller. The chiller is a medium to cool and stores the fluid. Figure 2.18 shows the hot stamping tool for forming process whilst Figure 2.19 shows the hot stamping tool for flat shape.

The die as shown in Figure 2.18 consists of an upper and lower member of the die that is used for forming the blank. The blank holder is the part of the die which holds the blank against the die to control metal flow. The punch, on the other hand, acts as a metal block that used for forming the blank. Figure 2.19 depicts the experimental apparatus employed by Merklein & Lechler, (2006) to determine the heat transfer coefficient from the hot stamping process to determine the heat transfer coefficient from the hot stamping process. A flat shaped samples is used in the study. A similar experimental setup (Figure 2.20) was also used by Hoffmann et al., (2007). In this project, the flat tool is used to study the cooling channel design in hot stamping.

2.5.3 Cooling channel system

The optimisation of a cooling system is able to reduce the cycle time, as the cooling part after the dies is closed is critical to ensure optimum cooling rate. There are some factors that affects the heat transfer between the drawn part and die such as heat transfer between surface parts, the heat conductivity of the material, the design of cooling duct and type of coolant (Karbasiyan & Tekkaya, 2010). There are also some constraints that ought to be considered in tool design. The constraints include the distance between loaded and unloaded of die surface and cooling duct, the distance between cooling ducts, the size of sealing plugs and position of cooling duct (Hu et al., 2013). The main function of cooling channel is to dissipate heat from the tool as well as to control the tool temperature. Temperature control is achieved by circulating a fluid through the cooling channel that is made by the drill hole (Steinbeiss et al., 2007).

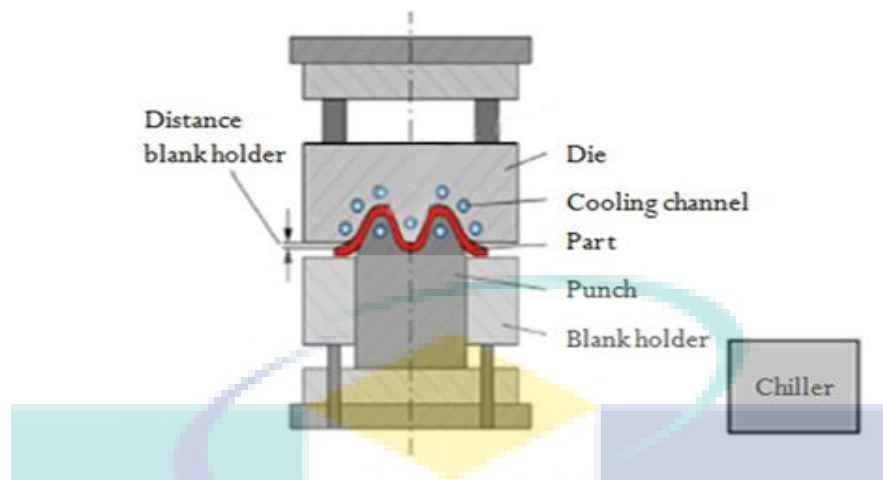


Figure 2.18 Tool design for the hot stamping process
Source: Karbasian & Tekkaya, (2010).

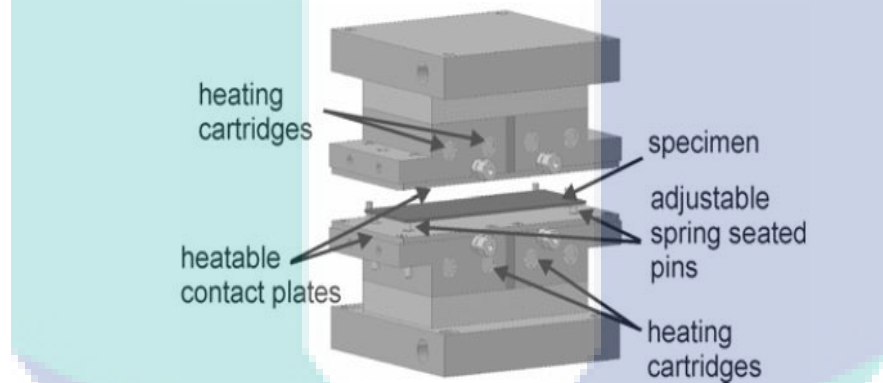


Figure 2.19 Schematic exposition of the quenching tool with integrated heating cartridges
Source: Merklein & Lechler, (2006).

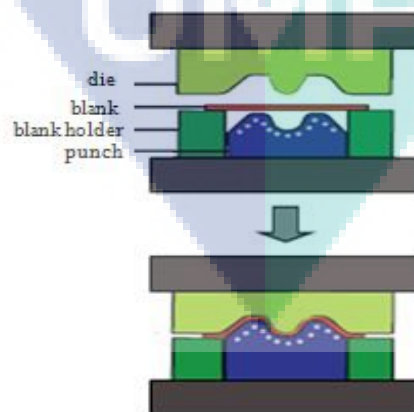


Figure 2.20 Schematic of a test hot stamping tool
Source: Hoffman et al., (2007).

The tool must be designed to cool efficiently in order to achieve maximum cooling rate and homogeneous temperature distribution of the hot stamped part. Therefore, the design of the tool is non-trivial as it must have cooling channels in the tool (Hu & Ying, 2017). Figure 2.21 shows, the cooling system with cooling ducts near to the tool contour is currently well known to be an efficient solution. However, the geometry of cooling ducts is restricted due to constraints in drilling. The cooling channel should be placed as near as possible for efficient cooling but sufficiently away from the tool contour to avoid any deformation in the tool during the hot forming process. All the generated solutions in the study were evaluated by optimum criteria such as efficient cooling rate and uniform cooling. It was found that the optimized profile of the channels for duct diameter is 8 mm (Hoffmann et al., 2007).

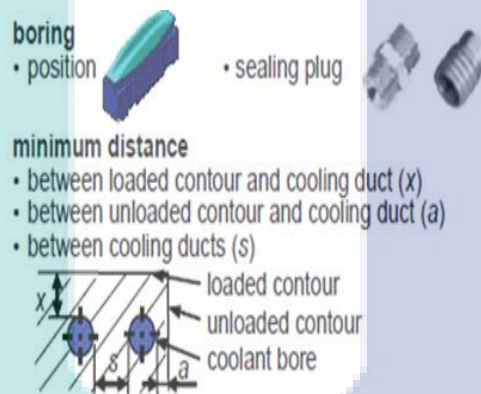


Figure 2.21 The constraints for optimizing cooling channel
Source: Hoffman et al. (2007).

2.5.4 Type of cooling channel

Cooling-channel configurations can be serial or parallel. Both configurations are illustrated in Figure 2.22. For parallel cooling channels, the flow is separate to the other channel, while for the serial, the flow moves in a single flow direction. Parallel cooling channels are drilled straight through. Due to the flow characteristics of the parallel design, the flow rate along various cooling channels were different. This depends on the flow resistance of each individual cooling channel. These varying flow rates in turn cause the heat transfer efficiency of the cooling channels to vary from one to another. As a result, cooling of the tool may not be uniform with a parallel cooling-channel configuration (Sositar Mold, 2011).

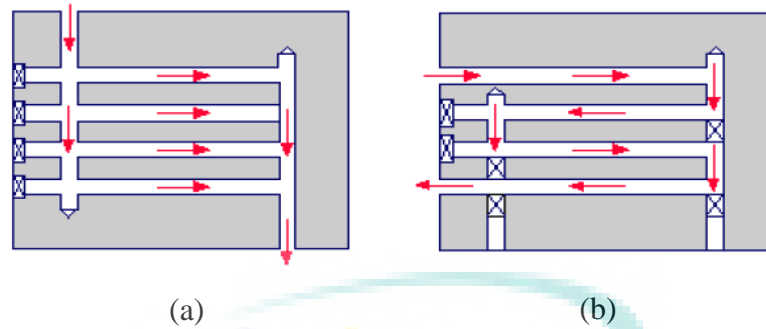


Figure 2.22 Cooling channel configuration (a) parallel cooling channel, and (b) serial cooling channel

Source: Sositar Mold, (2011)

Cooling channels connected in a single loop from the coolant inlet to its outlet are called serial cooling channels. This type of cooling-channel configuration is the most commonly recommended and used. By design, if the cooling channels are uniform in size, the coolant can maintain its (preferably) turbulent flow rate through its entire length. Turbulent flow enables heat to be transferred more effectively. Heat transfer of coolant flow discusses this more thoroughly (Sositar Mold, 2011). In this project the serial cooling channels are used, due to the channel can maintain the turbulent flow.

2.6 Die Design Optimization

Design of experiments (DOE) is a systematic, rigorous approach to engineering problem-solving that applies principles and techniques at the data collection stage to ensure the generation of valid, defensible, and supportable engineering conclusions. In addition, all of this is carried out under the constraint of a minimal expenditure of engineering runs, time, and money. There are four general engineering problem areas in which DOE may be applied, those are comparative, screening or characterising, modelling and optimizing. In the fourth case, the engineer is interested in determining optimal settings of the process factors; namely, to determine for each factor the level of the factor that optimises the process response. In this section, heuristic and taguchi method are presented.

2.6.1 Heuristic Method

Basically, heuristic methods are often resorted to solve real optimization (Martí & Reinelt, 2011). A heuristic method also called an approximation algorithm, an inexact procedure, or, simply, a heuristic. It is a well-defined set of steps for quickly

identifying a high-quality solution for a given problem, where a solution is a set of values for the problem unknowns and quality is defined by a stated evaluation metric or criterion (Barr et al., 1995). Beside that, heuristic also is used to specify the class problem from the decisions of some a priori knowledge (Coy et al., 2001). Barr et al., (1995), recommended an experimental step in order to systematically conduct the heuristic method as shown in Figure 2.23. Where is as the first step, a research experiment should have a purpose, stated clearly and defined prior to the actual testing. Then, in step 2 within a setup experiment there is a set of dependent variables such as the performance measures or results, that are affected by a set of independent variables. For the step 3, experiment design is the process of planning an experiment to ensure that the appropriate data is collected. Next, in step 4 data analysis refers to evaluating the recorded empirical data with statistical and nonstatistical techniques with respects to the experiment's purpose and goals. At this point, the requisite data should be available to test the hypotheses, verify assumptions, and measure variability. Lastly in step 5, the research need to thoroughly document the experimentation and all relevent factors, carefully analyze the resulting data, and present unbiased, supportable conclusions.

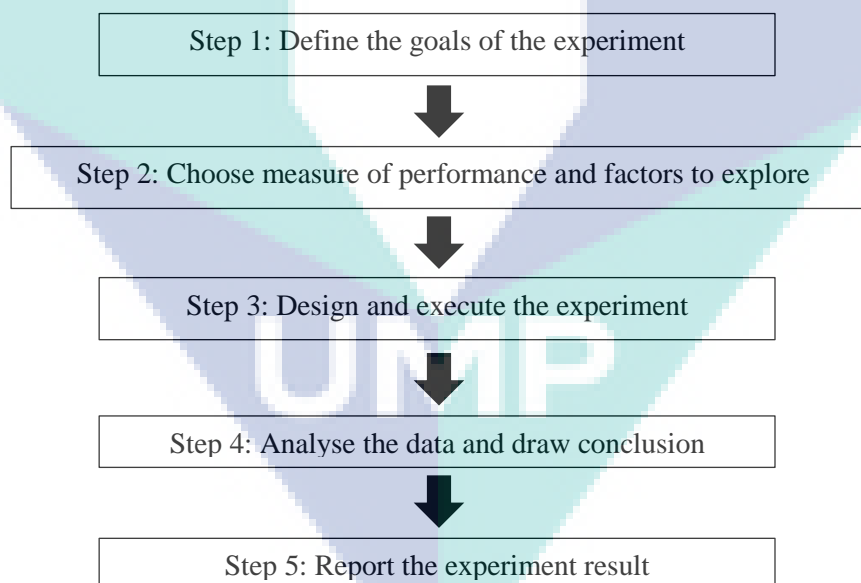


Figure 2.23 Experiment steps for Heuristic method

Source: Barr et al., (1995).

2.6.2 Taguchi Method

The Taguchi Method was proposed by Genichi Taguchi, a Japanese quality management consultant. The method explores the concept of quadratic quality loss function and employs a statistical measure of performance which is called the signal-to-noise (S/N) ratio. It provides a simple, efficient, and systematic approach to optimise the design for performance, quality, and cost (Roy, 2001). Taguchi is a part of the design of experiment (DOE) technique. There is a number of DOE that have been employed, screening DOE, characteristic DOE, Response surface method and Taguchi method. These techniques are divided into three main phase, which encompasses all experimentation, i.e. the planning phase, the conducting phase and finally the analysing phase (Roy, 2001).

The planning phase creates a standard orthogonal array (OA) for laying out of the experiment. Firstly, the number of factors and levels are defined, and it will use four factors, and three levels to represent the nine of trial number (L9) design. This design can reduce the total number of the experiments instead of the standard factorial design which uses 24 experiments (4 factor x 3 levels x 2 times). Then, the second phase is to conduct an experiment based on the suggestion of the total number of the experiment (Çakıroğlu & Acır, 2013).

The control factor that may contribute to the reduction of variation can be quickly identified by looking at the amount of variation present as the response. Taguchi has created a transformation of the repetition data to another value which is the response measure of the variation present. The transformation is the signal-to-noise ratio (S/N) (Canakci et al., 2013).

The Taguchi method was used to obtain optimum cooling channel design and the optimum parameters for the hot stamping process of a flat shape tool. Furthermore, the main effect analysis to utilised to ascertain the main effect factors. The two response results of the optimum cooling channel design were then analysed by the S/N ratio of the larger is better for cooling rate, and the smaller is better for von Mises stress value. Whilst for the optimum parameter for hot stamping process, the larger is better is used for the two response i.e. the tensile strength and the hardness value.

2.7 Summary

In order to achieve the tool with high cooling efficiency as well as having homogeneous temperature distribution throughout the tool, the heat transfer of the tool must be in perfect condition where, no temperature drops in the interface. This is called an ideal (perfect) thermal contact. So, to get an equivalent temperature, the tool must be design in a flat square shape with smooth surface, because the purpose of tool is for experimental heat transfer and not use for forming. The idea of these criteria was from the previous work of on heat transfer coefficient identification in hot stamping of high strength steels (Bosetti et al., 2010).

Another means of mitigating the present problem is by adding the cooling channel inside the tool. Main function of cooling channel is to dissipated heat from the tool as well as to control the tool temperature. Due to this, fluid is placed inside the tool, as the medium for cooling the tool. In addition, heat transfer coefficient can be determined by obtaining the velocity of fluid inside the cooling channel. The cooling system with cooling channel near to the tool contour is currently well known as an efficient solution. However, the cooling channel should be placed as near as possible for efficient cooling but sufficiently away from the tool contour to avoid any deformation in the tool during the hot forming process as reported by Hoffmann et al., (2007). All the generated solutions were evaluated by optimum criteria such as efficient cooling rate and uniform cooling.

The design criteria that need to be considered are the optimum diameter of cooling channels, the pitch between cooling channels and also the distance between cooling channel and loading surface. These criteria are required optimization in order to achieve the best hot stamping with higher cooling rate and low von Mises stress. Hoffmann et al., (2007) and Steinbeiss et al., (2007) employed Evolutionary Algorithm in their study. On the other hand, Jiang et al., (2012), Kumar et al., (2011), and Liu et al., (2013) optimised their results using numerical simulation. Conversely, Zhong-de et al., (2010) used theoretical analysis. From the literature survey, it was established that the heuristic method has yet been explored. Therefore this study employs this method to optimise the cooling channel parameters.

Due to the criteria discussed, the heat transfer experiment needs to be arranged to obtain the tool with high cooling efficiency as well as having homogeneous temperature distribution throughout the tool. Lin et al., (2014) and George et al., (2012) measured the heat transfer distribution of the tool by placing the thermocouple approximately 4 to 5 mm away from the loading counter. The experimental results obtained from the present study is compared with the FEA simulation results, to validate the FEA results. Namklang & Uthaisangsuk, (2016), validated their study by this method and acceptable agreement between was found between the experimental and FEA simulation results.

The mechanical properties, the tensile strength and hardness of the final product from the hot stamping process are examined. Naderi et al., (2011), Chang et al., (2011) and Wang & Lee, (2013) examined the effect of the heating temperature, heating time, thickness of the sample and the transfer time towards the strength and hardness of final product. In this study, the thickness of the sample, the heating temperature, and heating time is examined, while transfer time is fixed as the speed of the hydraulic press machine cannot be control.

CHAPTER 3

METHODOLOGY

3.1 Introduction

To achieve the aim and objectives of this project, there were several methods used. The sequence of the methods had been planned as shown in Figure 3.1 and has been applied for both type of product, which are flat test samples and U-shape bending. As for the first step, the samples were designed before starting the hot stamping process. The flat samples were cut by using wire cut, while for U-shape, was formed by using cold forming die. Hot stamping tool with cooling channel design was performed as to study the cooling performances in hot stamping tool. FEA was conducted as to obtain the heat transfer rate and von Mises stress (VMS). Heuristic and Taguchi method was used to optimize the cooling channel design. Then, hot stamping process experiment was conducted to get the temperature distribution of the blank product and tool. The result of the temperature distribution between FEA and experiment was expecting error less than 20 %. Lastly, tensile strength and hardness was measured to compare the initial strength of product with the final strength of the product. Next, the experimental and FEA, optimization results were presented and discussed in next chapter.

3.2 Material and Sample Preparations

Flat samples with tensile shape specification and U-shape part as a blank product were used. The flat samples are cut by using wire cut, while for U-shape, is formed by using cold forming die. The material used for the blank product was boron steel (22MnB5). Then, the hot stamping tool which is able to cover heat transfer distribution of the heated blank is being designed. The tool material used in this project is SKD61. Table 3.1 shows the mechanical properties of 22MnB5 and SKD61 steel at room temperature.

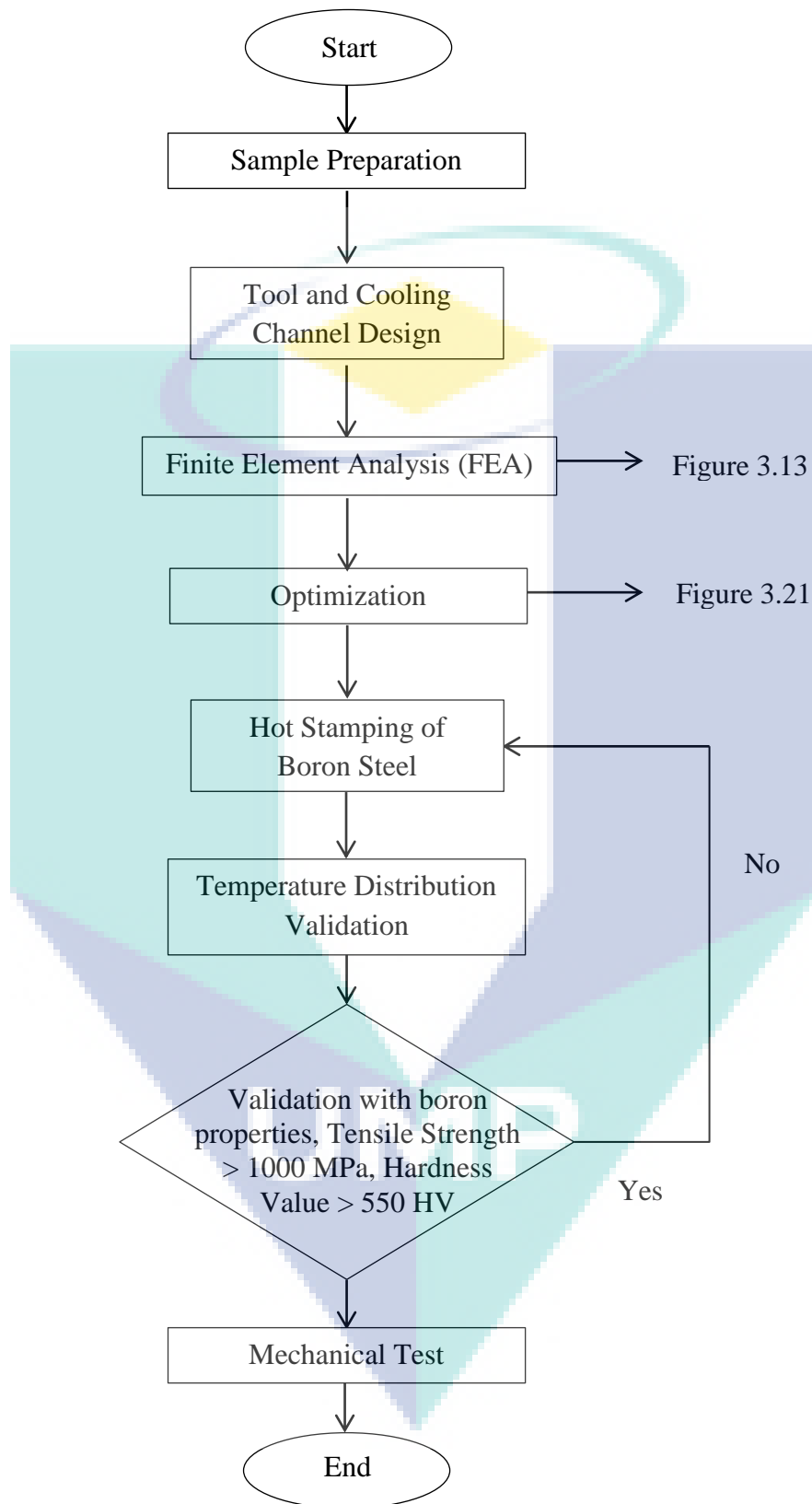


Figure 3.1 Research project flow chart

Table 3.1 Mechanical properties of 22MnB5 and SKD61 steel at room temperature

Mechanical properties	22MnB5	SKD61
Elastic Modulus (N/m ²)	212	200000
Poisson's Ratio	0.284	0.394
Mass Density (kg/m ³)	817	7700
Yield Strength (MPa)	505	550
Thermal Conductivity (W/m·K)	47.5	25

Source: Kumar et al. (2011) and Turetta (2008)

3.2.1 Flat Samples

An important factor that needs to consider in sheet metal forming is formability. The ability of the material to deform according to the specified geometry was determined by this factor. Thus, tensile test is one of the methods in mechanical testing that used to define formability. In the same time, this testing also derived some properties such as strength and strain hardening. Flat sample is cut into tensile test sample shape, E8M04 shown in Figure 3.2, where the G is the gage length, w is the width, L is the overall length, R is the radius fillet, b is the length of grip and C is the width of grip. Next, the samples will be stretched by using a universal testing machine. Then, the value of ultimate tensile strength will be recorded. In this project, the samples is cut from the raw material by using Sodick VZ 300L Edm wire cut, refer to Appendix A1. Figure 3.3 shows the process flow for the flat sample's fabrication.

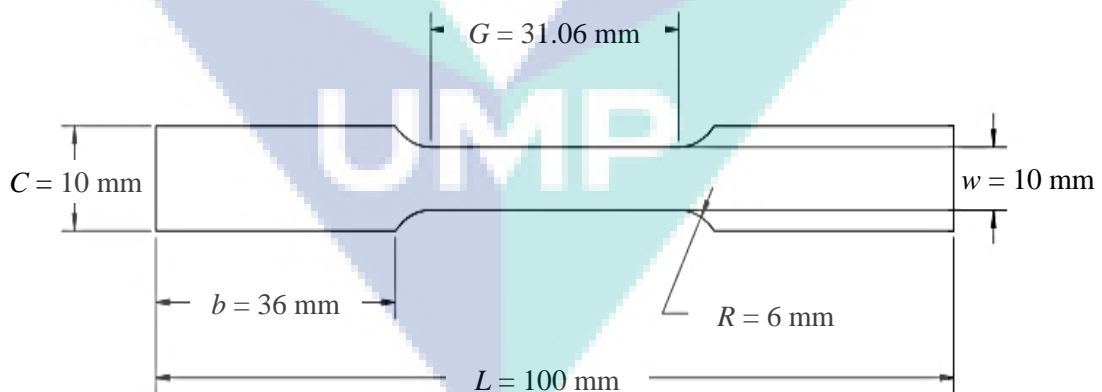


Figure 3.2 Flat sample, E8M04

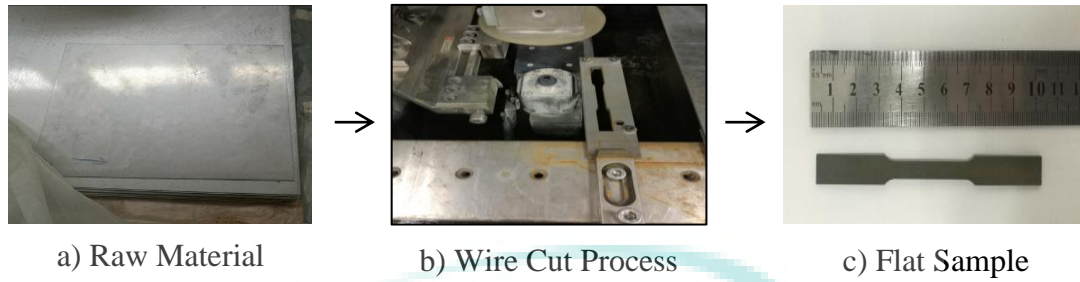
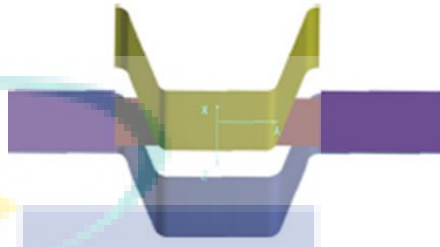
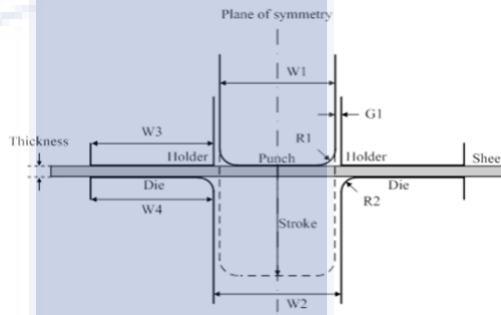
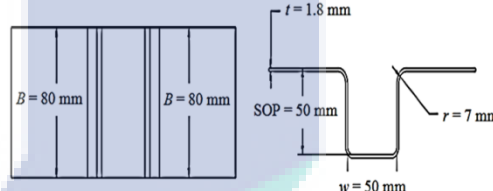


Figure 3.3 Process flow for flat sample fabrication

3.2.2 U-shape samples

A U-shaped sample geometry was chosen on the basis of the work of Hu et al. (2013) and Thanadngarn et al., (2013). Based on Hu et al. (2013), the blank size dimension used was 280 mm x 80 mm x 1.6 mm and the stroke of punch (SOP) is 51.6 mm. While Thanadngarn et al., (2013), the SOP used was 71.8 mm where the details of the dimension shown in Table 3.2. Therefore, in this research, the product was designed based on those details, with a different SOP length. This is because the higher the SOP length results to a higher length of spring used. Longer spring used caused shut height in cold die construction high as it not be able to fit into the desired machine. Thus, in order to minimize the length of spring, the SOP length of 50 mm was used on this product, and the dimension of the width of the part was 80 mm, which in accordance to Hu et al. (2013). As for the corner radius of this part, it was based on Thanadngarn et al., (2013). Whilst for the U-shape product design employed in this project was a combination of parameters from both researchers. In Table 3.2 shows the U-shape product for this project, where w is the width, r is the bending radius, B is the bending line length and t is the thickness of material. Next, in order to fabricate the U-shape samples, U-shape cold die need to be design and fabricated. Table 3.2 compares blank diameter, stroke punch (SOP) and schematic diagram of U-shape samples used in previous works and current study.

Table 3.2 Comparison on blank diameter, stroke of punch (SOP) and schematic diagram of U-shape samples used in previous works and current study

Author	Blank Size (mm)	Stroke of Punch (SOP) (mm)	Schematic Diagram
Hu et al. (2013)	280.0 x 80.0 x 1.6	51.6	
Thanadngarn et al. (2013)	360.0 x 30.0 x 1.2	71.8	
Current Work	250.0 x 80.0 x 1.8	50.0	



a) Raw Material



b) Cold Stamping Process



c) U-shape Sample

Figure 3.4 Process flow for U-shape samples fabrication

3.2.3 U-shape die

To design the U-shape die, the bending force needs to be calculated. The bending force can be estimated, if the outer moments of bending and the moments of the inner forces are equal, by assuming that, the process is one of a simple bending beam. Thus, the bending force is a function of the strength of the material, the length and thickness of the piece, and the die opening, in bending the sheet metal. Based on the U-shape, the bending line length, B is present at two locations, as shown in Table 3.2. B is determined to be 4 for the U-shape samples. The bending force may be computed through the following equation (Equation 3.1) (Misumi, 2015).

$$P = C/3 \times B \times t \times Ts \quad 3.1$$

Where, P represents the bending force (N), B is the bending line length (mm), t is the plate thickness (mm), and Ts is the tensile strength (MPa). As for C , it is the coefficient ranging from 1.0 to 2.0 (Boljanovic & Paquin, 2006). When the punch radius (R) and the radius of the die are small, larger coefficient will be used. Table 3.2 shows the parameters used for calculating the bending force. Hence, the value of bending force for the die is 244.6 kN.

While for the stripping force, the force used to form the material into U-shape was 10 % of the bending force, and the value of stripping force is 24.46 kN, based on Equation 3.2. In order to fit with die design, six springs were used as shown in the design. Thus, the stripping force should be divided by 6 to ensure that the spring able to withstand the force during the forming process (Lempco, 2000). Therefore, the type of spring that able to withstand the force needs to be identified.

$$Fs = 10\% \times P \quad 3.2$$

Besides that, the stiffness of the spring is 50 mm by following the length of stroke of punch (SOP) of the part design, as shown in Figure 3.5. In order to choose the suitable spring, Misumi catalog has been used as references, where this company is known in the die press area and is also available in Malaysia (Misumi, 2015).

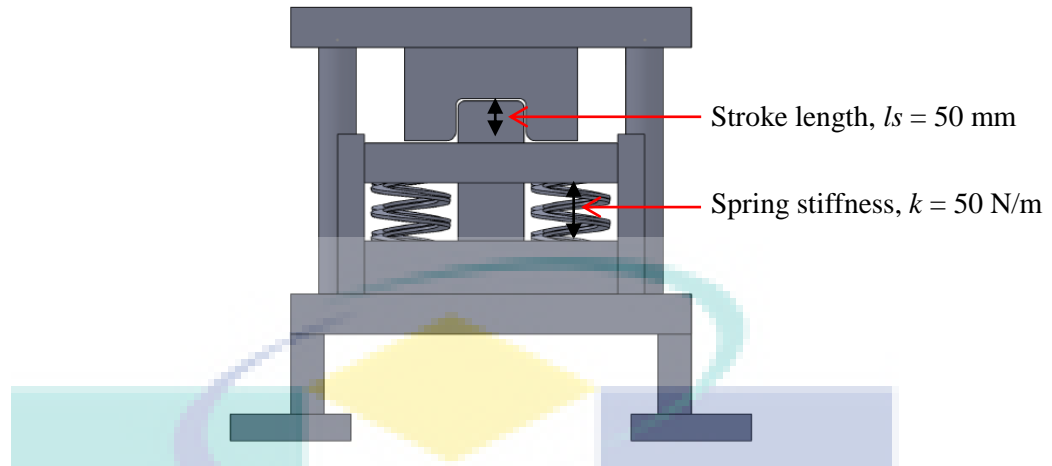


Figure 3.5 Die design during compression

After completing the calculation, the suitable spring selected from the Misumi catalog was SWM 50-200. The properties of this spring were; the load is 3920 N, while the stiffness was 50 N/m and the length of the spring was 200 mm. Figure 3.6 shows the complete die design for U-shape die.

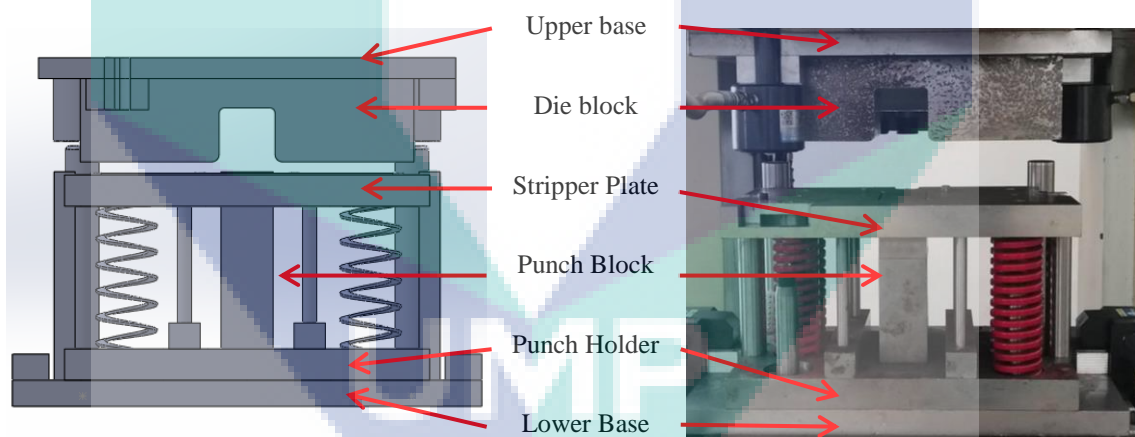


Figure 3.6 U-shape die design

3.3 Cooling Channel Design for Hot Stamping Tool

In order to study the cooling performance, the actual process of hot stamping in a laboratory scale experiment was replicated. The process was simplified into a simple compression of the flat samples and the U-shape samples in contact with the tool. To maintain the consistency and repeatability, the simplified process was designed to press

both samples in between the experimental tool without any permanent deformation of the samples. Without deformation, noise factors such as heat generated due to forming, sliding friction and imperfect contact due to thinning which may influence the black temperature are eliminated (Duncan & Panton, 1997). The tool size must cover the heat distribution of the blank. In order to suit the blank with the tool, the dimension of 140 mm x 70 mm x 40 mm for the flat tool upper and lower, as shown in Figure 3.7. Figure 3.8 details the dimension for the U-shape tool, i.e. 140 mm x 70 mm with stroke of punch (SOP) of 50 mm. Further discussion, it will be explained in the ensuing section with regards to the selected of cooling channel parameter.

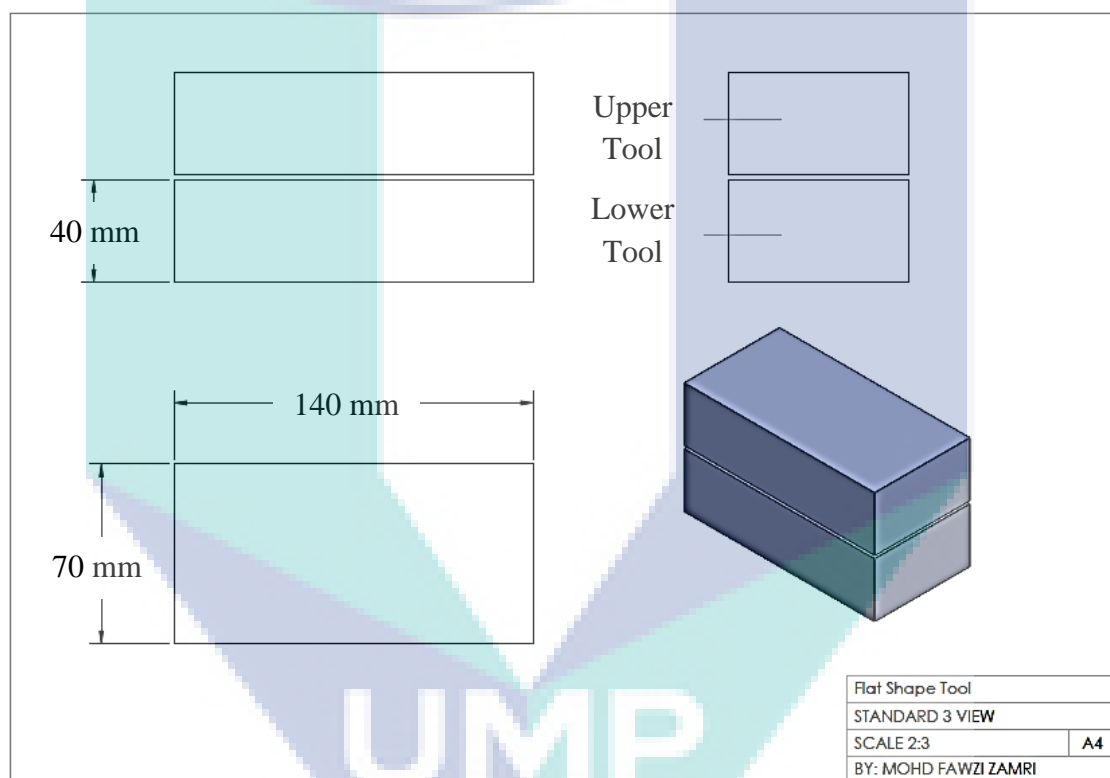


Figure 3.7 Hot stamping flat shape tool design

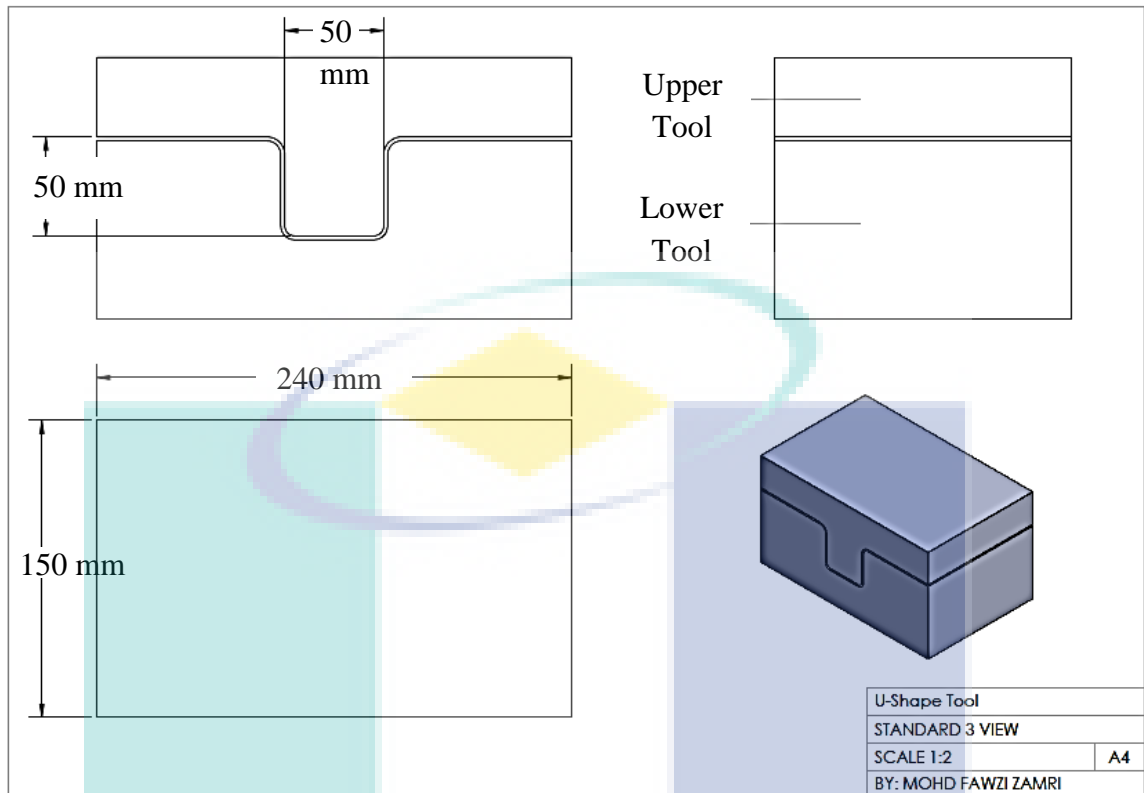


Figure 3.8 Hot stamping U-shape shape tool design

The 3D design of punch, die and blank product were modelled from the SolidWorks design software. Figure 3.9 and 3.10, shows the design of the hot stamping tool with cooling channel parameter that used in the simulation. The schematic model shows for both types of hot stamping tools, i.e. flat and U-shaped. The symbols of C_A , C_B , C_C and C_D represents the diameter of cooling channel (C_A), the pitch between cooling channel (C_B), distance cooling channel to tool surface (C_C) and distance cooling channel to wall tool (C_D). As for the parameter (C_A), the sizes of cooling channel were 6 mm, 8 mm, and 12 mm. The parameters chosen were based on the availability of the cooling hose by referring to (PME, 2004). Then, as for the parameters (C_B), (C_C) and (C_D) the dimensions were 6 mm, 8 mm, and 10 mm. Those parameters were taken from Hoffmann et al., (2007), Liu et al., (2013), and Lin et al., (2014) as the researchers have chosen 8 mm as their main parameter.

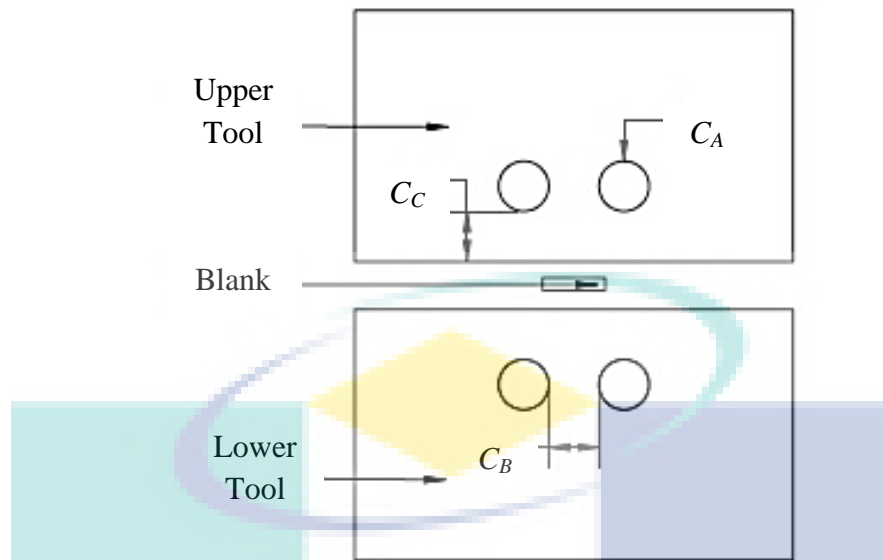


Figure 3.9 Flat hot stamping tool with cooling channel parameter

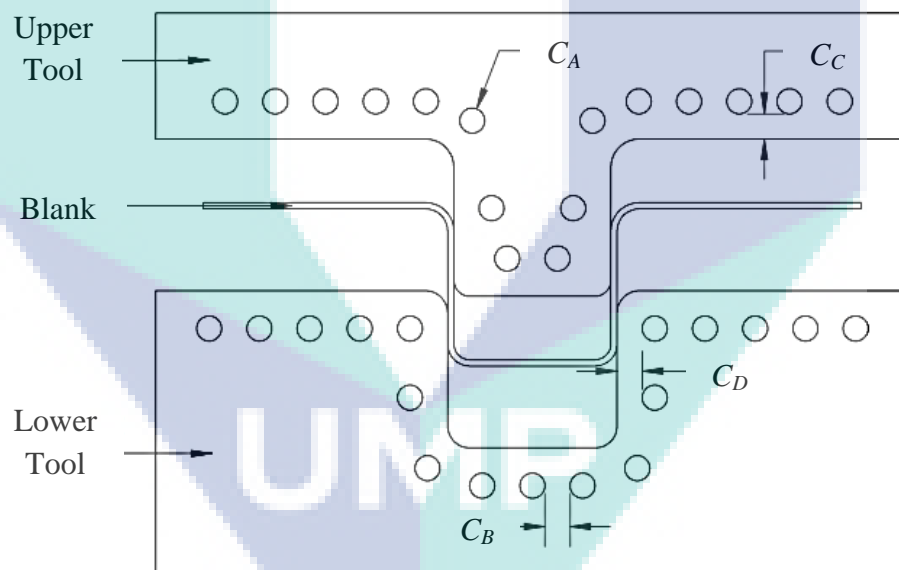


Figure 3.10 U-shape hot stamping tool with cooling channel parameter

3.4 Finite Element Analysis

Figure 3.11 shows, the flow chart of the FEA for analyzing the hot stamping tool. It begins by inserting the material data, namely, SKD61 and 22MnB5 for steel and the tool of the blank, respectively. Then, the model from SolidWorks was imported into the ANSYS software, and the constraints are defined. Suitable meshing technique was identified to reduce the percentage error of final results. The surface contact between blank and tool must be ensured (Tondini et al., 2011). FEA was simulated after all the parameters required are inputted. As the accuracy of the FEA was heavily dependent on the input parameters, therefore all the material properties, thermal properties and its temperature parameters such as thermal conductivity, specific heat and density were taken into account in the thermal analysis. These values were obtained from the literature (Lin et al., 2014), (Xiaoda et al., 2016), manufacturer catalogue (Assab, 2008) and others. Then, in order to select the optimum meshing type for FEA, meshing parameters such as coarse, medium and fine was done. The result with higher number of node and element, then, with lowest meshing and solution time was selected. Lastly, after the optimum result obtained from the meshing, thermal and static analysis was conducted.

In this analysis, the solid 3D model tool was assembled with the blank to observe the heat transfer for both parts. As for the first step of the analysis, the time taken to complete the analysis is set to be 10 s. Then, the thermal load was applied to the 3D model as the temperature of the blank was set as 900 °C and for the tool was 20 °C. Furthermore, the convection had been chosen as the heat transfer mechanism with a value of 4700 W/m²K (Hoffman et al., 2007). Next, connections advisor was selected, and contact set was chosen. Contact set function defines the contact between blank and tool. As for the thermal resistance value, it was set as 0.000213 m²K/W. After all the parameters were set, the mesh was run, and the analysis of results was obtained. This analysis was done to ensure that the tool obtained a high cooling efficiency with homogeneous temperature distribution. Thus, the dimension of the pitch between cooling channel and the diameter of the cooling channel were varied in the analysis. Mesh time taken for this analysis was only 10 s. This is because, in real industries, it takes only 8 to 10 s to press the small part.

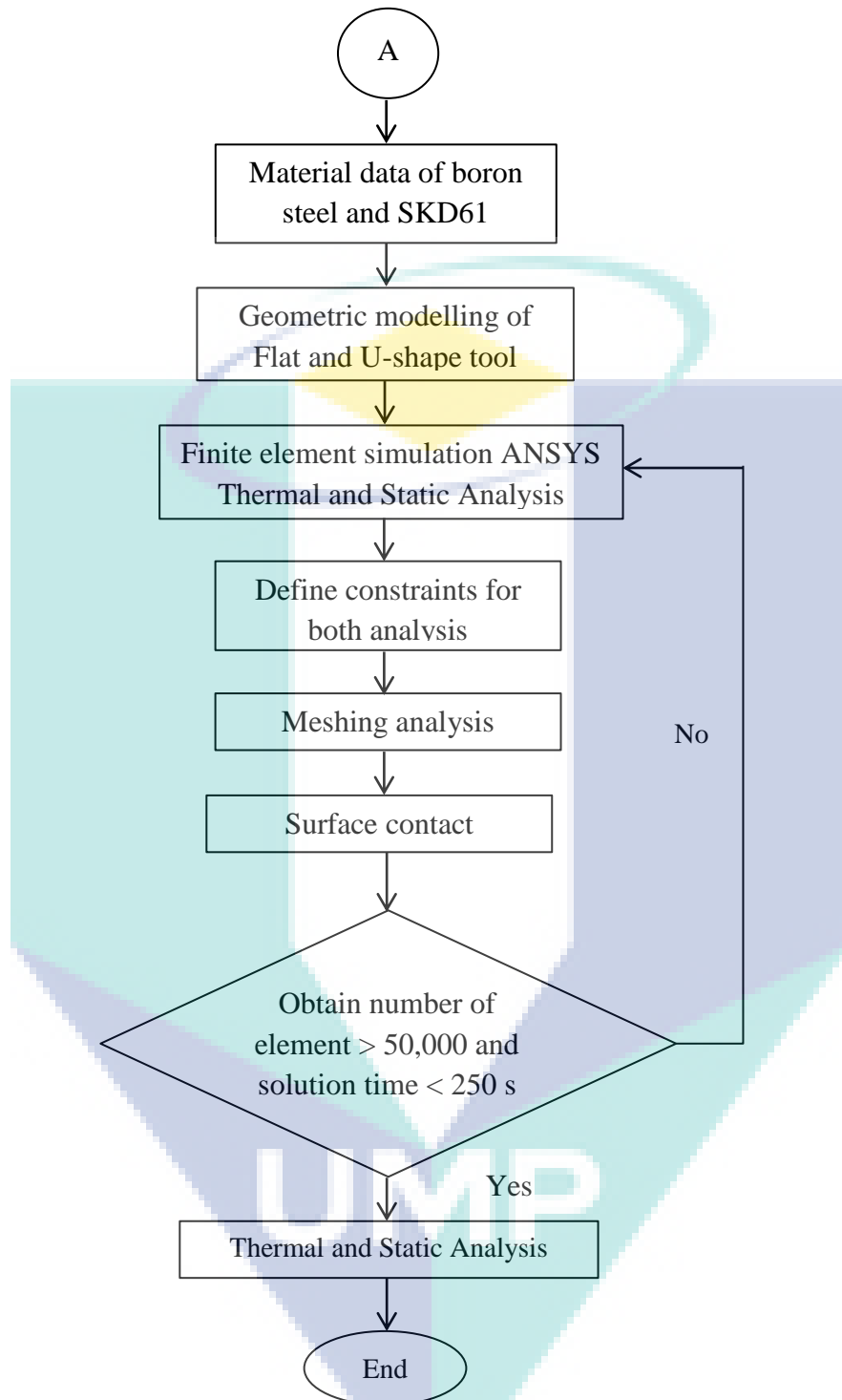


Figure 3.11 Flow chart of meshing in FEA of hot stamping

3.4.1 Material Data

The type of the materials used in this project were boron steel for the sheet metal and SKD61 for the tool component. As for the input material data, relevant engineering data with respect to thermal and static analysis were selected. For thermal analysis, the data needed were the mass density and thermal conductivity of tool and blank material, while for static analysis the data required were elastic modulus, poison's ratio, mass density and yield strength of the tool material. The data was used as an input into the menu of engineering in the ANSYS simulation software as boron steel and SKD61 were not available in the standard libraries of the software. These data were non-trivial as inaccurate data cause error to the output of the simulations.

3.4.2 Geometric Modelling

The model for this study was designed in SolidWork software. The FEA analysis, on the other hand, was performed via ANSYS simulation software. The working format for the aforementioned software were identical, i.e. SolidWorks saves the model in (.part) whilst FEA runs on (.igs) format. Therefore, the model developed via Solidworks were saved as (.igs) to allow the model to be imported in ANSYS prior to any FEA simulation works (Figure 3.12). The models imported were shown in Figure 3.13 and Figure 3.14, respectively. The effects of thermal and mechanical structural fields on the tool were completed by using ANSYS Workbench 15.0.

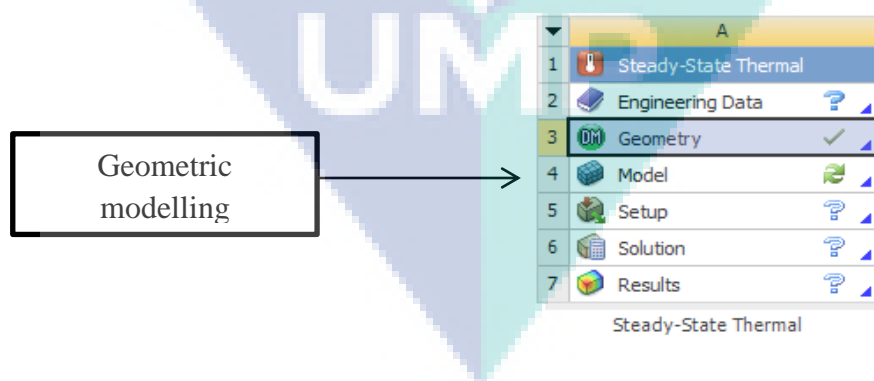


Figure 3.12 Toolbox of geometric modelling in ANSYS simulation software

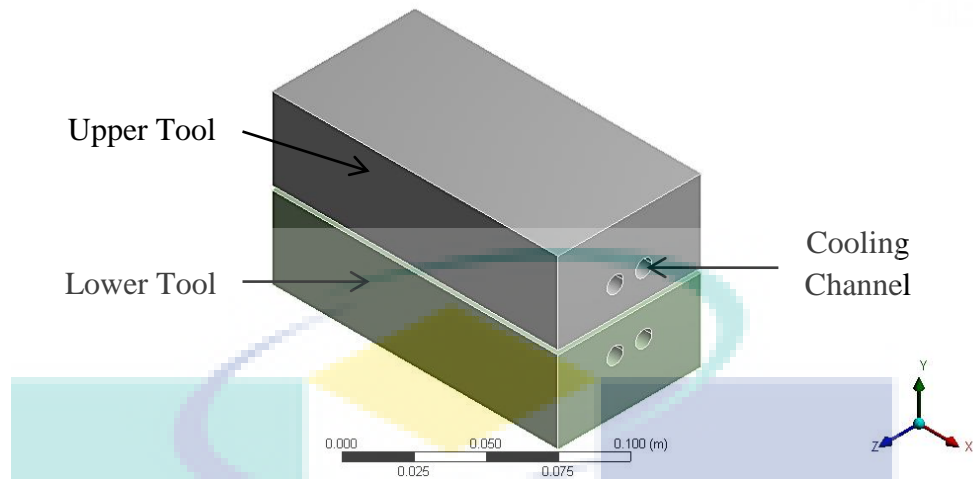


Figure 3.13 Flat hot stamping tool import on Ansys software

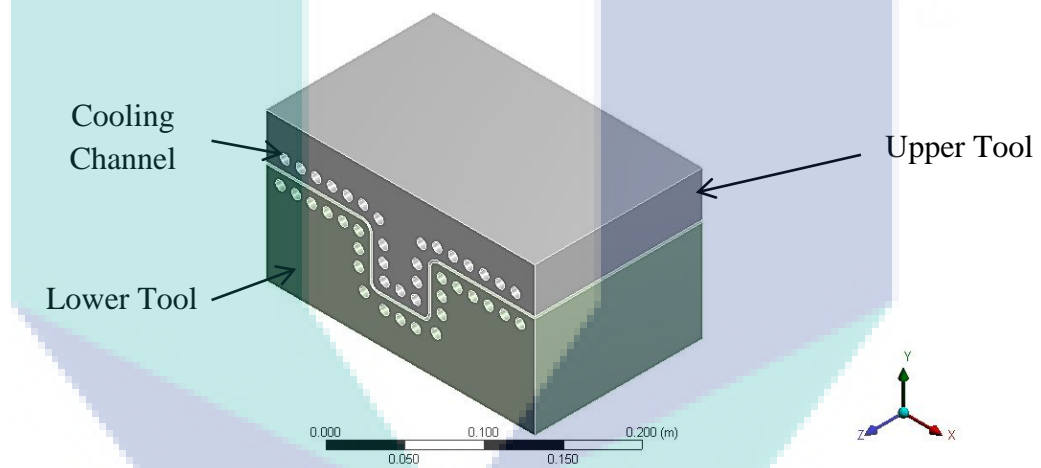


Figure 3.14 U-shape hot stamping tool import on Ansys software

3.4.3 Define Constraints

The boundary condition employed in the study are shown in Table 3.3. The data were taken from the simulation for analysis carried out by Hoffmann et al., (2007). The tool motion and deformation of the blank were not considered as this simulation was intended to evaluate the temperature distribution during quenching process. The blank was assumed to be in its initial homogeneous temperature (Maeno et al., 2014).

Table 3.3 Boundary condition for analysis

Parameters	Value
Thermal Contact Conductance ($\text{W/m}^2\text{°C}$)	2000
Initial Temperature of Sheet (°C)	850
Initial Temperature of Tool (°C)	20
Convection Surrounding ($\text{W/m}^2\text{°C}$)	10
Duration of Quenching Process (s)	10
Convection Cooling Channel ($\text{W/m}^2\text{°C}$)	4700

Source: (Hoffmann et al., 2007)

3.4.4 Meshing

ANSYS Meshing is a general-purpose, intelligent, automated high-performance product. It produces the most appropriate mesh for accurate, efficient multiphysics solutions. A mesh well suited for a specific analysis can be generated with a single mouse click for all parts in a model. Full controls over the options used to generate the mesh are available for the expert user who wants to fine-tune it. The power of parallel processing is automatically used to reduce the time taken for mesh generation (ANSYS, 2016). The ANSYS program can automatically mesh the model without specifying any mesh controls based on its default mesh. The meshing can be controlled by three means i.e. coarse, medium and fine which may vary the post processing results.

Local meshing controls were focussed on the cooling channel inside the hot stamping tool. This requires a fine mesh, as the cooling channel function was to control the strength and the cooling rate of the tool as well as to control the process. For a better analysis with a lower time consumption is therefore required. There were several types of local meshing controls such as method control, sizing control, contact sizing control, refinement control, mapped face meshing, match control, pinch control and inflation control.

Next, surface contact was happen when the heated blank with the hot stamping tool were been contact (Lv et al., 2016). In this analysis, the contact between blank and tool, was set as bonded. From literature review, the thermal contact conductance that gives the closest value to the experimental condition (Boron steel in contact with H13) is the thermal contact conductance (TCC) value between Boron steel and H11 Tool Steel. This is because, the thermal properties of H11 tool steel having the closest match with the SKD61 tool steel (Tondini et al., 2011). Then, the TCC value of $2000 \text{ W/m}^2\text{°C}$

was chosen. Figure 3.15 shows blank and the die were been position. Then the contact between the die and blank were happen and the temperature were been set up.

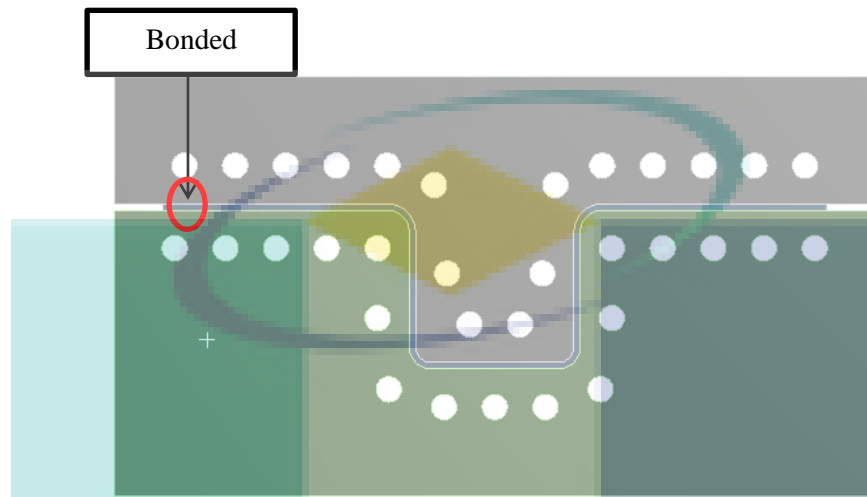


Figure 3.15 Thermal contact conductance between blank and die

Next, in this analysis, the refinement control and mapped face meshing were used to compare the quality of meshing element. This is primarily due to the suitability of the criteria in optimising the mesh quality of the cooling channel. This mesh quality criterion was measured by its “skewness”. Mesh skewness is one of the most important features that determines the quality of mesh. Apart from skewness, aspect ratio and mesh smoothness were also used to determine the quality. Skewness is basically defined on the geometrical orientation of a mesh. It is not defined "with respect to nearby meshes" as anticipated. It is measured as how much the generated mesh differs from the ideal mesh cell (Kumar & Visavale, 2013).

At this stage, the aforementioned thermal analysis carried out by the ANSYS software produce the results. These results will then be compared with using different geometric parameters that were used to design the cooling channel. The determination of the optimize cooling channel for the U-shaped model will be based on the parameters examined. Furthermore, the temperature distribution for this model was also investigated. FEA of the thermal analysis was compared to the actual experimental data. If the results are validated, the documentation and presentation stage are ensued. However, if the results are not acceptable, it must be reverted to the stage where the parameters are modified to satisfy the thermal analysis for hot press forming.

3.4.5 Thermal and Static Analysis

In this study, the combination of thermal analysis and static analysis were performed as shown in Figure 3.16. The thermal analysis was done to ensure the tool obtained high cooling efficiency with homogenous temperature distribution (Hoffmann et al., 2007). Static analysis, was conducted to ensure whether the ability of the tool able to withstand the pressure applied, apart from that the optimum distance between loading surfaces and cooling channel was also obtained. The results were then compared to the experiment data to ensure the validity of the results.

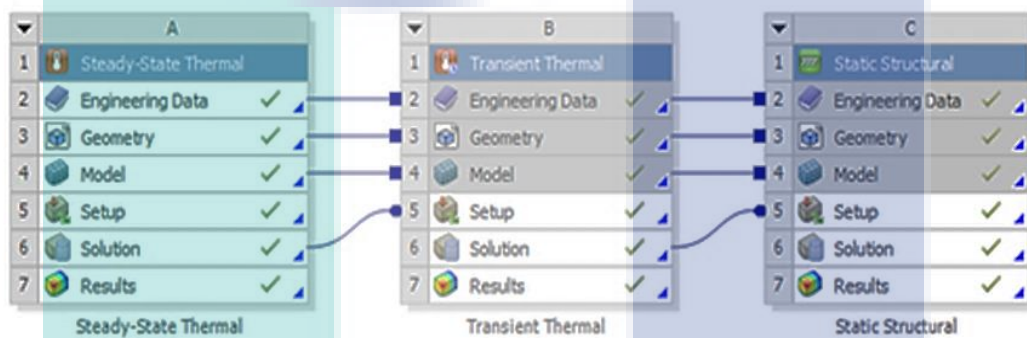


Figure 3.16 Setting interface of thermal and static analysis

The simulation begins with the steady state thermal analysis, in which the tool set to be in room temperature environment while the blank temperature in the austenitization temperature condition. The analysis time setting was set at 1 seconds, assuming that the hot stamping process has not started yet. As for the transient thermal analysis, the time was set for 10 seconds. The time considered was identical as the actual time of hot stamping process, by neglecting the punch motion. This was result in the cooling rate of the hot stamping tool. According to heat transfer rate given by Fourier' Law:

$$\dot{Q}_{conduction} = -kA \frac{dT}{dX} \quad 3.3$$

where k is thermal conductivity, A is the contact area and dT/dX is the temperature gradient.

$$\dot{Q}_{convection} = hA [T_f - T_s] \quad 3.4$$

where h is heat transfer coefficient, T_f is the surface temperature and T_s is represents the moving fluid temperature.

As for the static structural analysis, pressure was applied to get maximum von Mises stress values. According to hook's law:

$$F = [k]q \quad 3.5$$

where F is nodal vector factor, k is stiffness matrix and q is the nodal displacement vector. The parameters defined for the constraints, meshing, surface contact and static and thermal analysis are discussed in the subsequent section.

Next, FEA was used to define the optimized the cooling channel parameters. The thermal and static analysis were evaluated. In the static analysis, the value of the maximum von Mises stress (VMS) was measured; the value obtained must not exceed the yield strength of the tool material. As for the thermal analysis, the data on heat transfer of the tool was obtained. Consequently, the cooling rate for the tool can be determined. In order to acquire the rate of cooling, the following heat transfer formulas were used, (Equation 3.6, 3.7 and 3.8).

$$Q = \Delta U = mc_{avg} (T_2 - T_1) \quad 3.6$$

$$m = \rho v' \quad 3.7$$

where, m , c_{avg} , T , ρ and v' are the mass, the average specific heat evaluated at the average temperature, the temperature, the density and specific volume, respectively. Normally, the rate of heat transfer changes during the process with respect time. Thus, the rate of cooling for tool and blank can be determined by dividing the amount of heat transfer with a time interval (Cengal & Ghajar, 2011).

$$\dot{Q} = \frac{Q}{\Delta t}$$

3.8

Figure 3.17 (a) shows the region of the computed heat transfer rate. The example of the calculation is shown in the Appendix A3. While Figure 3.17 (b) shows the close-up scale of temperature and time range used for calculation in simulation. Time range between 3 to 6 s was chosen as it resulted in the best slope compare to other range of time. Besides that, the time range indicates where the material properties change from austenite to martensite. In hot stamping, material need to be in fully martensite as to achieve ultra high strength steel (Karbasian & Tekkaya, 2010).

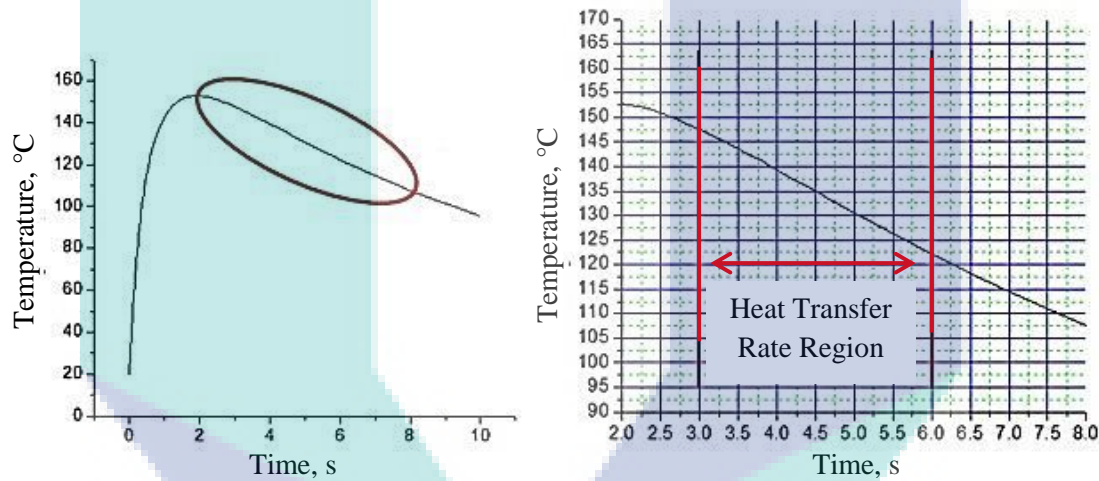


Figure 3.17 Thermal distribution in the hot stamping tool, (a) heat transfer distribution along 10 s, (b) close-up scale for heat transfer distribution

As been mention before, the static analysis was done to make sure whether the tool was able to withstand the pressure applied, apart from obtaining the optimum distance between loading surfaces and cooling channel (Lim et al., 2014). The exerted pressure in this experiment was 35 MPa. The maximum von Mises stress of the tool must not exceed the yield strength of the tool material. If the maximum von Mises stress in the tool is greater than the yield strength, the tool is failed. From this analysis, the fixed variable was the pitch between cooling channels which was 10 mm, whilst the manipulated variable was the distance between loading surface to the cooling channel with a different diameter of the cooling channel.

3.5 Cooling Channel Design Analysis

Figure 3.18 shows the flow in designing the cooling channel. In the flat tool section, the optimum cooling channel parameter from heuristic were compared with the optimum cooling channel from taguchi method. As result, the best parameter was chosen for fabrication and experiment was conducted for flat shape sample. Whilst for the U-shape sample, cooling channel optimisation using heuristic method was employed. Those result was evaluated based on the highest cooling rate and lower von Mises stress. Thus, the result obtained from the optimization were discussed briefly.

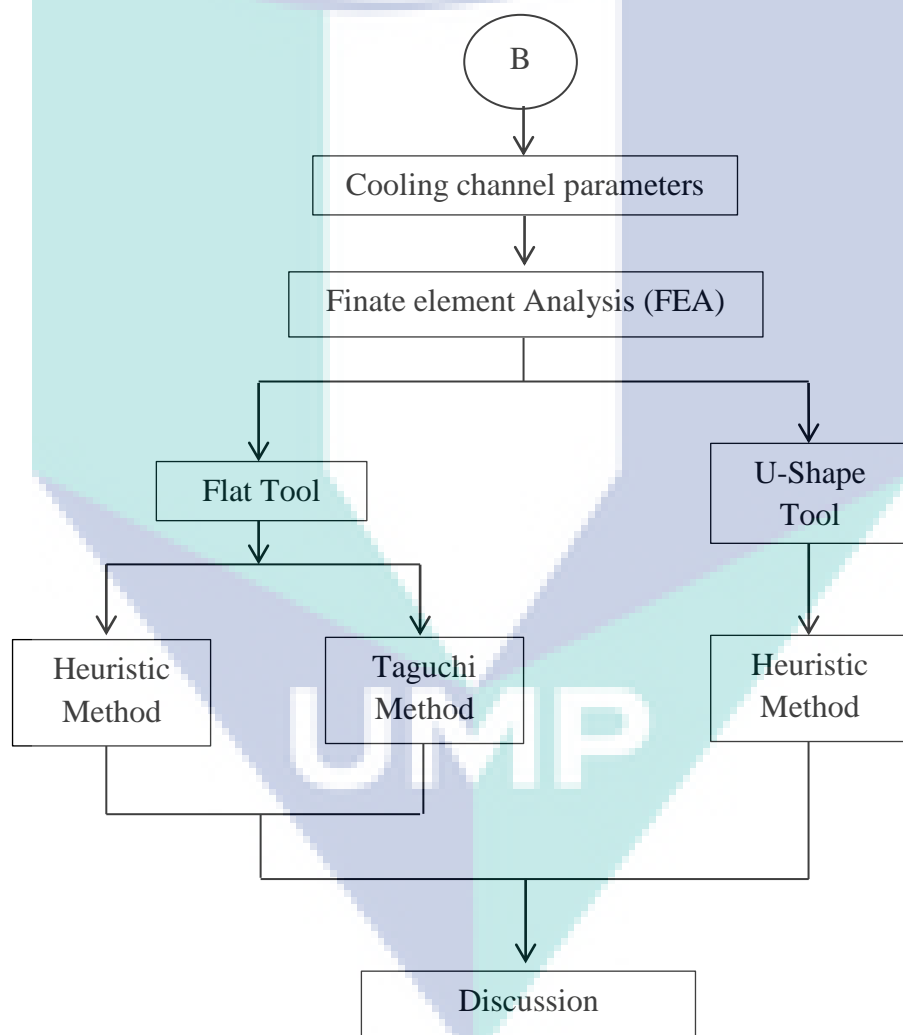


Figure 3.18 Sequence for cooling channel design analysis

3.5.1 Heuristic Method

Heuristic method used to optimise cooling channel parameters for hot stamping tool. The data were analyzed and recorded accordingly. The cooling channel optimization steps using Heuristic method is shown in Figure 3.19. On the basis of the works of Coy et al., (2001) and Díaz et al., (2016) the outputs of the parameters were determined to identify the best cooling channel parameters. The outputs considered were the highest cooling rate and lowest von Mises stress. As for this project, the parameter was selected and regrouped based on their criteria. As the first step to optimise the cooling channel parameter for flat shape, the parameter (C_A) 6 mm, 8 mm and 12 mm were chosen whilst fixing the parameters for (C_B) and (C_C) to be 8 mm. After the optimum parameter from (C_A) was selected, the parameter (C_B) is manipulated as (C_A) and (C_C) were fixed. Finally, parameter (C_C) was optimized as the (C_A) and (C_B) has been optimised. The steps were repeated for the U-shape tool cooling channel optimization, by considering an additional parameter (C_D). Table 3.4 shows the summary of the cooling channel parameters. Next, the input parameters were cooling channel design parameters while the output parameters were cooling rate and von Mises stress values. The output parameters were measured, until the input optimum parameter is obtained. Once the parameters were optimised for the hot stamping tool, the optimum parameter was validated, by conducting the hot stamping process experiment. The heat transfer distribution from the tool and blank were measured and analysed. Lastly, the data were recorded by comparing the heat transfer distribution of FEA with experimental.

Table 3.4 Heuristic approach for cooling channel parameter for flat and U-shape

Diameter of Cooling Channel, C_A	Pitch Between Cooling Channel, C_B	Distance Cooling Channel to Loading Surface, C_C	Distance Cooling Channel to Wall Tool, C_D
6 mm	6 mm	6 mm	6 mm
8 mm	8 mm	8 mm	8 mm
12 mm	10 mm	10 mm	10 mm

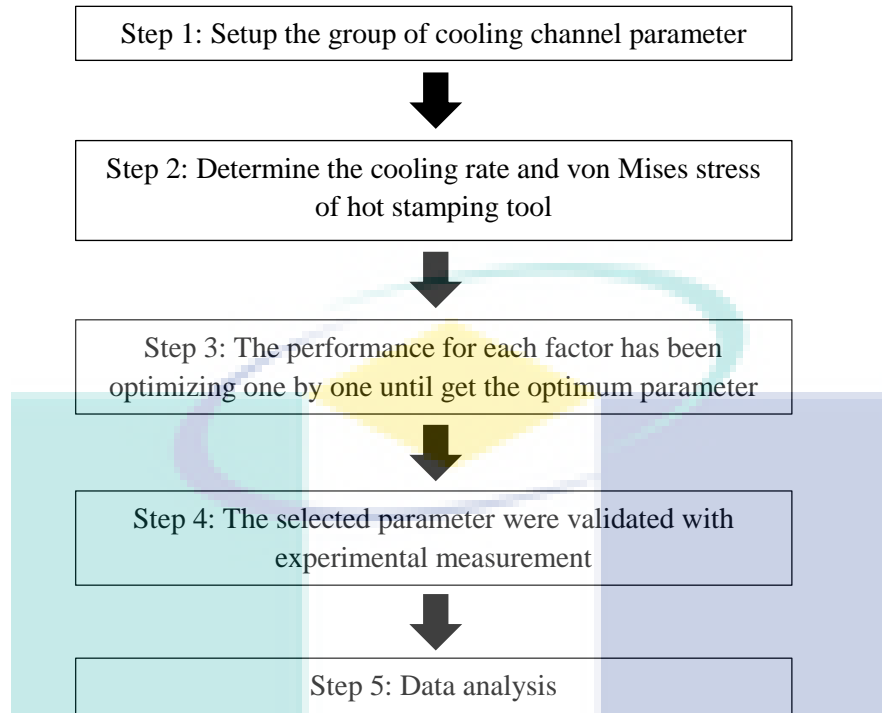


Figure 3.19 Cooling channel optimization steps using Heuristic method

3.5.2 Taguchi Method

Taguchi's design of experiment method was used in this project to evaluate the relative contribution of the cooling channel design towards the hot stamping tool. The main effect and Signal Noise Ratio (S/N Ratio) were employed to investigate the results, and the optimum parameters of the cooling channel can be established (Shahrom et al., 2013).

Table 3.5 lists the Taguchi test matrix for the tests to be performed on the tool structure that is able to withstand high forming load. Table 3.6 lists the tool cooling performance. To design the experiment matrix for three factors with three levels, the L9 orthogonal array (OA) was selected. The L9 array requires a minimum number of 9 test to investigate the hot stamping tool. The total should be known in two ways, namely using a table or MINITAB software (Yusoff et al., 2006). In this study, the factors that contribute towards the hot stamping tool are the diameter of cooling channel, the pitch between cooling channel and the distance cooling channel to loading surface (Zhang et al., 2010). Those factors results in the maximum VMS and cooling rate of the hot stamping tool.

Table 3.5 Factor and Level Description for flat shape cooling channel parameter

Factor	Factor Description	Level 1	Level 2	Level 3
C_A	Diameter of Cooling Channel (mm)	6	8	12
C_B	Pitch Between Cooling Channel (mm)	6	8	10
C_C	Distance Between Cooling Channel to Loading Surface (mm)	6	8	10

Table 3.6 L9 Test matrix for Flat shape cooling channel parameters

No. Simulation	Factor		
	C_A	C_B	C_C
1	6	6	6
2	6	8	8
3	6	10	10
4	8	6	8
5	8	8	10
6	8	10	6
7	12	6	10
8	12	8	6
9	12	10	8

Signal Noise Ratio (S/N Ratio) is the ratio between signals to noise. Signal is a desire value and noise related to undesire during the simulation process. The maximum VMS and cooling rate respond or variable respond were desired value and the other effect such as quantity of cooling channel, size of hot stamping tool and others were undesired value or noise. Basically there have three categories of S/N ratio, such as nominated as the better (Equation 3.9), smaller is better (Equation 3.10) and larger is better (Equation 3.11) (Shahrom et al., 2013). In this project, a smaller is better used for respond maximum VMS and larger is better for cooling rate.

Nominal is better

$$\frac{S}{N} = -10 \log_{10} \left[\sum_{i=1}^n \frac{1}{y_i^2} \right] \quad 3.9$$

Smaller is better

$$\frac{S}{N} = -10 \log_{10} \left[\sum_{i=1}^n y_i^2 \right] \quad 3.10$$

Larger is better

$$\frac{S}{N} = -10\log_{10}[\sigma^2] \quad 3.11$$

Where n is number of test and y_i is average of result.

3.6 Hot stamping of 22MnB5 steel

Researchers (Hoffmann et al., 2007), (Naganathan & Penter, 2012), (Karbasian & Tekkaya, 2010), had elaborated on the process of hot press forming. The blank is heated approximately from 850 °C to 950 °C and then placed on the water-cooled die. The cooling channel has a convection of 4700 W/m²°C with a temperature of 20 °C. This chill water aids to cool down the die and to allow the quenching process to transpire. After obtaining the optimum cooling channel parameter from the FE analysis, the tool design was finalised prior to the experiment. Two types of experiment were conducted in this study were flow rate and heat transfer experiment. The flow rate experiment was carried out to determine the velocity of the fluid inside the cooling channel, to ascertain the value of the heat transfer coefficient (Naganathan & Penter, 2012). The heat transfer experiment, on the other hand, was performed to determine the rate of cooling rate of the tool. As for fabrication, there are several types of machine have been used to fabricate the dies and tools for hot stamping. Beside using machines such as milling and turning on the fabrication site, mechanical press machine and mini hydraulic press, were used in conducting the hot stamping process experiment. Table 3.7 and 3.8 shows the specification of both machines.

Table 3.7 Mechanical press, OCP 80 specification

Parameter	Value
Tonnage Capacity (Tonne)	80
Die height (mm)	330
Stroke (mm)	150
Slide area (mm)	560 x 460

Table 3.8 Mini hydraulic press machine specification

Parameter	Value
Capacity (Tonne)	10
Bore diameter size (mm)	80
Rod diameter size (mm)	40
Stroke length (mm)	200

3.6.1 Flow rate experimental

In this experiment, convection had been chosen as the heat transfer mechanism. Convection is the mode of energy transfer between a solid surface and the adjacent liquid or gas that is in motion (Cengal & Ghajar, 2011). This involves the combined effects of conduction and fluid motion. The faster the fluid motion, the greater the convection heat transfers.

First, the water was circulated into the water tank, until there is no air bubble present in the tube. The tube was taken out from the water tank and placed it into the volumetric flask to measure the volume flow rate (Melissa, 2012). The volume flow rate filled in the volumetric flask is recorded until the water filled up to 1.5 litre. Table 3.9 shows the lists the results of the water flow rate of the hot stamping process experiment.

Table 3.9 Water flow rate for hot stamping process experiment

Volume of water (l)	Time (s)			Average Time (t)	Volume flow rate, \dot{v} (l/s)	Volume flow rate, \dot{v} (m^3/s)
	1	2	3			
1.5	23.19	23.50	23.34	23.34	64.267×10^{-3}	64.267×10^{-6}

To compute the heat transfer coefficient, volume flow rate, \dot{v} is required. In this experiment, the volume flow rate is used to determine the velocity of fluid flow to obtain the Reynolds Number, Re . The volume flow rate is the volume of the fluid flowing through a pipe or duct per unit time which may be determined based on the flow rate experiment. The calculation involved in order to determine the volume flow rate is:

$$\dot{v} = VA \quad 3.12$$

where, V is the average fluid velocity in the flow direction, and A is the cross-sectional area of the pipe or duct.

Re is defined as the flow regime that is a function of the ratio of the inertia forces to the viscous forces in the fluid (Cengal & Ghajar, 2011). Re is determined in this experiment to get the Nusselt Number, Nu which is used to compute the heat transfer coefficient. The formula of Re and Nu are given as follow:

$$Re = VL/\nu \quad 3.13$$

where V is the upstream velocity, L is the characteristic length of the geometry, and $\nu = \mu/\rho$ is the kinematic viscosity of the fluid. If the value of Re that flows in smooth tubes > 10000 , the flow is often turbulent.

$$Nu = hD/k = 0.023Re^{0.8}Pr^n \quad 3.14$$

where h is the heat transfer coefficient, D is the diameter cooling channel, k is the thermal conductivity and Pr is the Prandtl Number. If the fluid flowing through the cooling channel for heating, $n = 0.4$ and for cooling, $n = 0.3$. Thus, the heat transfer coefficient can be obtained by using Nusselt number formula (Pitts & Sissom, 1998). Appendix A2 shows the detail calculation for the heat transfer coefficient.

3.6.2 Heat transfer experiment

Taguchi method was used to determine the optimum parameters for the hot stamping process. Parameters such as cooling flow rate, heating temperature, pressure and holding time were used to obtain the optimum parameters in the hot stamping process. As for the cooling rate, the value was fixed by according to the power of motor water pump used. As for the thickness of material, the thickness were 1.8 mm, 2.0 mm and 3.0 mm, respectively. The temperature ranges between 800 °C to 900 °C with an interval of 50 °C and for the heating time during stamping is 4 to 8 s with an interval of 2 s. Table 3.10 shows the factor and level description of hot stamping process for Taguchi method while Table 3.11 shows the L9 Test Matrix for hot stamping process for flat shape. From the experiment, the optimum parameter for hot stamping process obtained for the flat shape was applied again in the U-shape experiment.

Table 3.10 Factor and level description of hot stamping process for Taguchi method

Factor	Factor Description	Level 1	Level 2	Level 3
t	Thickness of material, (mm)	1.8	2	3
T_h	Heating temperature, (°C)	800	850	900
t_m	Heating Time, (s)	4	6	8

Table 3.11 L9 Test Matrix hot stamping process for flat shape

No. Experiment	Factor		
	t	T_h	t_m
1	1.8	800	4
2	1.8	850	6
3	1.8	900	8
4	2	800	6
5	2	850	8
6	2	900	4
7	3	800	8
8	3	850	4
9	3	900	6

Figure 3.20 shows the schematic of experimental setup for hot stamping tool. Furnace used to heat up the boron steel blank to the austenization temperature while the chiller was used to cool down the hot stamping tool and maintain the initial tool temperature at 18 °C in every experiment done. As to quench boron steel sample, hot stamping tool was used. The hydraulic press machine was used to apply the pressure to the hot stamping tool.

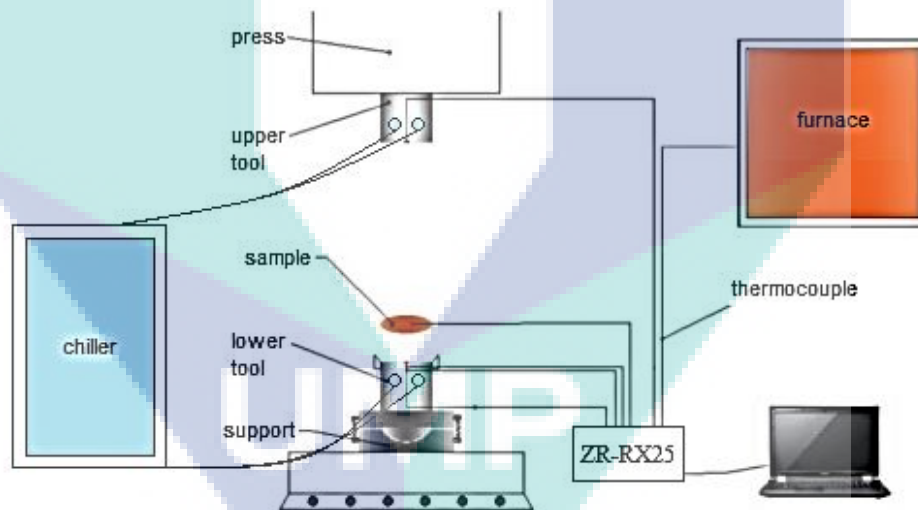


Figure 3.20 Schematic of experimental setup for hot stamping tool

The details of the heat transfer experiment performed were explained in this subsection. Prior the hot stamping experiment, the blank was heated to the temperature 800 °C, 850 °C, and 900 °C inside the furnace. The heated blank, must then be transferred quickly to the tool as to avoid heat lost before pressing process begins. Then, the blank was stamped on the tool with a pressure of 20 MPa by using mini hydraulic press machine. During the stamping process, the heat transfer was examined.

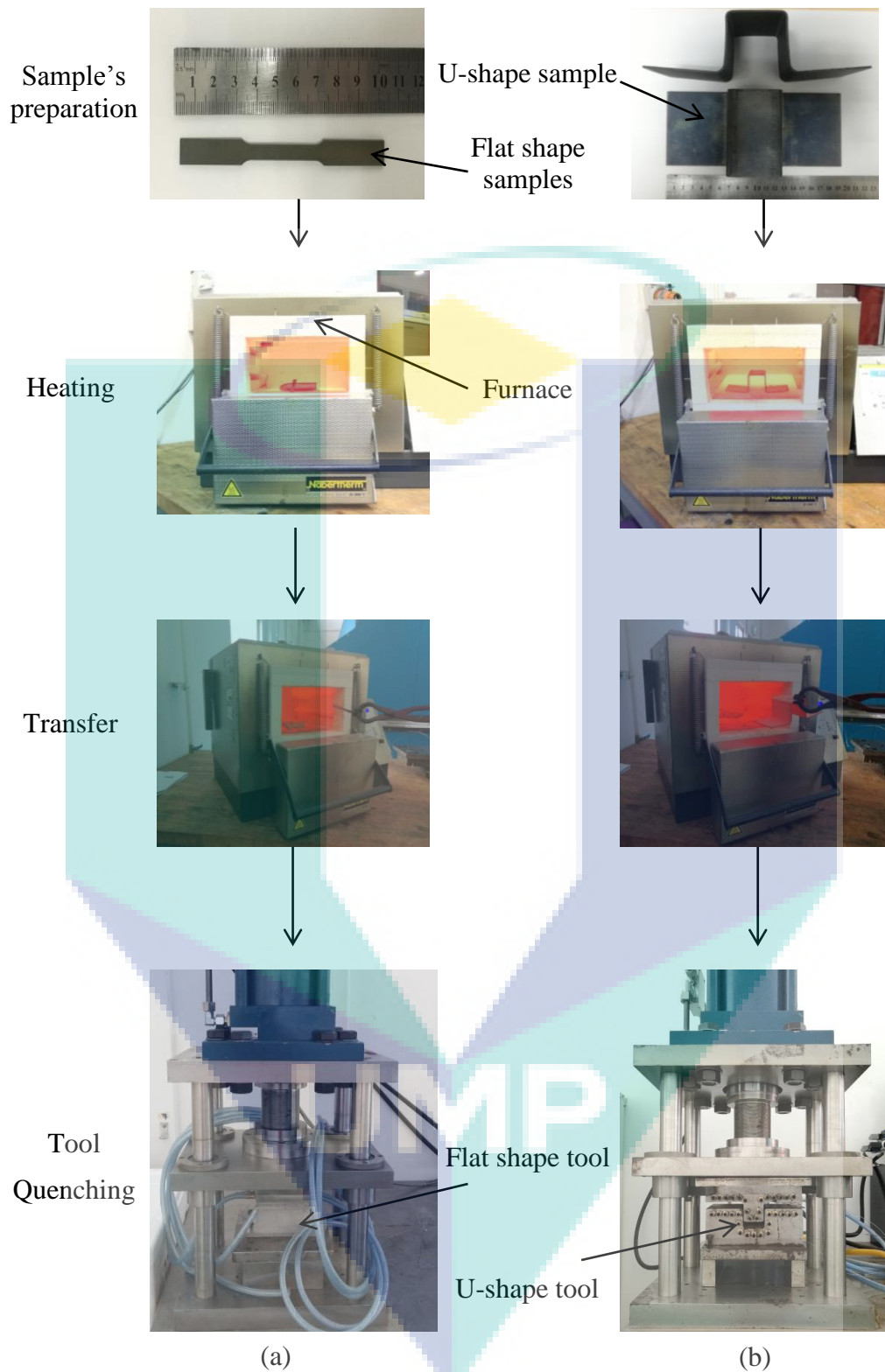


Figure 3.21 Hot stamping process flow for (a) Flat shape; (b) U-shape sample

The temperature of the blank and the tool were recorded by means of a thermocouple. The results were then compared with the simulation result. Figure 3.21 shows the flow of the hot stamping process for flat tool and U-shape tool. Next, the hot stamping product will be measured and analysed by conducting the tensile test and the hardness measurement.

The thermocouple was placed inside the tool to measure its temperature as shown in the Figure 3.25. The function of the thermocouple in this experiment is to record temperature during hot stamping process. Lin et al., (2014) and George et al., (2012) measured the heat transfer distribution of the tool by placing the thermocouple approximately 4 to 5 mm away from the loading counter. Then, the data of temperature was collected by using a data logger. The data logger used in this experiment was ZR – RX25 Data Logger which is designed to measure a wide range of temperatures using any thermocouple that has a miniature size thermocouple connector. Besides, this data logger has the low conversion time as 10 temperature measurements can be taken for every second. The location of thermocouple need to be change based on other reseacher work. since the value of the temperature distribution enable to capture. The optimum location to capture the tool temperature is 0.05 mm away for the loading counter (Figure 3.25), due to the 4 to 5 mm range enable to capture the desired temperature distributon.



Figure 3.22 Thermocouple location for (a) flat shaped tool, (b) u-shaped tool

After the result was obtained, the rate of cooling for the tool need to be determined in order to get the minimum time required for the tools to cool down from a high temperature. This was to ensure the flat and U-shape tool has a high cooling efficiency.

3.6.3 Tensile Test Measurement by Universal Tensile Machine

The samples was clamped using the upper and lower jaw of the Universal Tensile Machine, (UTM). Table 3.12 lists the specification for UTM machine. The process was stopped when it reached the required strain value. The raw results are in the form of force versus elongation. It covers from the elastic phase to the plastic phase until the samples fractures. Then data then was processed to generate the true stress versus true strain curve.

Table 3.12 Universal Tensile Machine Specification

Capacity	3369
Load Capacity (kN)	50
Maximum Speed (mm/min)	500
Minimum Speed (mm/min)	0.005
Maximum Force at Full Speed (mm/min)	25
Maximum Force at Full Load (mm/min)	250
Return Speed (mm)	500
Total Crosshead Travel (mm)	1122
Total Vertical Test Space (mm)	1193
Space Between Columns (mm)	420
Height (mm)	1582
Width (mm)	756
Depth (mm)	707
Weight with Typical Load Cell (kg)	141
Maximum Power Requirement	700

3.6.4 Hardness Measurement by Vickers Microhardness Machine

Once the tensile test had been performed, the sample was then cut into small pieces to measure the hardness measurement (Figure 3.30). Table 3.13 lists the specification of the Vickers hardness machine. Next, the mounting process was followed, where the mixture between 10 ml of resin and 20 ml of powder. The mixture was held for approximately 2 to 3 minutes after the mixture was poured into reference sample case. The sample was then subjected to the grinding and polishing processes. An 800-grade grain size of sand paper and liquid of diamond were used to polish the sample. The hardness value was measured by using microhardness, hardness readings measured with a test force 0.5 N and diamond shapes for the reference sample using the Vickers hardness tester machine.

Table 3.13 Wilson Vickers 402 MVD specifications

Parameter	Capacity
Hardness scale	Vickers and Knoop
Test load (kN)	10-2000
Dwell time (s)	5-99
Eyepiece magnification	10x
Maximum specimen height (mm)	85
x-y stage dimension (mm)	100 x 100
x-y stage travel range (mm)	25 x 25
Minimum reading (mm)	0.01
Operating temperature (°C)	10 – 38
Machine dimension (mm)	513 x 320 x 470
Weight (mm)	36
Power supply (VAC)	110-220

3.7 Summary

This chapter outlines the design process and analysis for this research of hot stamping process in order to achieve the objectives. This research start with the preparations of material and sample of flat and U-shape that had been explained in Section 3.2. Next, in Section 3.3, the design of cooling channel for hot stamping was explained. Finite element analysis (FEA) was conducted in Section 3.4 which involve in obtaining the material data, geometric modelling, meshing and thermal and static analysis. In Section 3.5, cooling channel design analysis was conducted by using Taguchi and Heuristic method. Lastly, the experiment of hot stamping using boron steel was conducted involving flow rate experiment, heat transfer experiment, tensile test measurement by Universal Tensile machine and hard measurement by using Vickers Microhardness Machine.

CHAPTER 4

RESULTS AND DISCUSSION

4.1 Introduction

This chapter explains in details on the results, analysis, and discussions based on chapter 3 methodology. Firstly, it started with the finding of the optimum FEA method including the meshes of different relevance center and mesh quality criteria. The result with higher number of node and element, then, with lowest meshing and solution time was selected. Next, thermal and static analysis of cooling channel design was conducted for both flat and U-shape sample. Then, those results had been optimized by using heuristic method and compared with taguchi method for flat sample. The experiment validation of hot stamped boron steel for heat transfer distribution and mechanical testing were done, based on optimum cooling channel parameter from the optimization method. The data and findings collected throughout the project were discussed.

4.2 Finite Element Analysis

4.2.1 Meshing

In order to have a fair comparison between the mesh sizes of different relevance center, it is essential to maintain the simulation parameters. This was applied on the part body and blank for the hot stamping simulation. Figure 4.1 shows the FEA simulation of three different mesh size application on flat tool. Figure 4.2 shows the FEA simulation of U-shape tool used in this study. Both figures show the differences between coarse, medium and fine mesh size. Table 4.1 and Table 4.2 summarised the results for meshing model. It illustrates the number of nodes, elements, meshing time and solution time for each meshing type. Table 4.1 tabulates difference in the number of nodes and elements for each mesh control for the flat tool. This can be clearly seen in

Figure 4.1 where fine meshing was employed. This type of mesh was used at the cooling channel and the flat tool. It is observed that the meshing time and the solution time does not vary much. Table 4.2, on the other hand, tabulates the number of nodes and elements for each mesh control for the U-shape tool. Figure 4.2 illustrates the full fine mesh employed for this particular tool. It is apparent that the meshing time, as well as the simulation time, varies significantly between the type of meshes. Therefore in this study, the medium sized mesh was utilised as it provides reasonable accuracy with a bearable computational burden.

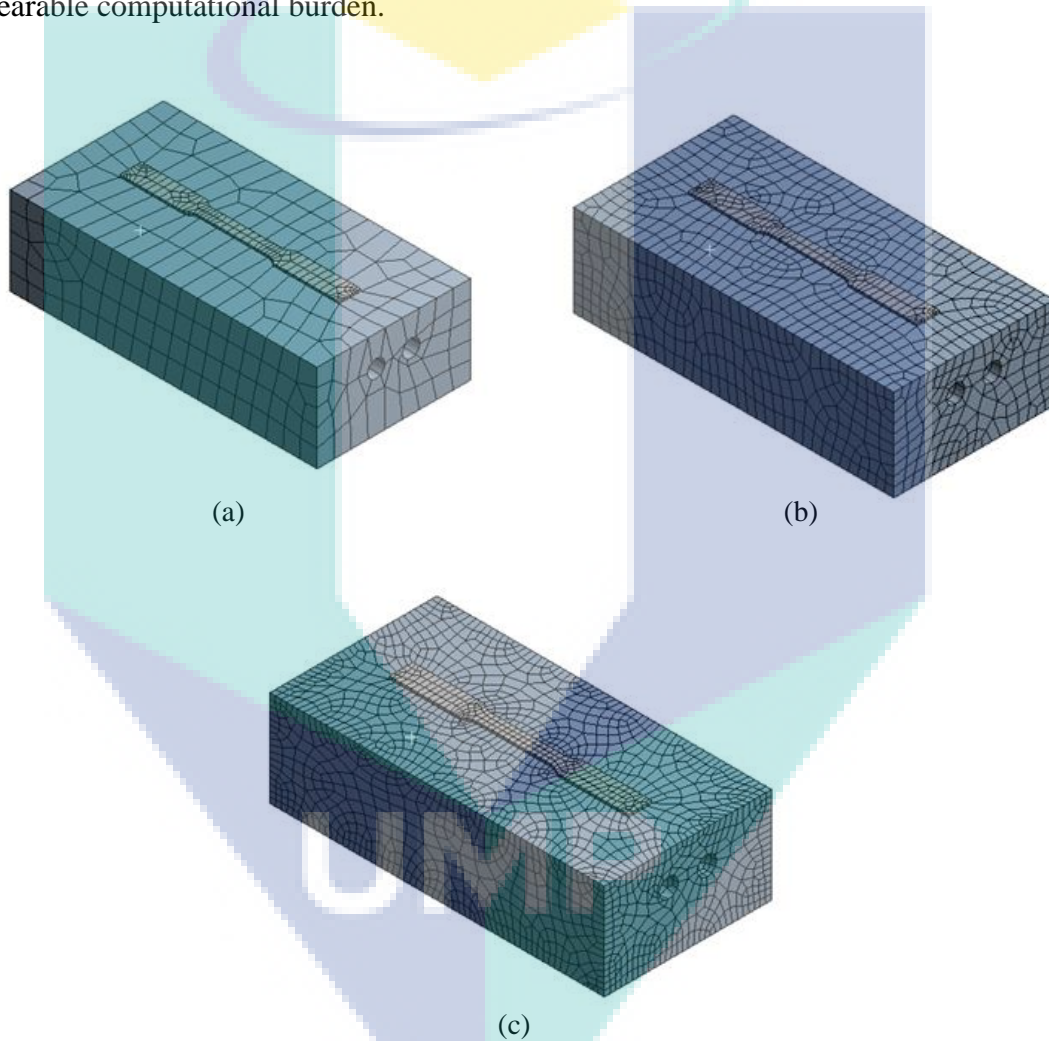


Figure 4.1 Flat shape tool meshing structure at (a) Coarse; (b) Medium and (c) Fine, mesh size at FEA simulation

Table 4.1 Meshing results for coarse, medium and fine meshing for flat tool

Sizing Control	Coarse	Medium	Fine
Node	39965	85264	158819
Element	26338	56044	105688
Meshing Time (s)	5	7	11
Solution Time (s)	122	234	388

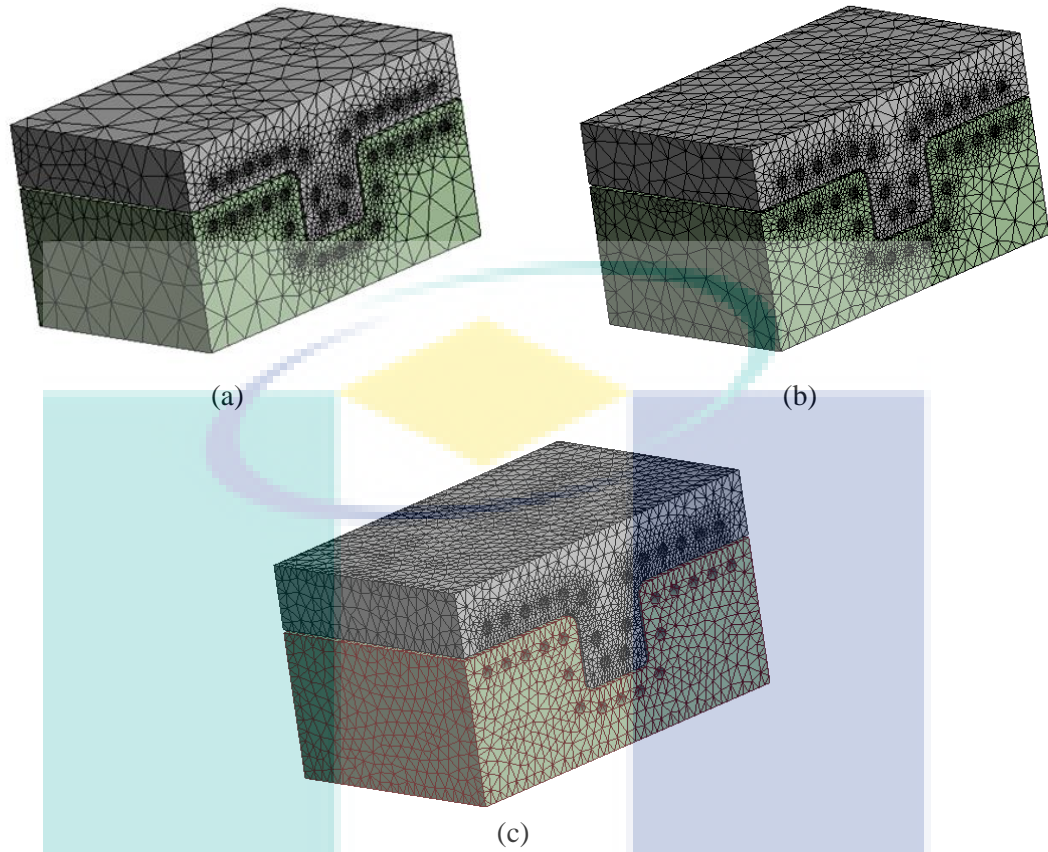


Figure 4.2 U-shaped tool meshing structure at (a) Coarse; (b) Medium and (c) Fine, mesh size at FEA simulation

Table 4.2 Meshing results for coarse, medium and fine meshing for U-shape tool

Sizing Control	Coarse	Medium	Fine
Node	86977	134436	340786
Element	45732	71533	223431
Meshing Time (s)	16	22	120
Solution Time (s)	180	429	2400

Based on Figure 4.3, by choosing a mapped mesh, the chart for mesh quality criteria indicated a lower quality result. Conversely, the refined mesh, (Figure 4.4) the chart shows a convergence towards zero, which suggest that the mesh quality was acceptable (ANSYS, 2016). In this project, a refinement control mesh was chosen due to this fact.

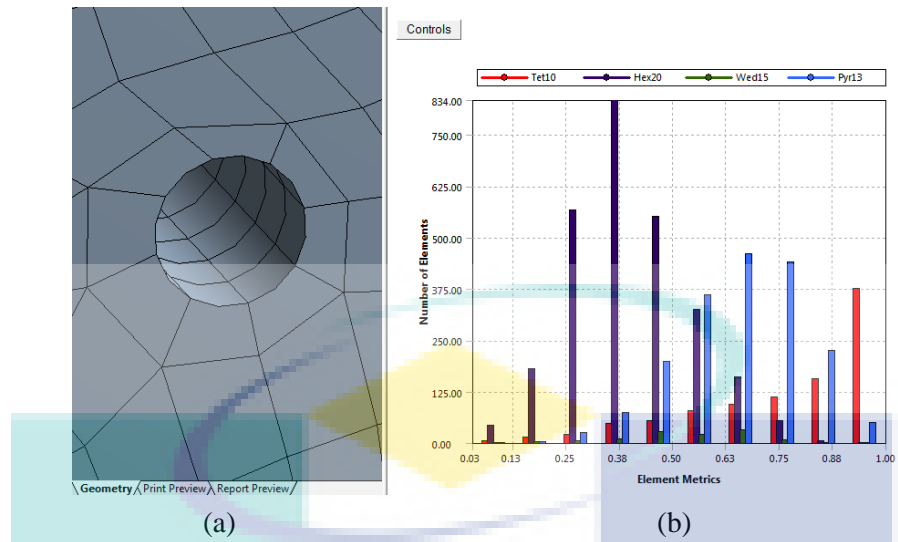


Figure 4.3 Local meshing control for hot stamping tool (a) Mapped mesh (b) Mesh quality criteria chart of mapped mesh.

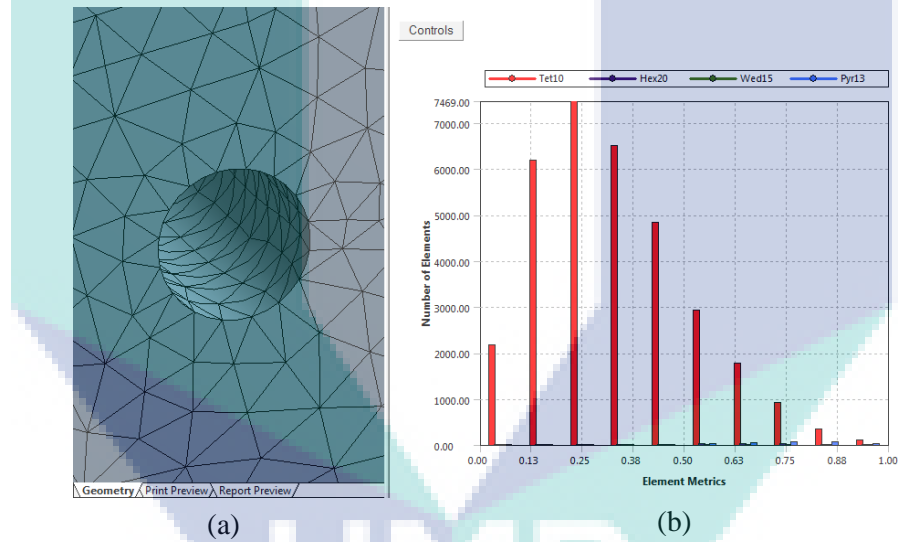


Figure 4.4 Local meshing control for hot stamping tool (a) Refined mesh (b) Mesh quality criteria chart of refined mesh.

4.2.2 Thermal and Static Analysis for flat and U-shaped

Figure 4.5, 4.6, and 4.7 shows the example of heat transfer distribution and von Mises stress value for cooling channel parameter $C_A = 8$ mm, $C_B = 10$ mm, $C_C = 8$ mm and $C_D = 8$ mm. Figure 4.5 shows the steady state condition for both hot stamping tool. The initial temperature heated blank during thermal analysis was 850 °C and the initial temperature for die and punch were 20 °C.

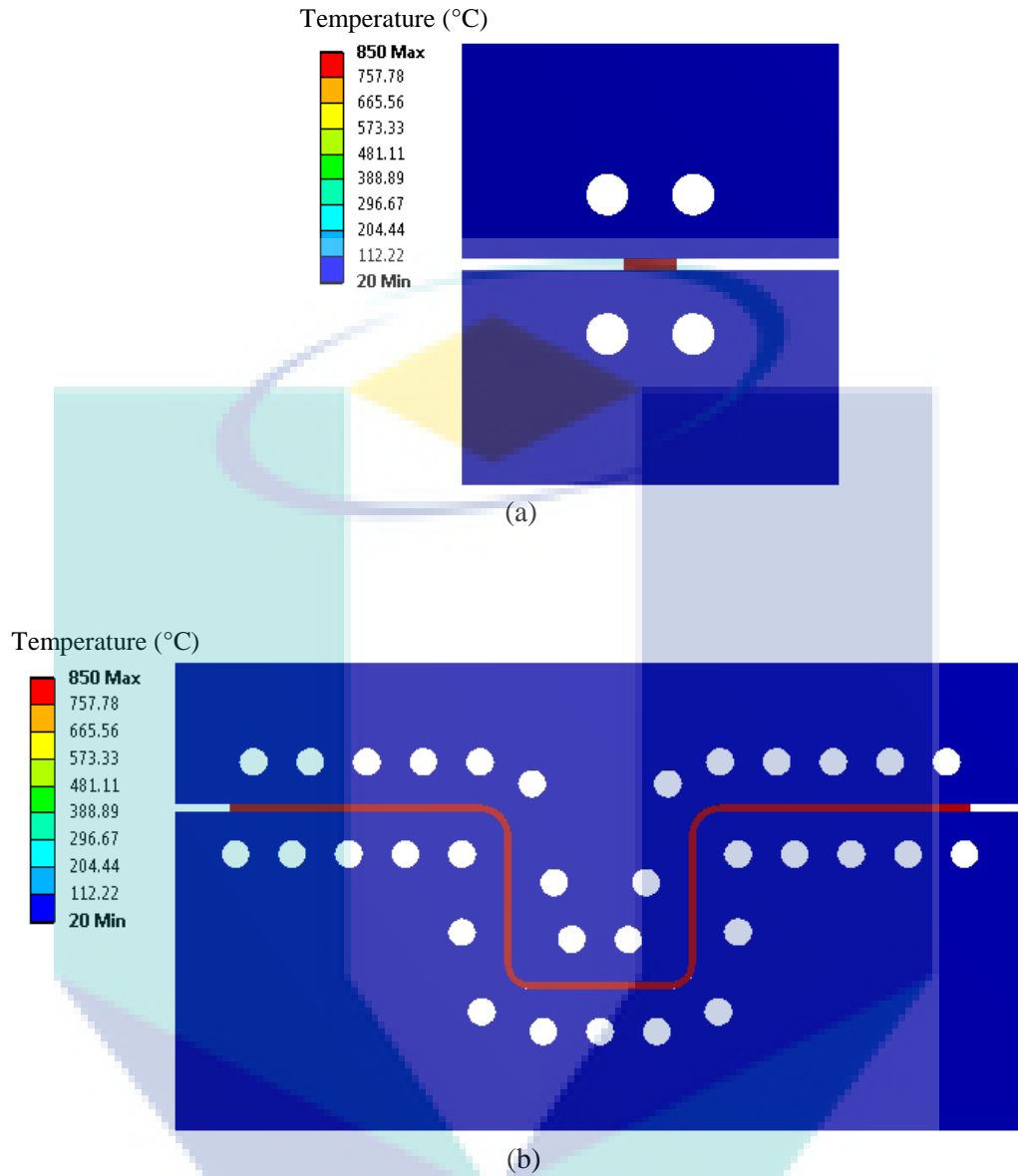


Figure 4.5 Steady state condition for hot stamping simulation of a) flat sample, b) U-shape sample

Subsequently, the data of the sample temperature was collected after 10 s and recorded as shown in Figure 4.6. Next, the lowest temperature was chosen for each diameter of the cooling channel as the cooling rate of the sample was attained with the lowest temperature. The temperature distribution for the hot stamping sample was measured, and cooling rate based on Equation 3.3, 3.4 and 3.5 was calculated.

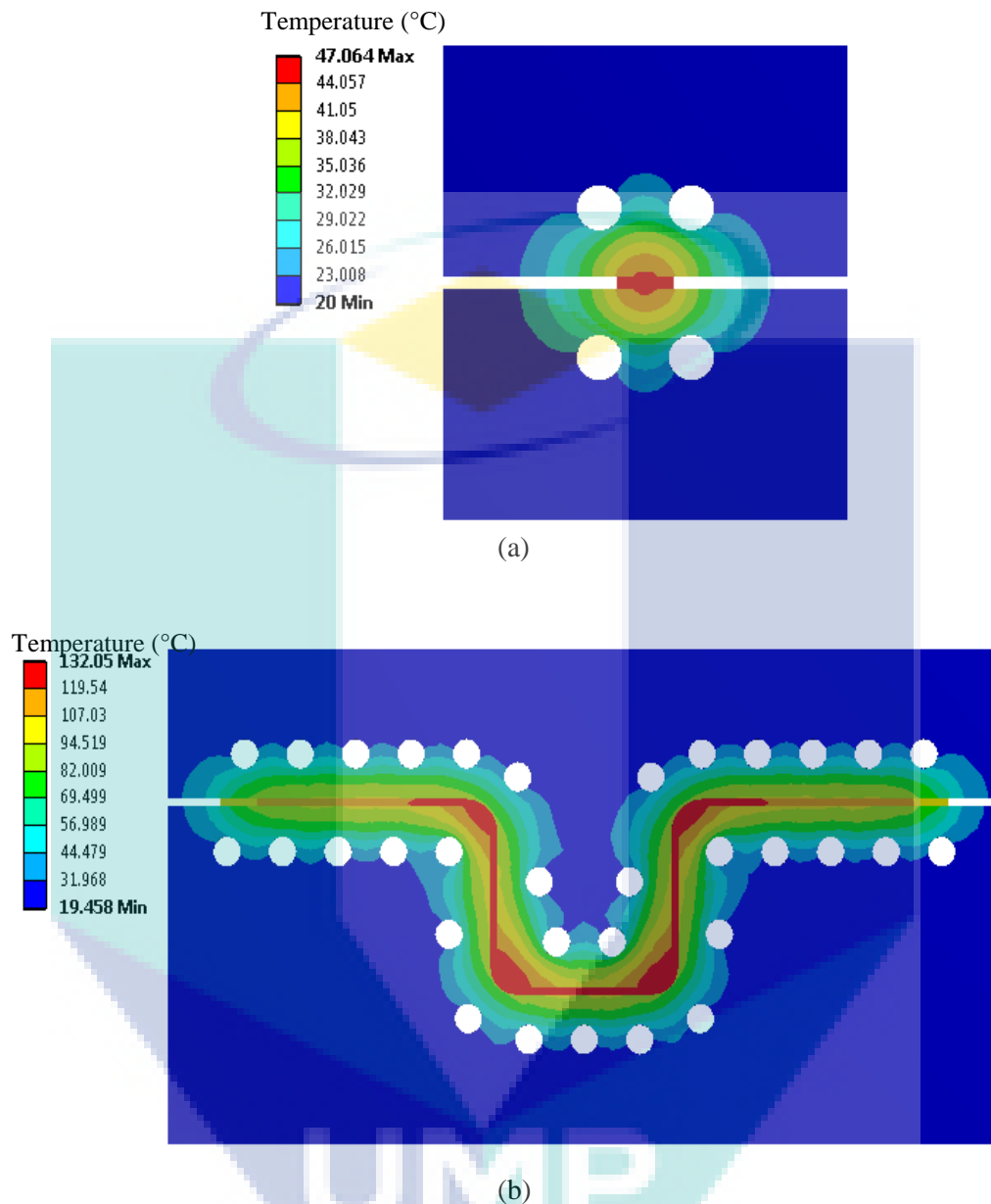


Figure 4.6 Transient thermal with 10 s quenching time for hot stamping simulation
a) flat sample, b) U-shape sample

Figure 4.7 shows the result for the von Mises stress analysis. Then, the highest value of von Mises stress was taken from the simulation. Based on Figure 4.7 (a), the higher value was 38.13 MPa for flat shaped tool. While for U-shaped, the higher value was 114.12 MPa for upper U-shaped tool (Figure 4.7 b) and the higher value for lower U-shaped tool (Figure 4.7 c) was 107.04 MPa.

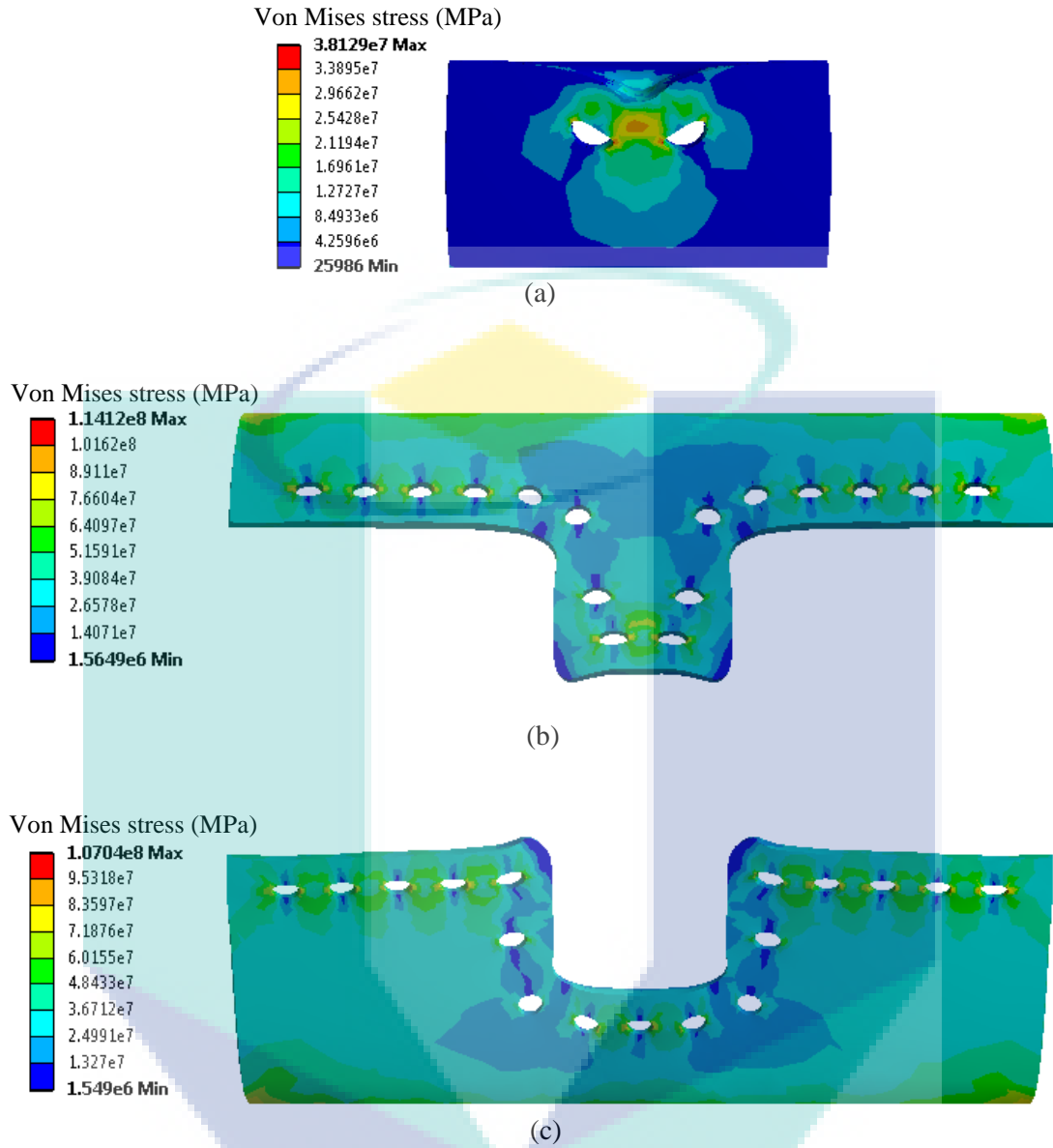


Figure 4.7 Von Mises stress distribution based on static stress analysis on; (a) flat tool, (b) upper U-shape tool and (c) lower U-shape tool

4.3 Design Optimization

4.3.1 Heuristic Method for Flat Sample

Table 4.3 shows the result of the heat transfer rate and von Mises stress affected by parameter (C_A). The result suggests that with an increasing value for (C_A), the value of the heat transfer rate and von Mises stress also increases. As for the heat transfer rate, the percentage increase between 6 mm and 8 mm was 0.22 %, while the percentage increase between 8 mm and 12 mm was 3.57 %. Hence, the total percentage increase of

cooling rate was 3.8 %. As for the von Mises stress, the percentage increase between 6 and 8 was 3.98 %, while the percentage increase between 8 mm and 12 mm was 2.8 %. Hence, the total percentage increase of von Mises stress was 6.89 %.

Table 4.3 Cooling channel design performance for parameter (C_A) for flat tool

No. Simulation	Cooling parameter (mm)			Heat transfer rate (kJ/s)	Von Mises Stress (MPa)
	C_A	C_B	C_C		
1	6	8	8	22.045	36.670
2	8	8	8	22.094	38.129
3	12	8	8	22.882	39.197

For parameter (6,8,8) mm the result indicates that both the cooling rate and von Mises stress were the lowest amongst other configurations. Whilst, for parameter (12,8,8) mm the results were on the other extreme. As cooling channel size increased, the heat transfer area and affected stress also increased. Hence the optimum cooling channel design for parameter (C_A) was (8,8,8) mm where the value lies between the highest heat transfer rate and the lowest von Mises stress value.

Table 4.4 shows the result of heat transfer rate and von Mises stress affected by parameter (C_B). The result shows that with the increasing value for (C_B) the value of the heat transfer rate increases whilst the von Mises stress decreases. As for the heat transfer rate, the percentage of increase between 6 mm and 8 mm was 0.55%, while the percentage of increase between 8 and 12 was 0.67 %. Hence, the total percentage increase of heat transfer rate was 1.22 %. As for the von Mises stress, the percentage of decrease between 6 mm and 8 mm is 5.03%, while the percentage of decrease between 8 mm and 12 mm was 13.32 %. Consequently, the total percentage of decrease of the von Mises stress was 17.68 %. As cooling channel distance increase, the heat transfer area increase and the stress decreased when the rigidity of structure increased.

Table 4.4 Cooling channel design performance for parameter (C_B) for flat tool

No. Simulation	Cooling parameter (mm)			Heat transfer rate (kJ/s)	Von Mises Stress (MPa)
	C_A	C_B	C_C		
4	8	6	8	21.974	40.148
2	8	8	8	22.094	38.129
5	8	10	8	22.242	33.049

It is apparent that the parameter of (8,10,8) mm gives the highest heat transfer rate with lowest von Mises stress value. Therefore, the value for parameter (C_B), was selected to be 10 mm and used in the analysis for parameter (C_C).

Table 4.5 shows the result of heat transfer rate and von Mises stress affected by parameter (C_C). The result shows that with an increasing value for (C_C), both the values of the heat transfer rate and von Mises, stress decreases. The percentage of decrease between 6 and 8 and between 8 and 12 are 3.28 % and 1.33%, respectively for the heat transfer rate. The accumulated percentage of decrease is 4.57%. As for the von Mises stress, the percentage of decrease between 6 and 8 is 20.98%, while the percentage of decrease between 8 and 12 is 1.61%. Hence, the total percentage of decrease for von Mises stress is 22.25%.

Table 4.5 Cooling channel design performance for parameter (C_C) for flat tool

No. Simulation	Cooling parameter (mm)			Heat transfer rate (kJ/s)	Von Mises Stress (MPa)
	C_A	C_B	C_C		
6	8	10	6	22.997	41.826
5	8	10	8	22.242	33.049
7	8	10	10	21.946	32.518

For parameter (8,10,6) mm the result suggests that the values of heat transfer rate and the von Mises stress are the highest. The lowest values for both criteria is the (8,10,10) mm configuration. If tool surface distance increase, the heat transfer decrease from hot sheet metal to cooling channel (Lim et al., 2016). It is similar for von Mises stress when increasing (C_C) for the tool due to the rigidity increase. Therefore, the optimum cooling channel design for parameter (C_C) is (8,10,8) mm as it lies in the middle. Therefore the optimum value of parameter (C_C) selected for this analysis was 8 mm.

Hence, based on heuristic optimization method, the optimum parameters for the cooling channel design for the flat shape tool are 8 mm, 10 mm, 8 mm and for C_A , C_B and C_C , respectively. From the analysis it also apparent that parameter C_C , gives the highest percentage of difference as compared to other parameters. This in turn suggest that parameter C_C is the most significant parameter (Hoffmann et al., 2007).

Based on the observations made, it was obvious that the temperature evolution was influenced by the different parameters for the design of cooling channel system to the hot stamping tool. The results suggest that 8 mm for the cooling channel diameter (C_A), 10 mm for the pitch between the cooling channel (C_B), 8 mm for the distance between the cooling channel and the tool surfaces (C_C) were the optimum parameters for the design of a cooling channel for the flat shape designed tool. Table 4.6 lists these parameters, while Figure 4.8 show the flat tool design with optimum cooling channel parameter.

Table 4.6 Optimum cooling channel design for flat tool

Parameter	C_A	C_B	C_C
Value (mm)	8	10	8

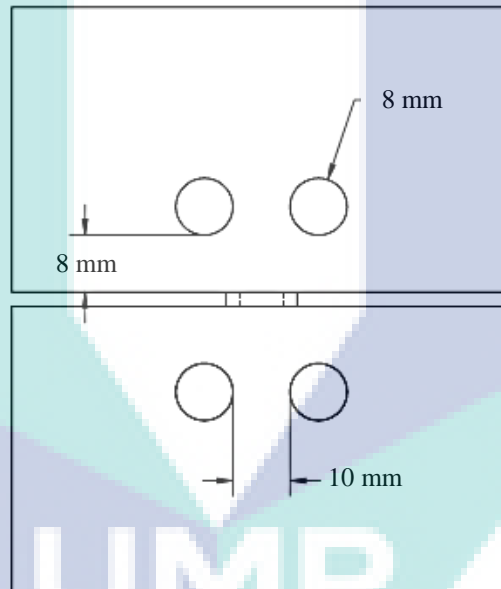
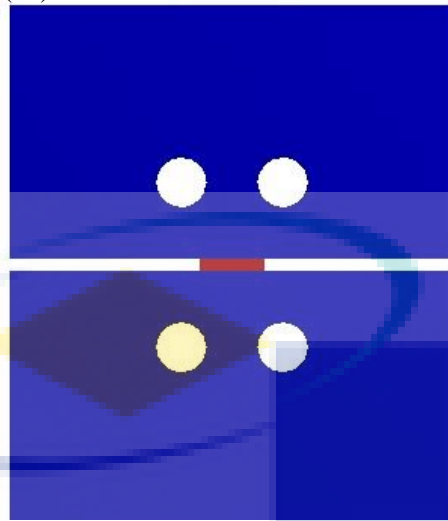
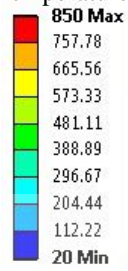


Figure 4.8 Flat tool design with optimum cooling channel parameter

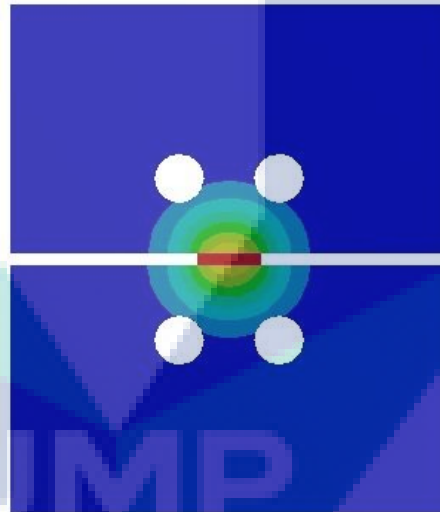
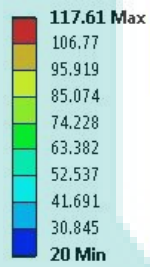
Figure 4.9 shows the blank and tool condition of thermal distribution for 0, 4, 8, 10 s. This quenching step took 10 s. In the simulations, the heat transfer occurs from blank to tool with cooling channels could be clearly observed. The temperatures of the upper tool and lower tool continuously decreases with the increasing holding time. Hence, this tool with the optimised cooling channel design was used in next experiment.

Temperature (°C)



(a)

Temperature (°C)



(b)

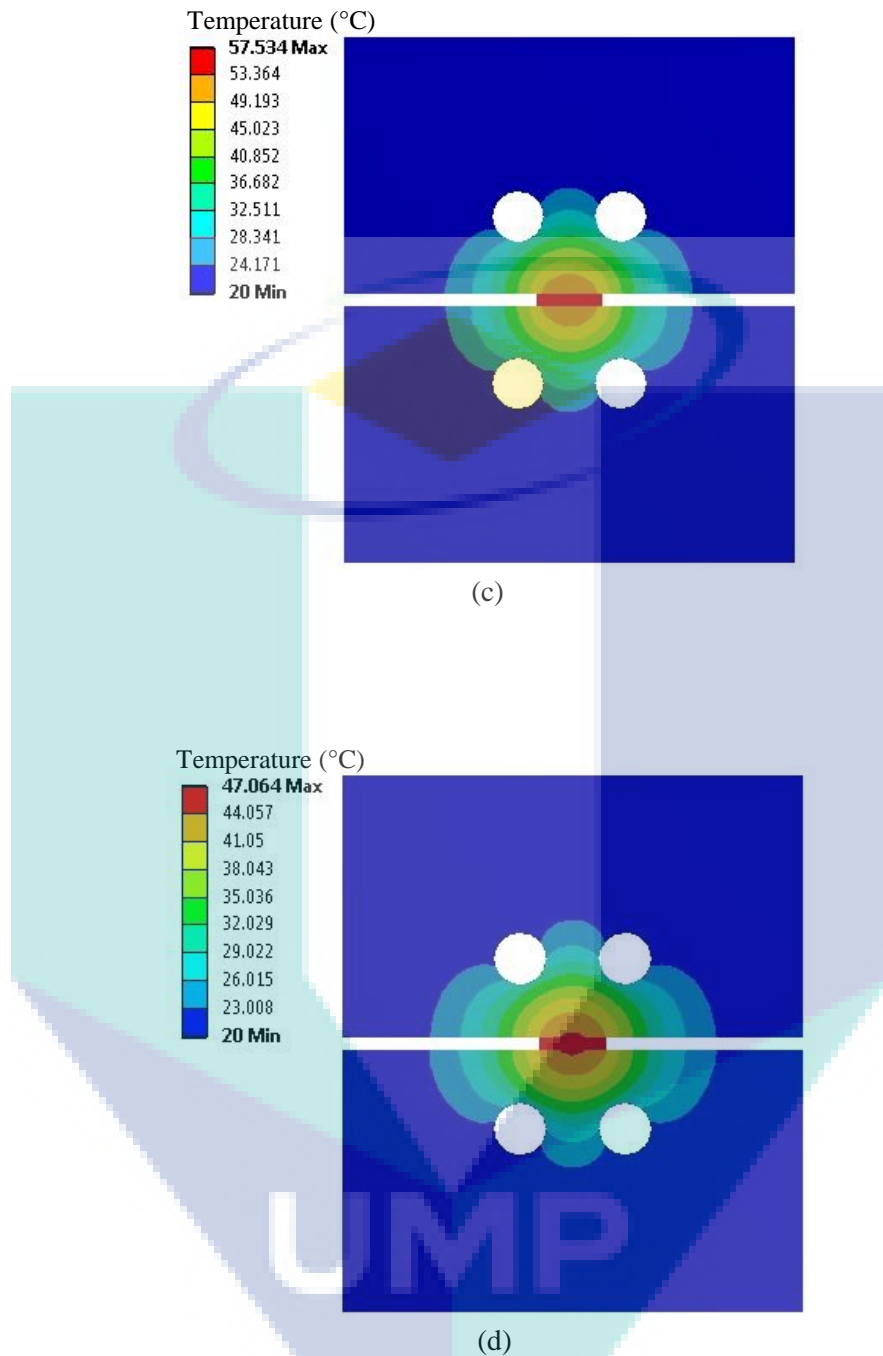


Figure 4.9 Blank and Tool Condition of flat tool of thermal distribution for holding time for flat tool at (a) 0 s, (b) 4 s, (c) 8 s and (d) 10 s

4.3.2 Heuristic Method for U-Shape Sample

(i) Effect of cooling channel diameter (C_A) on heat transfer rate and stress distribution

For this simulation study, the different value of cooling channel diameter (C_A) that used were 6 mm, 8 mm, and 12 mm. Other parameters were held constant such as

the pitch between the cooling channel (C_B), the distance between the cooling channel and the tool surface (C_C) and the distance between the cooling channel for the wall on tool surfaces (C_D) by set the value of 8 mm, 8 mm and 8 mm. Table 4.7 shows the cooling rate decrease as (C_A) increase for upper and lower tool. Maximum von Misses fluctuate when increasing (C_A). Based on the results, the optimum parameter is 8 mm for highest heat transfer rate and lowest stress for the upper and lower tools.

Table 4.7 Effect of cooling channel diameter (C_A) on heat transfer rate and von Mises stress

No. Simulation	Cooling Channel Diameter, (C_A) (mm)	Heat transfer rate, (kJ/s)		Von Mises Stress, (MPa)	
		Upper Tool	Lower Tool	Upper Tool	Lower Tool
1	6	8.298	14.368	123.960	169.200
2	8	8.246	13.300	113.610	109.970
3	12	7.563	12.775	132.750	151.670

(ii) **Effect of the pitch between the cooling channels (C_B) on heat transfer rate and stress distribution**

For this simulation, the pitch between the cooling channel (C_B) were varied between 6 mm, 8 mm, and 10 mm. Again, other parameters were held constant such as the cooling channel diameter (C_A), the distance between the cooling channel to the tool surface (C_C) and the distance between the cooling channel for the wall on tool surfaces (C_D) with the value of 8 mm, 8 mm and 8 mm. Table 4.8 shows shows the cooling fluctuate as (C_B) increase for upper and lower tool. It is similar for von Misses fluctuate when increasing (C_B). Based on the results, the optimum parameter is 8 mm for highest cooling rate and lowest stress for the upper and lower tools.

Table 4.8 Effect of pitch between cooling channels (C_B) heat transfer rate and von Mises stress

No. Simulation	Pitch between Cooling Channel, (C_B) (mm)	Heat transfer rate, (kJ/s)		Von Mises Stress, (MPa)	
		Upper	Lower	Upper	Lower
4	6	7.838	11.262	122.15	131.67
2	8	8.246	13.300	113.61	109.97
5	10	7.587	11.709	116.57	125.03

(iii) Effect of the distance between the cooling channel and the tool surfaces (C_C) on heat transfer rate and stress distribution

In this analysis, value of the distance between the cooling channels and the tool surfaces (C_C) were varied between 6 mm, 8 mm, and 10 mm. Similarly, other parameters such as the cooling channel diameter (C_A), the pitch between the cooling channel (C_B), and the distance between the cooling channel for the wall on tool surfaces (C_D) were set to be 8 mm, 8 mm and 8 mm, respectively. Table 4.9 shows the cooling fluctuate as (C_C) increase for upper tool, while it is decreasing as (C_C) increase for lower tool. It is similar for von Mises fluctuate when increasing (C_C) for both tools. Based on the results, the optimum parameter is 8 mm for highest cooling rate and lowest stress for the upper and lower tools.

Table 4.9 Effect of distance between cooling channel to tool surfaces (C_C) heat transfer rate and von Mises stress

No. Simulation	Distance between Cooling Channel to Tool Surfaces (C_C)	Heat transfer rate, (kJ/s)		Von Mises Stress, (MPa)	
		Upper	Lower	Upper	Lower
6	6	8.606	14.639	114.87	112.03
2	8	8.816	14.113	113.61	109.97
7	10	7.467	13.300	121.51	124.81

(iv) Effect of the distance between the cooling channel for the wall on tool surfaces (C_D) on heat transfer rate and stress distribution

In this simulation study, the distance between the cooling channels for the wall on tool surfaces (C_D) were changed between 6 mm, 8 mm, and 10 mm. Parameters (C_A), (C_B), and (C_C) were held constant with the value of 8 mm, 8 mm and 8 mm, respectively. Table 4.10 lists whilst Figure 4.16 depicts the cooling fluctuate as (C_D) increase for upper tool, while it is decreasing as (C_D) increase for lower tool. It is similar for von Mises fluctuate when increasing (C_D) for both tools. Based on the results, the optimum parameter is 10 mm for upper tools and 8 mm for lower tools.

Table 4.10 Effect of the distance cooling channels to wall tool (C_D) heat transfer rate and von Mises stress

No. Simulation	Distance between Cooling Channel to Wall Tool (C_D)	Heat transfer rate, (kJ/s)		Von Mises Stress, (MPa)	
		Upper	Lower	Upper	Lower
8	6	8.696	15.692	120.86	126.15
2	8	7.587	14.640	113.61	109.97
9	10	9.506	13.396	115.62	113.06

Based on results analysis heat transfer rate and von Mises stress varies with different geometric parameters for the design of the cooling channel system to the hot stamping tool (Table 4.11). These make the optimization for the cooling channel for this U-shaped design, the following values were selected i.e. 8 mm, 8 mm, 8 mm, 8 mm and 10 mm for the cooling channel diameter (C_A), the pitch between the cooling channel (C_B), the distance between the cooling channel and the tool surfaces (C_C), the distance between the cooling channel for the wall on tool surfaces (C_D), the upper tool and lower tool, respectively. Figure 4.10 shows the schematic design of of U-shape tool with optimised cooling channel parameter.

Table 4.11 Optimum cooling channel design for U-shape tool

Parameter	Value (mm)	
	Upper Tool	Lower Tool
C_A	8	8
C_B	8	8
C_C	8	8
C_D	10	8

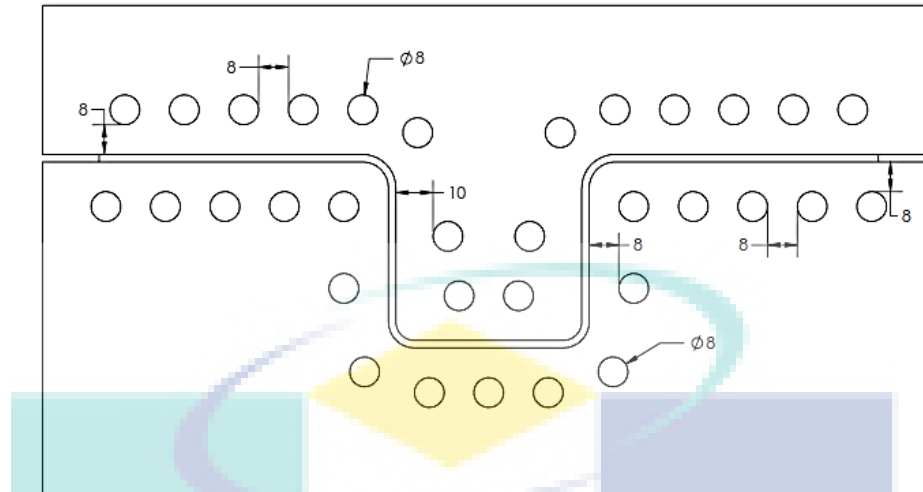
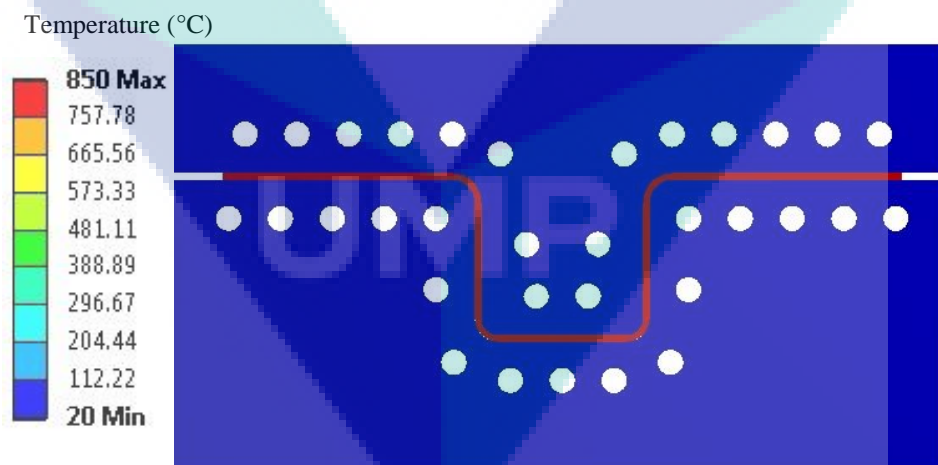


Figure 4.10 U-shape tool design with optimum cooling channel parameter

Figure 4.11 illustrates the blank and tool condition of thermal distribution for 0, 4, 8, 10 s. This quenching step took 10 s. In the simulations, the heat transfer transpires from the blank to the tool with cooling channels could be easily observed. The temperatures of the upper tool and lower tool continuously decreases with the increase in holding time. Hence, this tool with the optimised cooling channel design used in the ensuing experiment.



(a)

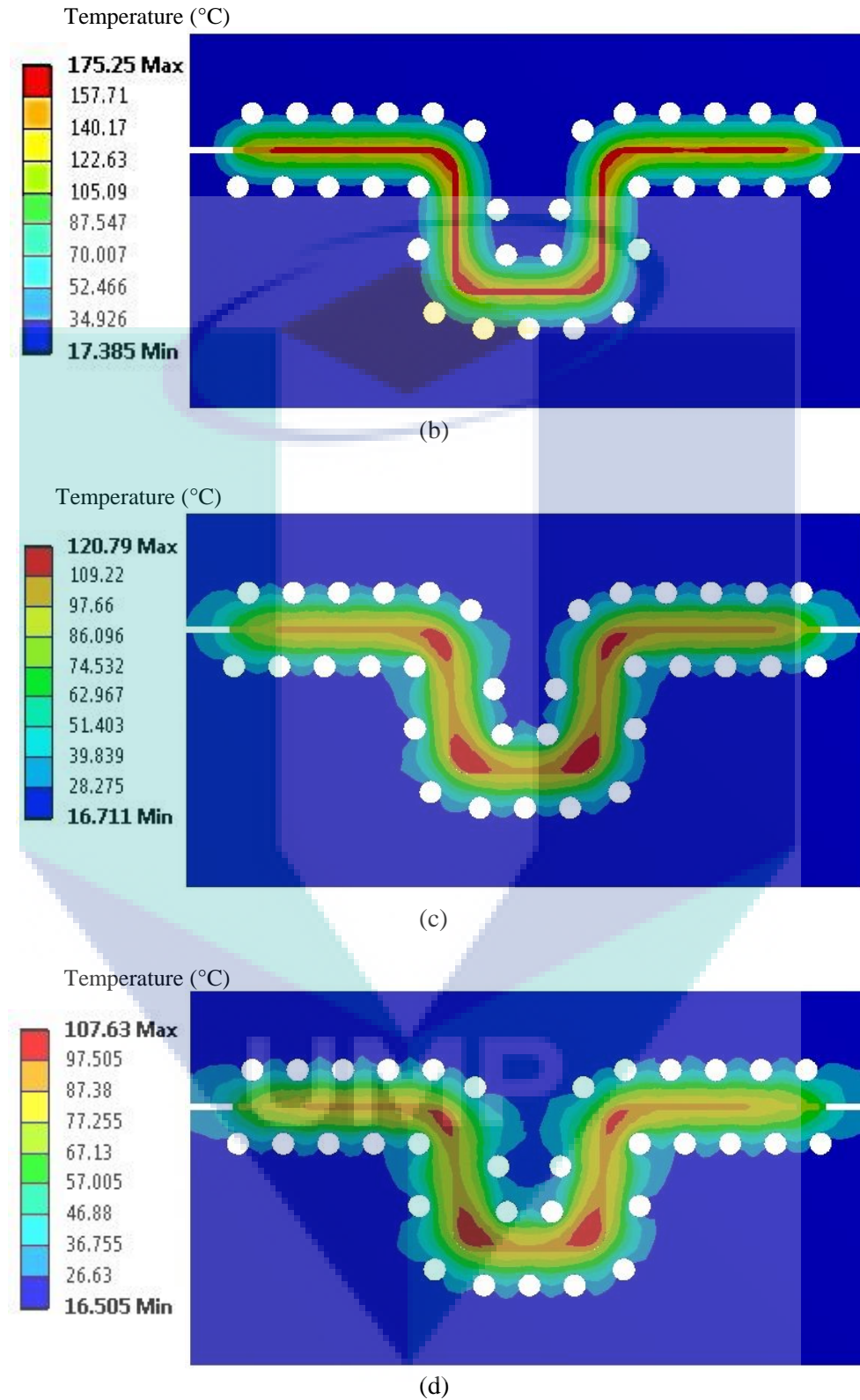


Figure 4.11 Blank and tool condition of U-shape tool of thermal distribution for holding time for flat tool at (a) 0 s, (b) 4 s, (c) 8 s and (d) 10 s

4.3.3 Taguchi Method

The value for the maximum VMS and cooling rate were obtained after conducting the FEA for all nine DOE. Each result represents one FEA in the OA as shown in Table 4.12. The table summarizes the maximum VMS value and the rate of cooling for hot stamping tool under constant of C_A , C_B , and C_C . All the results are analysed by conducting the main effect, and S/N Ratio. Result shows, cooling channel with parameter $C_A = 6$ mm, $C_B = 6$ mm and $C_C = 6$ mm shows value of 24.813 kJ/s which was higher cooling compare to other. While for VMS, parameter $C_A = 6$ mm, $C_B = 10$ mm and $C_C = 10$ mm shows value of 31.977 which was the lowest value of VMS. Next, confirmation test was carried out to compare the simulation results and the predicted results of the minimum value of maximum VMS and higher value of cooling rate.

Table 4.12 Result of Cooling rate and VMS from the Taguchi method for flat tool

No. Experiment	Factor			Result	
	C_A	C_B	C_C	Heat transfer rate (kJ/s)	Maximum von Mises stress (MPa)
1	6	6	6	24.813	43.536
2	6	8	8	22.094	36.164
3	6	10	10	20.142	31.977
4	8	6	8	21.974	40.148
5	8	8	10	21.715	35.515
6	8	10	6	22.997	41.826
7	12	6	10	22.108	37.657
8	12	8	6	23.697	41.845
9	12	10	8	20.332	33.473

(i) Main Effect

Table 4.13 summarizes the average main effect for maximum VMS and heat transfer rate that are obtained from each factor i.e. C_A , C_B , and C_C array at each level (Level 1, level 2 and level 3). The main effect graph for heat transfer rate and maximum VMS under a constant diameter of cooling channel, pitch between cooling channel and distance cooling channel to loading surface is represented by Figure 4.12 and 4.13 based on the results obtained in Table 4.13. From the results, cooling channel with parameter $C_A = 6$ mm, $C_B = 6$ mm and $C_C = 6$ mm shows higher cooling compare to other. While for VMS, parameter $C_A = 6$ mm, $C_B = 10$ mm and $C_C = 10$ mm shows the lowest value of VMS. The quality of characteristics analysis in the current study is the

smaller is better for maximum VMS value and larger is better for cooling rate due to the optimization in designing the cooling system for hot stamping tool (Hoffmann et al., 2007). It can be observed that the parameters and their levels of combination for cooling rate are C_A1 , C_B1 , and C_C1 and for the maximum VMS, the combination is C_A1 , C_B3 , and C_C3 .

Table 4.13 Average main effect for cooling rate and VMS for taguchi method of flat tool.

Parameters (mm)	Average Main Effect							
	Heat transfer rate (kJ/s)				Maximum von Mises stress (MPa)			
	Level 1	Level 2	Level 3	Rank	Level 1	Level 2	Level 3	Rank
C_A	22.35	22.23	22.05	3	33.76	34.07	35.59	3
C_B	22.97	22.50	21.16	2	35.83	34.77	32.82	2
C_C	23.84	21.47	21.32	1	37.33	34.51	31.59	1

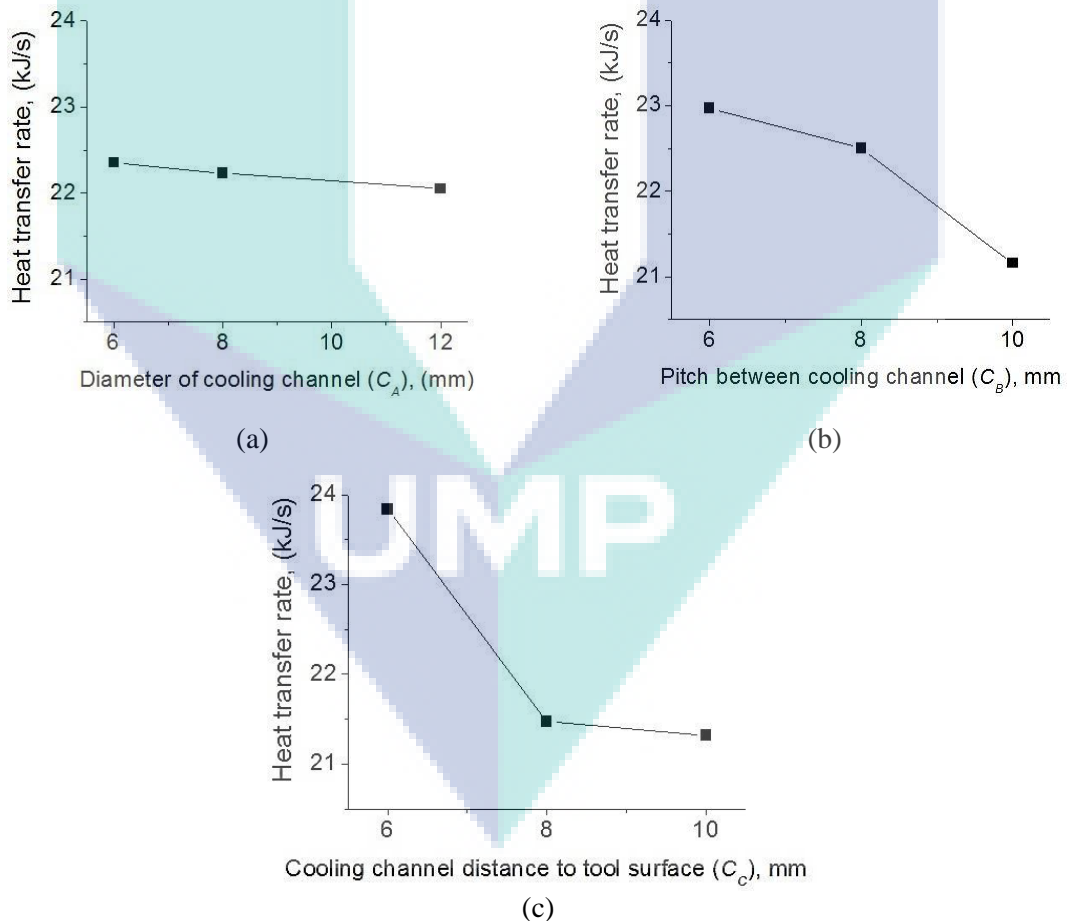


Figure 4.12 Main effect plot for heat transfer rate of flat tool (a) Diameter of cooling channel (b) Pitch between cooling channel (c) Cooling channel distance to tool surface.

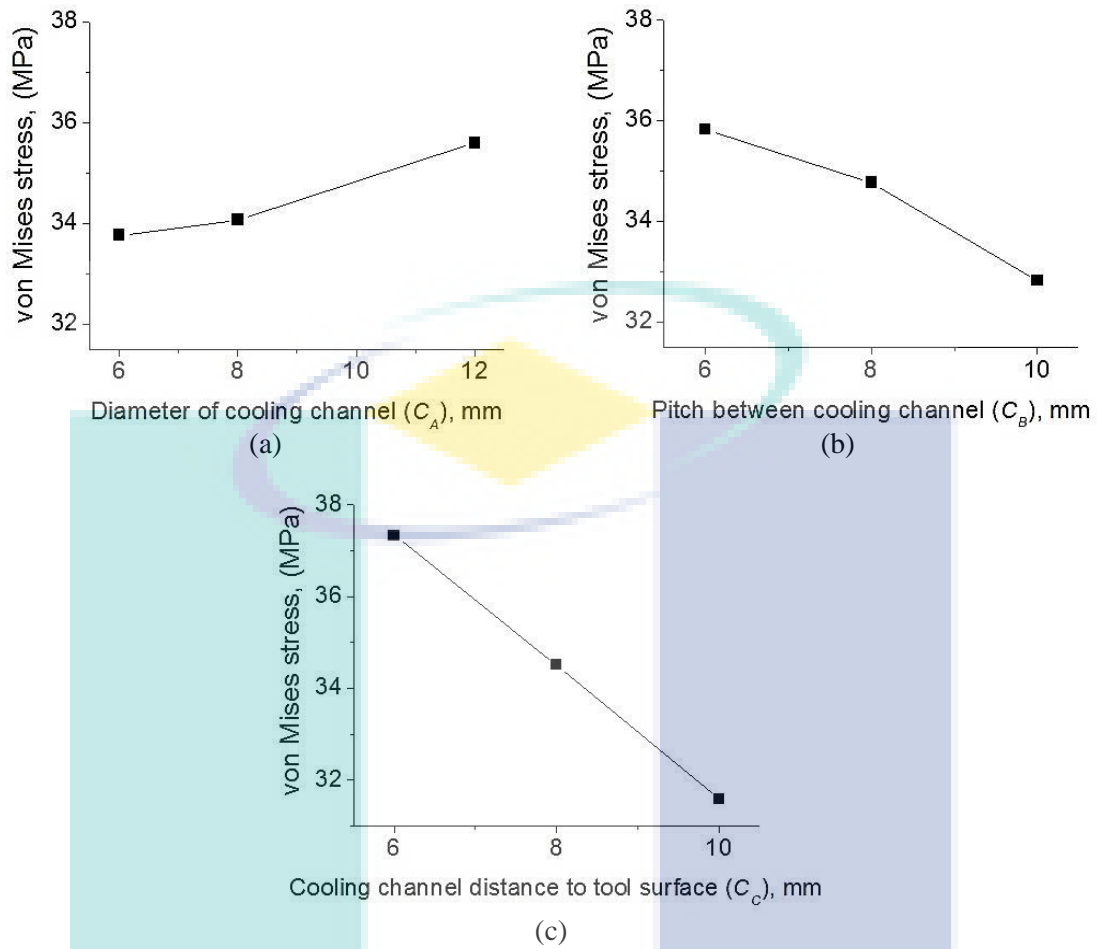


Figure 4.13 Main effect plot for maximum von Mises stress (VMS) of flat tool (a) Diameter of cooling channel (b) Pitch between cooling channel (c) Cooling channel distance to tool surface.

(ii) Analysis of S/N ratio

From Table 4.14, it is evident that 27.8936 dB was the highest value for S/N ratio of cooling rate, and 30.0968 dB was the lowest value for S/N ratio of the maximum VMS. Compared to the main effect, that suggest the optimum level for cooling rate were C_{A1} , C_{B1} , and C_{C1} , and maximum VMS were C_{A1} , C_{B3} , and C_{C3} , similar optimal result with the S/N ratio analysis was attained. Finally, the validation result was verified based on the suggested optimal process parameters combinations. However, it was worth mentioning that validation was not required as the optimal parameters combination and their levels coincidentally were the same as the experiment in OA for cooling rate and maximum von Mises stress (Yusoff et al., 2006).

Table 4.14 Respond value and S/N ratio for flat tool

No. Simulation	Larger is better		Smaller is better	
	Heat transfer rate (kJ/s)	S/N Ratio (dB)	Maximum von Mises stress (MPa)	S/N Ratio (dB)
1	24.813	27.8936	43.536	32.7770
2	22.094	26.8855	36.164	31.1655
3	20.142	26.0821	31.977	30.0968
4	21.974	26.8382	40.148	32.0733
5	21.715	26.7352	35.515	31.0082
6	22.997	27.2334	41.826	32.4289
7	22.108	26.8910	37.657	31.5169
8	23.697	27.4939	41.845	32.4329
9	20.332	26.1636	33.473	30.4939

4.3.4 Heuristic and Taguchi Method Comparison

Results obtained from both the DOE method indicate discrepancies with the optimization of the cooling parameter for the hot stamping flat tool. The results obtained from the Heuristic method was (8,10,8) mm while based on the Taguchi method the results indicates (6,6,6) mm and (6,10,10) mm respectively. In hot stamping tool, lower maximum VMS and higher cooling rate value were the criteria that were of importance. Figure 4.14 illustrates the temperature distribution for cooling channel design obtained from the FEA. From the result, it evident although that the trend of each cooling design were the same, but the results of the the tool performances were different. The tool with parameter (8,10,8) mm gives a better cooling performance as the tool had less maximum temperature achieved after the heated blank is transferred to the tool. Figure 4.15 depicts the results of the cooling parameters that were selected.

The parameter of (6,6,6) mm resulted in the highest heat transfer rate of 24.813 kJ/s and maximum VMS of 43.536 MPa. As for parameter (6,10,10) mm the results show the lowest heat transfer rate of 20.142 kJ/s and minimum VMS of 31.977 MPa. This result was achieved due to the major difference in the distance to the loading surface, C_C where the distance for (6,8,6) mm was the shortest which was 6 mm and for (6,10,10) mm it has the longest distance which was 10 mm. From this observation, it was proven that the distance of cooling channel to loading surface was a major factor in designing hot stamping tool (Hoffmann et al., 2007), (Karbasiyan & Tekkaya, 2010) and (Kumar et al., 2011). This was true as when the distance was near to the loading surface, it result in a higher heat transfer rate and high maximum VMS that will affect

the deformation of the tool. This observation was in contrast for a longer distance from the loading surface. In this study, it was evident that parameter (8,10,8) mm from heuristic method provides the optimum results where it had a Heat transfer rate of 22.242 kJ/s and VMS of 33.049 MPa.

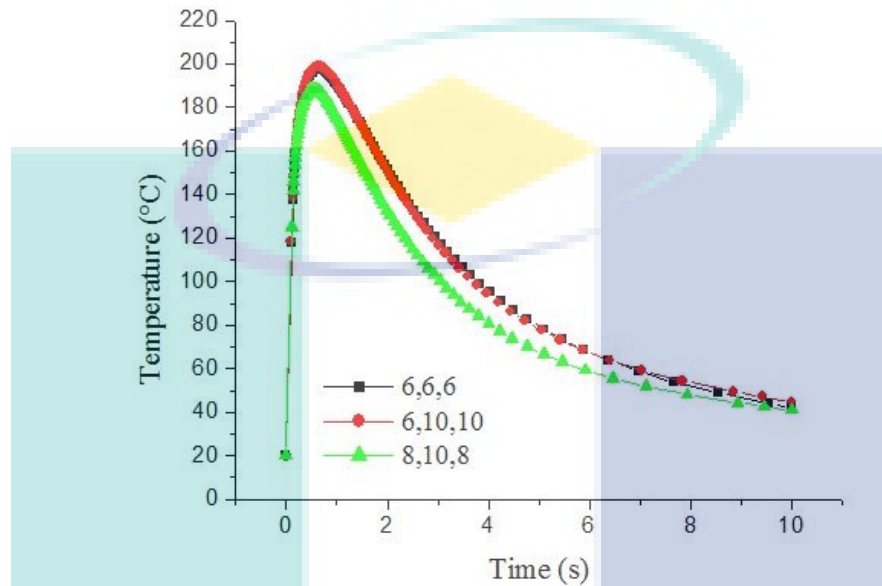


Figure 4.14 Temperature distribution for cooling channel design of flat tool between heuristic and taguchi method

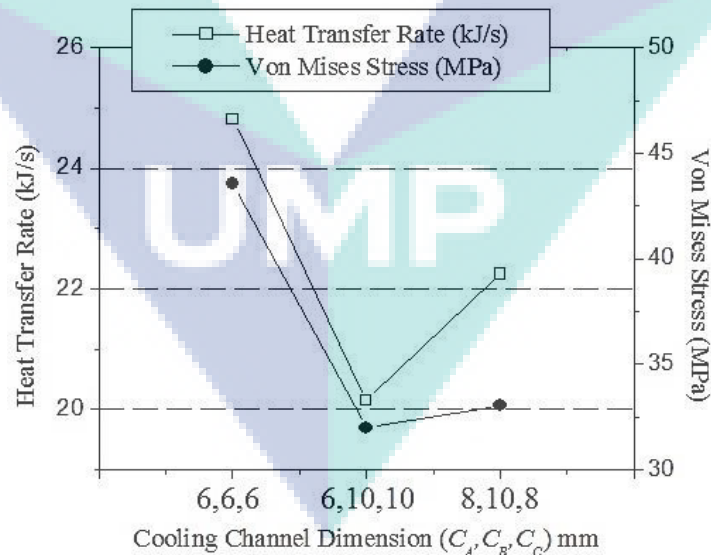


Figure 4.15 Cooling channel design performance for flat shape tool based on heuristic versus taguchi method.

4.4 Experiment Validation of Hot Stamped 22MnB5 Steel

4.4.1 Validation of FEA Thermal Analysis with Experiment for Flat Tool

FEA simulations of the hot stamping process were conducted by applying aforementioned materials and thermal properties. The temperature evolutions of the blank and tool during the process determined by the experiments and calculated by the simulations were compared and presented in Figure 4.16. The comparison of heat transfer distribution between FEA and experiment result in Figure 4.16 shows an average percentage error for blank heat distribution of 1.83 % and 2.67 % for the tool. The results showed an acceptable agreement between the experiments and FE simulations due to tool lower value of percentage error, and the similar pattern of the distribution (Namklang & Uthaisangsuk, 2016).

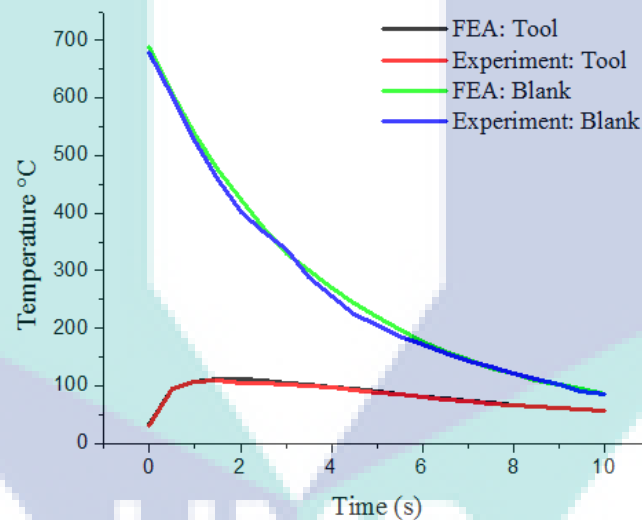


Figure 4.16 Comparison of heat transfer distribution between FEA and experiment for flat tool

4.4.2 Validation of FEA Thermal Analysis with Experiment for U-shaped tool

As mentioned before the FEA simulations of the hot stamping process were conducted by applying all mentioned material and thermal properties. The temperature evolutions of the blank and tool during the hot stamping of U-shaped blank were compared and presented in Figure 4.17. The results compare temperature distribution of blank and tool from experimental and FEA simulation. The result validates the simulation result for the upper tool, lower tool and blank. The result indicates that the temperature distribution trend of the blank and tool are almost identical.

The percentage error of the heat transfer distribution between FEA and experimental results shows the average percentage error for the blank heat distribution for the upper tool, lower tool, and the blank were 16.65 %, 17.95 %, and 7.92 %, respectively. The higher error of the U-shape as compared to the flat shape is attributed to the time taken to close the U-shape tool is greater than the flat tool. For the U-shape tool, the upper die is opened widely due to the punch stroke for the U-shape is 50 mm. As the speed for the hydraulic press machine is slow, the heated blank is not at its optimum temperature (reduction of temperature due to air exposure). The results obtained showed an acceptable agreement between the experimental and FEA simulation results (Namklang & Uthaisangsuk, 2016).

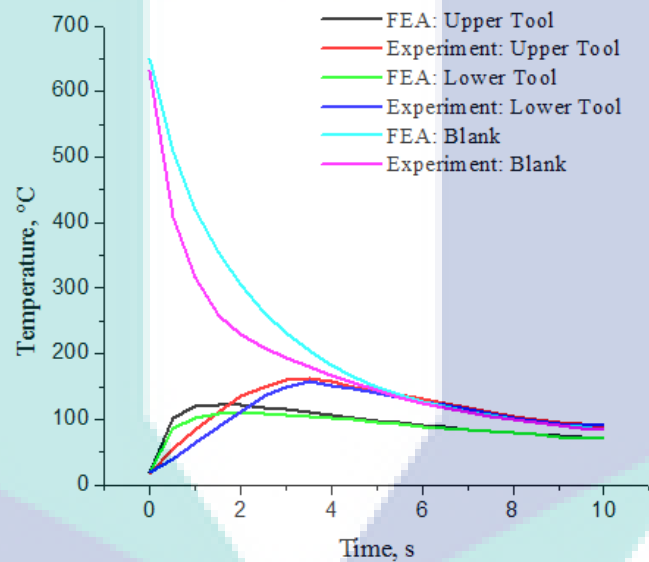


Figure 4.17 Comparison of heat transfer distribution between FEA and experiment for U-shape tool

4.4.3 Experimental Analysis of Hot Stamping for Flat shaped tool

The tensile strength and hardness properties were obtained after conducting the experiment for all nine DOE. Each result represents properties of hot stamped blank. The tensile strength and hardness decreased as the thickness of the material increased. As temperature and heating time increased, the tensile strength and hardness properties increased. Table 4.15 summarizes the tensile strength and hardness for boron steel sample at different sample thickness, heating temperature and heating time. The highest tensile strength was 1034.745 MPa and the highest value of hardness was 588 HV. Those result was represented based on the combination parameter of t_1 , T_{h3} and t_{m3} at

1.8 mm, 900 °C and 8 s respectively. All the results were analysed by conducting the main effect, S/N Ratio and (ANOVA). The increasing of heating temperature increases the value of tensile strength (Chang et al., 2011) The increasing of heating temperature and heating time also increases the value of hardness (Merklein & Lechler, 2008).

Table 4.15 Value of tensile strength and hardness

No. Experiment	Factor			Result	
	t (mm)	T_h (°C)	t_m (s)	Tensile Strength (MPa)	Hardness (HV)
1	1.8	800	4	696.604	372
2	1.8	850	6	1001.430	492
3	1.8	900	8	1034.745	588
4	2.0	800	6	515.598	179
5	2.0	850	8	499.962	238
6	2.0	900	4	590.817	218
7	3.0	800	8	482.814	215
8	3.0	850	4	462.095	204
9	3.0	900	6	642.154	294

(i) **Main Effect**

Table 4.16 summarizes the average main effect for tensile strength and hardness which obtain from each factor i.e. t, T_h , and t_m array each level (Level 1, level 2 and level 3). The main effect graph for tensile strength and hardness for boron steel blank under constant of thickness, heating temperature and heating time were shown based on the result tabulated in Table 4.16. The quality of characteristics analysis in the experiment result was the higher is better for both tensile strength and hardness in setup the hot stamping process parameter. From Figure 4.18 and 4.19 it shows that the parameters and their levels of combination for highest value of tensile strength were t1, T_h 3 and t_m 2 and highers value for hardness, the combinations were t1, T_h 3 and t_m 2.

Table 4.16 Average main effect for tensile strength and hardness

Symbol	Parameters	Average Main Effect							
		Tensile Strength (MPa)				Hardness (HV)			
		Level 1	Level 2	Level 3	Rank	Level 1	Level 2	Level 3	Rank
t	Thickness (mm)	910.9	535.5	529.0	1	496.0	255.3	264.7	1
T_h	Temperature (°C)	565.0	654.5	755.9	2	211.7	313.0	323.3	2
t_m	Heating Time (s)	583.2	719.7	672.5	3	237.7	377.0	357.3	3

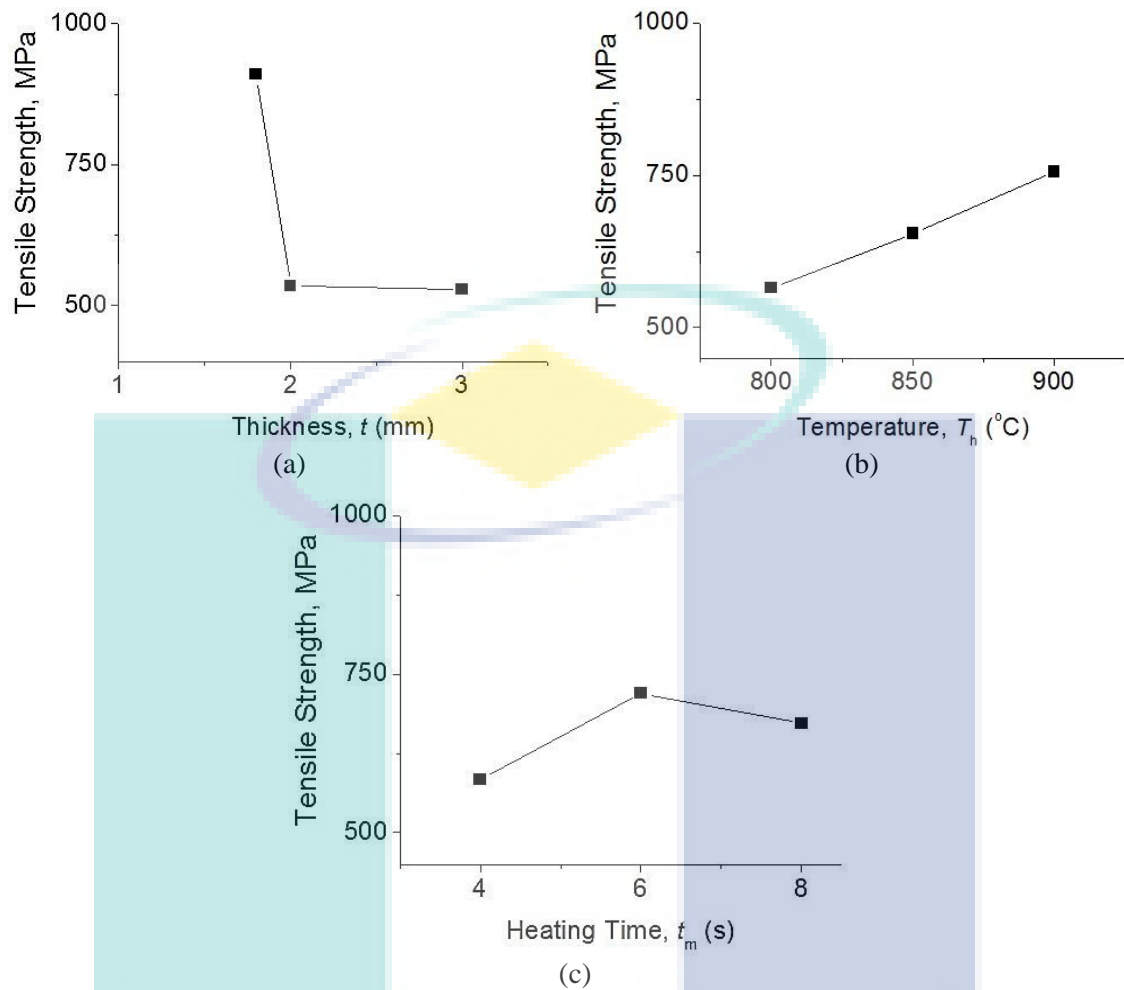


Figure 4.18 Main effects plot for tensile strength of flat tool (a) thickness (b) temperature (c) heating time

(ii) Analysis of S/N ratio

All values for S/N ratio were listed in Table 4.17. From the table, it could be observed that 60.2967 dB was the highest value for S/N ratio of tensile strength, whilst 55.8338 dB was the highest value for S/N ratio of hardness. Compared to the main effect, it shows that the optimum level of tensile strength and hardness are different to that of the S/N ratio analysis.

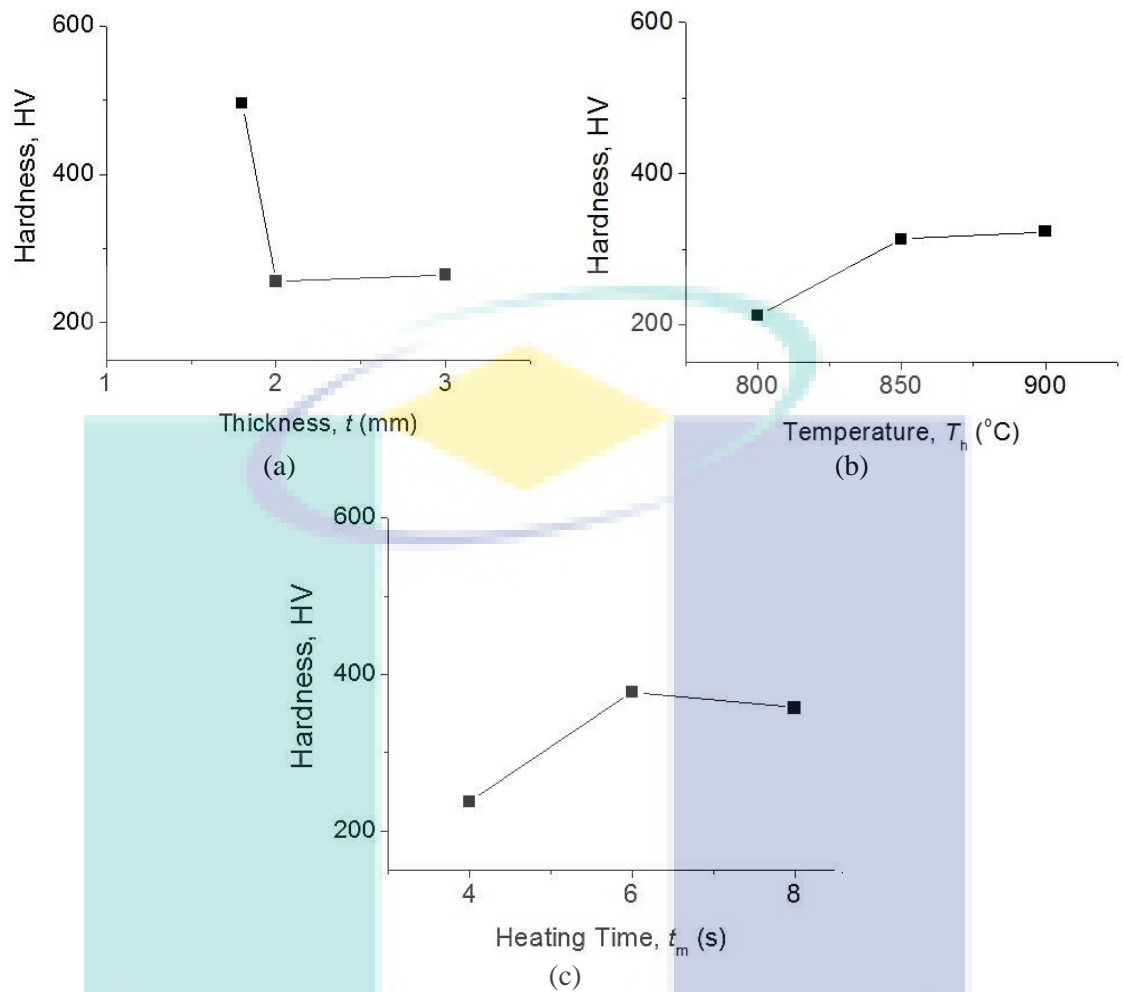


Figure 4.19 Main effects plot for hardness of flat tool (a) thickness (b) temperature (c) heating time

Table 4.17 S/N ratio analysis

No. Experiment	Larger is better		Larger is better	
	Tensile Strength (MPa)	S/N Ratio (dB)	Hardness (HV)	S/N Ratio (dB)
1	696.60	56.8597	372	51.4109
2	1001.43	60.0124	492	53.9271
3	1034.74	60.2967	588	55.8338
4	515.60	54.2462	179	45.0571
5	499.96	53.9787	238	47.5315
6	590.82	55.4291	218	46.7691
7	482.81	53.6756	215	46.6488
8	462.10	53.2946	204	46.1926
9	642.15	56.1528	294	49.3669

Since the both corresponding value of the main effect and analysis of S/N ratio were different, a new experimental parameter was introduced to prove the result of the Taguchi method is valid. From Table 4.18 it shows that the corresponding value from the Taguchi method gives the better result for tensile strength and hardness. It was

observed that the strength of boron steel increases with the increase of temperature and heating time, but the strength slightly reduce if the heating time is more the heating point of boron steel (Chang et al., 2011) and (George et al., 2012). Thus, from this experiment, the best parameter for the hot stamping process for a material of 1.8 mm thickness were 900 °C and 6 s for heating temperature and heating time, respectively. This parameter was used for U-shape hot stamping process.

Table 4.18 Result of responding value from Taguchi method for flat tool experiment

No. Experiment	Factor			Result	
	t (mm)	T_h (°C)	t_m (s)	Tensile Strength (MPa)	Hardness (HV)
2	1.8	850	6	1001.43	492
Optimum	1.8	900	6	1050.56	602
3	1.8	900	8	1034.75	588

4.4.4 Experimental Analysis of Hot Stamping for U-shaped tool

As for the U-shape experiment, the hot stamping process parameter was taken from the best parameter from flat shape experiment. The tensile tests were carried out for samples taken from the bottom, wall and flange locations of the stamped parts, as illustrated in Figure 4.20. The comparison of tensile strength for 3 sample of boron steel raw material before and after quenching process. Sample 1 to 3 shows an increase of tensile strength up to 1150 MPa in experiment 1 to experiment 3 compare to the tensile strength of as-received boron steel blank which was only 600 MPa. The strength of boron steel had increased up to 51.08 % after the quenching process. The value of tensile strength after quenching was around 1500 MPa (Merklein & Lechler, 2008). Based on Wang & Lee, 2013, transfers time more than 20 s will affect the strength of boron steel around 1200 MPa. Hence, the result comparable. As for the hardness, the hardness level for sample 1 to 3 from experiment 1 to 3 were almost similar. The hardness levels for boron steel recorded were only up to 100 HV for all samples. However, compare to the raw material of boron steel, the hardness resulted up to 600 HV for all samples in all experiment after quenching process. As a result, hardness of boron steel had been increase up to 82.56%. The value of hardness was around 514 HV (Merklein & Lechler, 2008). Since, the hardness obtain was higher compare to normal

trend, the result was acceptance. Table 4.19 shows the summarise result for the tensile strength and hardness.

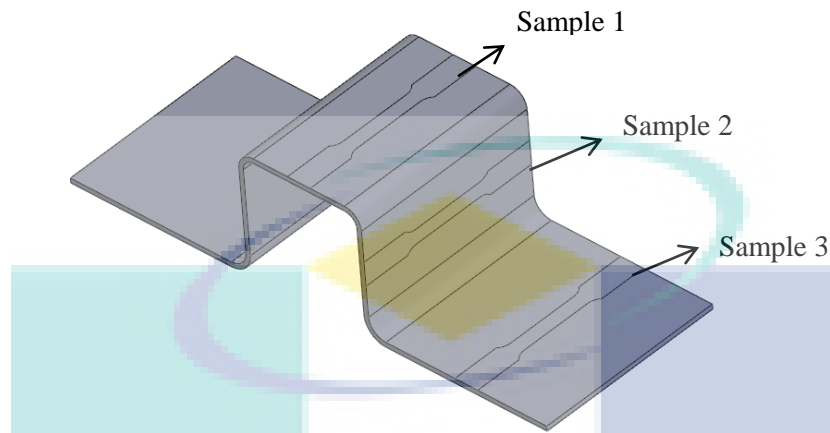


Figure 4.20 Locations on stamped sample for tensile specimen and hardness test

Table 4.19 Summarise result tensile strength and hardness for U-shape

Sample	Tensile Strength (MPa)			Hardness (HV)		
	x_i	x_{ii}	x_{iii}	y_i	y_{ii}	y_{iii}
Original	523.67	545.28	541.32	105	109	105
1	1079.13	1114.73	1097.81	588	625	597
2	1030.55	1110.67	1104.65	567	617	609
3	1069.54	1109.89	1101.12	579	610	607

4.5 Summary

In FEA, the medium sized mesh was utilized on the hot stamping tool as it provides reasonable accuracy with a bearable computational burden. Next, by choosing refined mesh which focused on the cooling channel, it resulted in higher quality of FEA. In this study, heuristic method was introduced during cooling channel optimization for hot stamping tool. This approached was able to acquire the tool cooling channel design with high performance in terms of high Heat transfer rate and low von Mises stress. The results suggest that 8 mm for the cooling channel diameter (C_A), 10 mm for the pitch between the cooling channel (C_B), 8 mm for the distance between the cooling channel and the tool surfaces (C_C) were the optimum parameters for the design of a cooling channel for the flat shape designed tool. Besides that, the cooling channel for U-shaped design, the following values were selected i.e. 8 mm, 8 mm, 8 mm, 8 mm

and 10 mm for the cooling channel diameter (C_A), the pitch between the cooling channel (C_B), the distance between the cooling channel and the tool surfaces (C_C), the distance between the cooling channel for the wall on tool surfaces (C_D), the Upper tool and lower tool, respectively. From the comparison of both method heuristic and taguchi, heuristic method provides the best results in optimizing cooling channel design for flate shape sample. In order to validate the simulation results with the experimental, the heat distributions were measured and compared. Based on the flat shape tool, the average percentage error for the blank heat distribution was 1.83 % and for the tool was 2.67 %. As for the U-shape tool, the average percentage error for the upper tool, lower tool, and the blank heat distribution are 16.65 % 17.95 % and 7.92 %, respectively. The results obtained demonstrated an acceptable agreement between the experimental and FEA simulation results. The value of the tensile strength and the hardness values were also measured. The strength of boron steel was observed to increase to up to 51.08 % after the quenching process, whilst the hardness of boron steel increased to up to 82.56 % from its initial condition. As a concluding remark, it was apparent that the cooling channel design parameters obtained from the heuristic method are able to achieve high tensile strength and hardness of output sample.

CHAPTER 5

CONCLUSION

5.1 Conclusion

The cooling channel design for hot stamping process was developed and the analysis and experimental had been successfully carried out. The process of hot stamping had involved material and sample preparations, designing cooling channel, analysis and experimental for both flat and U-shape sample. In material and sample preparations, flat and U-shape sample were prepared. Then, cooling channel was design. Finite Element Analysis (FEA) was conducted which involve in obtaining the material data, geometric modelling, meshing and thermal and static analysis. The cooling channel design analysis was conducted by using Taguchi and Heuristic method. The experiment of hot stamping using 22MnB5 steel was conducted involving flow rate experiment, heat transfer experiment, tensile test measurement and hard measurement. All the experimental results were analyzed and discussed thoroughly. Hence, by this study, cooling channel design by means of a heuristic method in hot stamping tool was designed and developed. Thus, some recommendations for future study were suggested in Section 5.3.

In conjunctions of research objectives, the conclusions of this research were stated as follows:

- (i) The optimised parameters for C_A , C_B , and C_C obtained from the aforementioned technique for the flat tool were 8 mm, 10 mm and 8 mm (8,10,8) mm respectively. While for U-shape, the best parameters for the upper tool are (8,8,8,10) mm for parameters C_A , C_B , C_C , and C_D , respectively. Conversely, the optimum parameters for the lower tool, were (8,8,8,8) mm respectively. The results obtained were optimised for high heat transfer rate, and low von

Mises stress as suggested by (Hoffmann et al., 2007). As for the flat shape tool, the heuristic method was validated in contradiction of the Taguchi method. Based on the Taguchi method, the parameters suggested that provides the highest maximum VMS and heat transfer rate were (6,8,6) mm. On the other hand, the lowest maximum VMS and heat transfer rate may be obtained through the following parameters i.e. (6,10,10) mm. However, the suggested parameters achieved by means of the heuristic method that results in a higher heat transfer rate and a lower von Mises stress was (8,10,8) mm.

- (ii) Simulation of thermal distribution resulted in, the heat distribution was measured and compared. Based on flat shape tool, the average percentage error for the blank heat distribution was 1.83 % and for the tool was 2.67 %. As for the U-shape, the average percentage error for the blank heat distribution of the upper tool was 16.65 %, 17.95 % for the lower tool and 7.92 % for the blank. The higher error of the U-shape as compared to the flat shape was attributed to the time taken to close the U-shape tool was greater than the flat tool. For the U-shape tool, the upper die was opened widely due to the punch stroke for the U-shape was 50 mm. As the speed for the hydraulic press machine was slow, the heated blank was not at its optimum temperature (reduction of temperature due to air exposure). The results obtained showed an acceptable agreement between the experimental and FEA simulation results (Namklang & Uthaisangsuk, 2016).
- (iii) Based on hot stamping experiment, the suitable thickness of the material, heating temperature and heating time parameters were 1.8 mm, 900 °C and 6 s, respectively. The strength of boron steel was observed to increase to up to 51.08 % after the quenching process, whilst the hardness was increased up to 82.56 % from its initial condition. The value of the tensile strength measured was approximately 1200 MPa, which was slightly lower from the usual trend. This was mainly due to the longer transfer time of the blank product from the furnace to the tool, in addition to the waiting time for the machine to press the heated blank. Based on Wang & Lee, (2013) a longer transfer time, resulted in a lower value of tensile strength.

5.2 Recommendations

There were some constraints faced whilst carrying out the experimental testing. The press speed of the hydraulic press machine used was very slow, this might result in a cooler blank before the quenching process transpires. Besides that, the hot stamping direct method can be conducted to eliminate the transfer time of the heated blank. Moreover, different tool materials such as the HTCS 150 could be used, where it has a higher material conductivity as compared to the current tool investigated. Furthermore, the cooling channel design can be optimised by using other intelligent optimization techniques such as Neural Networks and the likes. As for the quenching medium, instead of using water, nano coolant can be introduced as owing to its high conductivity.



UMP

REFERENCES

- Abdul Hay, B., Bourouga, B., & Dessain, C. (2010). Thermal contact resistance estimation at the blank/tool interface: experimental approach to simulate the blank cooling during the hot stamping process. *International Journal of Material Forming*, 3(3), 147–163.
- Altan, T., & Tekkaya, A. E. (2012). Sheet Metal Forming Process and Application. *ASM International*, 133–156.
- ANSYS. (2016). ANSYS Meshing. Retrieved from <http://www.ansys.com/products/platform/ansys-meshing>
- Assab. (2008). Supreme Hot Work Tool Steel Catalogue. (4th Edition) Assab Group.
- Banabic, D. (2010). Sheet Metal Forming Processes. *Springer*.
- Bar-Meir, G. (2009). Fundamental of Die Casting Design. *Springer*
- Barr, R. S., Golden, B. L., Kelly, J. P., Resende, M. G., & Stewart JR, W. R. (1995). Designing and Reproting on Computational Experiment with Heuristic Methods. *Journal of Heuristics*, 9–32.
- Boljanovic, V., & Paquin, J. (2006). *Die Design Fundamental* (3rd Edition) Industrial Press Inc.
- Bosetti, P., Bruschi, S., Stoehr, T., Lechler, J., & Merklein, M. (2010). Interlaboratory comparison for heat transfer coefficient identification in hot stamping of high strength steels. *International Journal of Material Forming*, 3(S1), 817–820.
- Çakıroğlu, R., & Acir, A. (2013). Optimization of cutting parameters on drill bit temperature in drilling by Taguchi method. *Measurement*, 46(9), 3525–3531.
- Canakci, A., Erdemir, F., Varol, T., & Patir, A. (2013). Determining the effect of process parameters on particle size in mechanical milling using the Taguchi method: Measurement and analysis. *Measurement*, 46(9), 3532–3540.
- Cengal, Y. A., & Ghajar, A. J. (2011). Heat and Mass Transfer. In *Fundamental and Application (McGraw-Hill)* (p. 9–16, 25–28, 423–426, 488, 489).
- Chang, Y., Meng, Z. H., Ying, L., Li, X. D., Ma, N., & Hu, P. (2011). Influence of hot press forming techniques on properties of vehicle high strength steels. *Journal of Iron and Steel Research International*, 18(5), 59–63.
- Coy, S. P., Golden, B. L., Runger, G. C., & Wasil, E. (2001). Using experimental design to find effective parameter settings for heuristics. *Journal of Heuristics*, 7(1), 77–97.

- Cui, J., Sun, G., Xu, J., Huang, X., & Li, G. (2015). A method to evaluate the formability of high-strength steel in hot stamping. *Materials & Design*, 77, 95–109.
- Dhillon. (2002). Engineering Maintenance A Modern Approach. *CRC Press*.
- Díaz, J., Rusu, C., & Collazos, C. A. (2016). Experimental Validation of a Set of Cultural-Oriented Usability Heuristics: e-Commerce Websites Evaluation. *Computer Standards & Interfaces*, 50(October 2016), 160–178.
- Duncan, J., & Panton, S. (1997). Introduction to sheet metal forming. *Composite Materials Series*, (33), 1–25.
- George, R., Bardelcik, A., & Worswick, M. J. (2012). Hot forming of boron steels using heated and cooled tooling for tailored properties. *Journal of Materials Processing Technology*, 212(11), 2386–2399.
- Hafizuddin. (2014). Dies design structure & manufacturing concept. *Proton Workshop*
- Hoffmann, H., So, H., & Steinbeiss, H. (2007). Design of Hot Stamping Tools with Cooling System. *CIRP Annals - Manufacturing Technology*, 56(1), 269–272.
- Holman, J. (2009). Heat Transfer. *McGraw-Hill*. Retrieved from <http://www.ncbi.nlm.nih.gov/pubmed/21128847>
- Hu, J., Marciniak, Z., & Duncan, J. (2002). Mechanics of Sheet Metal Forming (2nd ed.). *Butterworth-Heinemann*.
- Hu, P., Ma, N., Liu, L., & Zhu, Y. (2013). Theories, Methods and Numerical Technology of Sheet Metal Cold and Hot Forming. *London: Springer London*.
- Hu, P., & Ying, L. (2017). Hot Stamping Advanced Manufacturing Technology of Lightweight Car Body. *Springer London*.
- IISI. (2009). AHSS guideline v4.1. Retrieved from www.worldautosteels.org
- Incropera, F., Dewitt, D., Bergman, T., & Lavine, A. (2002). *Fundamentals of Heat and Mass Transfer*. *John Wiley and Sons Ltd*.
- Iron, I., & Institute, S. (2002). Ultra-Light Steel Autobody Advanced Vehicle Concepts (ULSAB-AVC). *Internal Iron and Steel Institute*.
- Jiang, C., Shan, Z., Zhuang, B., Zhang, M., & Xu, Y. (2012). Hot stamping die design for vehicle door beams using ultra-high strength steel. *International Journal of Precision Engineering and Manufacturing*, 13(7), 1101–1106.
- Karbasian, H., & Tekkaya, a. E. (2010). A review on hot stamping. *Journal of Materials Processing Technology*, 210(15), 2103–2118.

- Kim, H., Kimchi, M., & Altan, T. (2009). Control of Springback in Bending and Flanging Advanced High Strength Steels (AHSS). *International Automotive Body Congress (IABC)*, 1–18.
- Kolleck, R., Veit, R., Merklein, M., Lechler, J., & Geiger, M. (2009). Investigation on induction heating for hot stamping of boron alloyed steels. *CIRP Annals - Manufacturing Technology*, 58, 275–278.
- Kumar, D. D., Shirsat, V., Sharma, V., & Sarpate, C. (2011). Design Optimization of Hot Forming Tools by Numerical Thermal Analysis. *KLT Automotive and Tubular Product LTD*.
- Kumar, P., & Visavale, G. (2013). Grid Generation for Cfd Simulation: Insights With Demo. Retrieved from <http://www.learncax.com/blog/2013/03/22/grid-generation-for-cfd-simulation-insights-with-demo/>
- Lee, M., Kim, S., Nam, H., & Chang, W. (2009). Application of hot press forming process to manufacture an automotive part and its finite element analysis considering phase transformation plasticity. *International Journal of Mechanical Sciences*, 51(11–12), 888–898.
- Lempco. (2000). Die Set Engineering Handbook and Catalog. *Lempco Group*.
- Lempco. (2004). Die Set Engineering Handbook and Catalog. *Lempco Group*.
- Lim, S. K., Azmi, W. H., & Yusoff, A. R. (2016). Investigation of thermal conductivity and viscosity of Al₂O₃/water – ethylene glycol mixture nanocoolant for cooling channel of hot-press forming die application. *International Communications in Heat and Mass Transfer*, 78, 182–189.
- Lim, W. S., Choi, H. S., Ahn, S. Y., & Kim, B. M. (2014). Cooling channel design of hot stamping tools for uniform high-strength components in hot stamping process. *International Journal of Advanced Manufacturing Technology*, 70(5–8), 1189–1203.
- Lin, T., Song, H., Zhang, S., Cheng, M., & Liu, W. (2014). Cooling Systems Design in Hot Stamping Tools by a Thermal-Fluid-Mechanical Coupled Approach. *Advances in Mechanical Engineering*, 2, 1–13.
- Liu, H., Lei, C., & Xing, Z. (2013). Cooling system of hot stamping of quenchable steel BR1500HS: optimization and manufacturing methods. *The International Journal of Advanced Manufacturing Technology*, 69(1–4), 211–223.
- López-Chipresa, E., Mejía, I., Maldonado, C., Bedolla-Jacuindea, A., El-Wahabib, M., & Cabrera, J. M. (2008). Hot Flow Behavior of Boron Microalloyed Steels. *Material Science and Engineering: A*, 480(1–2), 49–55.
- Lundström, E. (2012). Schuler Academy. *Proton Training*.

- Lv, M., Gu, Z., Li, X., & Xu, H. (2016). Optimal Design for Cooling System of Hot Stamping Dies. *ISIJ International*, 1–9.
- Maeno, T., Mori, K., & Nagai, T. (2014). CIRP Annals - Manufacturing Technology Improvement in formability by control of temperature in hot stamping of ultra-high strength steel parts. *CIRP Annals - Manufacturing Technology*, 63(1), 301–304.
- Martí, R., & Reinelt, G. (2011). The Linear Ordering Problem, Exact and Heuristic Methods in Combinatorial Optimization (Vol. 175, pp. 17–41). Berlin, Heidelberg: Springer Berlin Heidelberg.
- Melissa, B. (2012). Fluid Flow Rates. Retrieved from <http://www.education.com/science-fair/article/fluid-flow-rates/>
- Merklein, M., & Lechler, J. (2006). Characterisation of the Flow Properties of the Quenchenable Ultra High Strength Steel 22MnB5. *CIRP Annals - Manufacturing Technology*, 55(1).
- Merklein, M., & Lechler, J. (2008). Determination of Material and Process Characteristics for Hot Stamping Processes of Quenchenable Ultra High Strength Steels with Respect to a FE-based Process Design, *International Journal Material Manufacturing*. 1(1), 411–426.
- Misumi. (2015). Misumi Press Stock Booklet 2015. Retrieved from <http://www.misumi-techcentral.com/tt/en/press/2012/06/126-press-forming-force-3-bending-force.html>
- Mori, K., Maeno, T., & Maruo, Y. (2012). Punching of small hole of die-quenched steel sheets using local resistance heating. *CIRP Annals - Manufacturing Technology*, 61(1), 255–258.
- Mori, K., Maki, S., & Tanaka, Y. (2005). Warm and Hot Stamping of Ultra High Tensile Strength Steel Sheets Using Resistance Heating. *CIRP Annals - Manufacturing Technology*, 54(1), 209–212.
- Mori, K., Saito, S., & Maki, S. (2008). Warm and hot punching of ultra high strength steel sheet. *CIRP Annals - Manufacturing Technology*, 57, 321–324.
- Naderi, M. (2007). *Hot Stamping of Ultra High Strength Steels*.
- Naderi, M., Ketabchi, M., Abbasi, M., & Bleck, W. (2011). Analysis of microstructure and mechanical properties of different high strength carbon steels after hot stamping. *Journal of Materials Processing Technology*, 211(6), 1117–1125.
- Naganathan, A. (2010). *Hot Stamping of Manganese Boron Steel*.
- Naganathan, A., & Penter, L. (2012). Hot Stamping. In *Sheet Metal Forming-Processes and Applications* (pp. 133–156).

- Namklang, P., & Uthaisangsuk, V. (2016). Description of microstructures and mechanical properties of boron alloy steel in hot stamping process. *Journal of Manufacturing Processes*, 21, 87–100.
- Pitts, D., & Sissom, L. (1998). *Schaum's outline of theory and problems of heat transfer. 2nd Edition. McGraw-Hill.*
- PME. (2004). Mould and Die Standards Components. Retrieved from <http://www.docfoc.com/pme-mould-die-standard-components-pdf>
- Roy, R. . (2001). *Design of Experiments Using The Taguchi Approach*. USA: John Wiley.
- Seok, H., & Koc, M. (2008). Numerical investigations on springback characteristics of aluminum sheet metal alloys in warm forming conditions. *Journal of Material Processing Technology* 204, 370–383.
- Sever, N. K., Mete, O. H., Demiralp, Y., Choi, C., & Altan, T. (2012). Springback Prediction in Bending of AHSS-DP 780. In *NAMRI/SME* (Vol. 40).
- Shahrom, M. S., Yusoff, A. R., & Lajis, M. A. (2013). Taguchi Method Approach for Recycling Chip Waste from Machining Aluminum (AA6061) Using Hot Press Forging Process. *Advanced Materials Research*, 845, 637–641.
- Shapiro, A. (2009). Finite element modeling of hot stamping. *Steel Research International*.
- Skrikerud, M., Megahed, M., & Porzner, H. (2010). Simulation of Hot Stamping Process.
- So, H., Faßmann, D., Hoffmann, H., Golle, R., & Schaper, M. (2012). An investigation of the blanking process of the quenched boron alloyed steel 22MnB5 before and after hot stamping process. *Journal of Materials Processing Technology*, 212(2), 437–449.
- SositarMold. (2011). Cooling Channel Configuration. Retrieved from <http://www.moldchina.org/cooling-channel-configuration.html>
- Srithananan, P., Kaewtatip, P., & Uthaisangsuk, V. (2016). Micromechanics-based modeling of stress-strain and fracture behavior of heat-treated boron steels for hot stamping process. *Materials Science and Engineering A*, 667, 61–76.
- Steinbeiss, H., So, H., Michelitsch, T., & Hoffmann, H. (2007). Method for optimizing the cooling design of hot stamping tools. *Production Engineering*, 1(2), 149–155.
- Thanadngarn, C., Sirivedin, K., Engineering, M., Thai-german, T. S. I., Buakaew, V., Neamsup, Y., ... Limited, C. (2013). The Study of the Springback Effect in the UHSS by U-bending Process, 6, 19–25.

- Tondini, F., Bosetti, P., & Bruschi, S. (2011). Heat transfer in hot stamping of high-strength steel sheets. In *Journal of Engineering Manufacture* (Vol. 225, pp. 1813–1824). Proceedings of the Institution of Mechanical Engineers, Part B.
- Turetta, A. (2008). *Investigation of Thermal, Mechanical and Microstructural Properties of Quenchenable High Strength Steels In Hot Stamping Operations*. Università Degli Studi Di Padova.
- Wang, S., & Lee, P. (2013). Investigation of Die Quench Properties of Hot Stamping. *China Steel Technical Report*, 2(26), 22–31.
- Xiaoda, L., Xiangkui, Z., Ping, H., & Xianghui, Z. (2016). Thermo-mechanical coupled stamping simulation about the forming process of High-Strength Steel sheet. *International Journal of Control and Automation*, 9(1), 93–102.
- Yanagimoto, J., Oyamada, K., & Nakagawa, T. (2005). Springback of High-Strength Steel after Hot and Warm Sheet Formings. *CIRP Annals - Manufacturing Technology*, 54(1), 213–216.
- Yusoff, A. R., Ghazalli, Z., & Che Hussain, H. (2006). Determining Optimum Edm Parameters in Drilling Small Holes By Taguchi Method. In *Proceedings of ICOMAST2006 International Conference on Manufacturing Science and Technology*.
- Zhang, Z., Li, X., Pan, L., & Wei, X. (2010). Numerical Simulation on Hot Forming of B Pillar.
- Zhang, Z., Li, X., Zhao, Y., & Li, X. (2014). Heat transfer in hot stamping of high-strength boron steel sheets. *Metallurgical and Materials Transactions B: Process Metallurgy and Materials Processing Science*, 45(4), 1192–1195.
- Zhong-de, S., Mi-Ian, Z., Chao, J., Ying, X., & Wem-juan, R. (2010). Basic Study On Die Cooling System Of Hot Stamping Process. *International Conference on Advanced Technology of Design and Manufacture*, 67(0 2), 5–8.

APPENDIX A1 **G-CODE FOR CUTTING FLAT SAMPLES**

```
(      = ON OFF  IP  HRP  MAO  SV   V   SF  C  PIK  CTRL  WK  WT  WS  WP  PC  SK);
C000 = 005 014 2215 000 240 +040.0 8.0 0102 0 000 0000 020 120 100 045 0000 00;
C001 = 006 014 2215 000 251 +030.0 8.0 0102 0 000 0000 020 120 100 045 0000 00;
H000 = +000000.0100 ;
H001 = +000000.1470 ;
( FIG-1 1T ALL CIRCUMFERENCE);
G54;
G90;
G92X-3.0Y1.0Z0;
G29;
T94;
T84;
C000;
G42H000G01X-1.0Y1.0;
C001X0.0;
H001;
M98P0001;
T85;
G149G249;
M02;
;
N0001;
G01X0.0Y30.0;
G03X2.0Y34.4721I-4.0J4.4721;
G01Y65.5279;
G03X0.0Y70.0I-6.0J0.0;
G01Y100.0;
X10.0;
Y70.0;
G03X8.0Y65.5279I4.0J-4.4721;
G01Y34.4721;
G03X10.0Y30.0I6.0J0.0;
G01Y0.0;
X0.0;
Y1.0;
G40H000X-3.0;
M99;
```

APPENDIX A2

CALCULATION FOR HEAT TRANSFER COEFFICIENT

Volume flow rate

Volume flow rate, $\dot{v} = VA$

where, $\dot{v} = 65.789 \times 10^{-6} \text{ m}^3/\text{s}$

$D = 8\text{mm}$

$A = \pi D^2/4$

$= 5.027 \times 10^{-5} \text{ m}^2$

hence, $V = \dot{v}/A$

$= 1.309 \text{ m/s}$

Reynolds Number, $Re = VD/v$

where, $V = 1.309 \text{ m/s}$

$D = 8\text{mm}$

$v = 1 \times 10^{-6} \text{ m}^2/\text{s}$

hence, $Re = VD/v$

$= 10480$

*since the value of $Re > 10000$, it is usually
turbulent

Heat Transfer Coefficient

Nusselt number, $Nu = hD/k = 0.023Re^{0.8}Pr^n$

where, $k = 0.589 \text{ W/m.K}$

$Pr = 7.01$

$n = 0.3$

hence, $h = (k/D)(0.023Re^{0.8}Pr^{0.3})$

$= 4997.55 \text{ W/m}^2.\text{K}$

APPENDIX A3
CALCULATION OF HEAT TRANSFER RATE FOR SIMULATION 5 U-
SHAPE LOWER TOOL

Heat transfer

$$\text{Heat transfer, } Q = \Delta U = mc_{avg} (T_2 - T_1)$$

$$\text{where, } m = 1.73 \text{ kg}$$

$$c_{avg} = 0.52 \text{ kJ/kg.K}$$

$$\text{hence, } Q = mc_{avg} (T_2 - T_1)$$

$$= (1.73)(0.52)(147.5 - 122.2)$$

$$= 22.76 \text{ kJ}$$

Heat transfer rate

$$\text{Heat transfer rate, } \dot{Q} = \frac{Q}{\Delta t}$$

$$= \frac{22.76}{6-3}$$

$$= 7.587 \text{ kJ/s}$$

APPENDIX B1

INTERNATIONAL MANUFACTURING ENGINEERING CONFERENCE,
ADVANCED MATERIALS RESEARCH VOL. 903 (2014) PP 163-168

COMPARISON OF COOLING PERFORMANCE BETWEEN HIGH THERMAL CONDUCTIVITY STEEL (HTCS 150) AND HOT WORK TOOL STEEL (SKD 61) INSERT FOR EXPERIMENTAL TOOL USING FINITE ELEMENT ANALYSIS

**Zahari Taha^{1, a}, Ahmad Razlan Yusoff^{1, b}, Mohamad Farid Mohamad Sharif^{1, c},
M.A. Hanafiah Saharudin^{1, d} and Mohd Fawzi Zamri^{1, e}**

¹Faculty of Manufacturing, Universiti Malaysia Pahang, Malaysia

ABSTRACT

In hot stamping, the tool cooling system plays an important role in optimizing the process cycle time as well as maintaining the tool temperature distribution. Since the chilled water is forced to circulate through the cooling channels, there is a need to find the optimal parameters of the cooling channels that will cool down the tool efficiently. In this research paper, the cooling channel parameters that significantly influence the tool cooling performance such as size of the cooling holes, distance between the cooling holes and distance between the cooling holes and the tool surface contour are analyzed using the finite element method for both static and thermal analysis. Finally the cooling performance of two types of materials is compared based on the optimized cooling channel parameters.

UMP

APPENDIX B2

ADVANCES IN MATERIALS AND PROCESSING TECHNOLOGIES, 2015 VOL.
1, NOS. 1–2, 27–35

HEURISTIC OPTIMISATION OF COOLING CHANNEL DESIGN IN THE HOT STAMPING DIE FOR HOT STAMPING PROCESS

Mohd Fawzi Zamri¹ and Ahmad Razlan Yusoff¹

¹Faculty of Manufacturing, Universiti Malaysia Pahang, Malaysia

ABSTRACT

In hot stamping process, similar die is used as in cold stamping process but with additional cooling channels. The cooling channel systems are integrated into the die design to control the heat transfer rate for quenching process of hot blanks. During quenching process, the die is effectively cooled to achieve the optimum heat transfer rate and homogeneous temperature distribution on hot blanks. In this paper, heuristic method with finite element analysis (FEA) of static analysis and thermal analysis are applied to determine the cooling channel size, pitch size between channels and channel distance to the blanks surface. This static analysis identifies either the tool able to stand the pressure applied or not, while the thermal analysis is to ensure the die obtains the high cooling efficiency with homogenous temperature distribution. In this heuristic method, each parameter of the cooling channels inside the die are optimised and benchmarked with traditional Taguchi method. The results showed that the heuristic method coincides with Taguchi method even better and achieved the acceptance error between FEA in temperature distributions.

**EXPERIMENTAL VALIDATION FOR HOT STAMPING PROCESS BY USING
TAGUCHI METHOD**

Mohd Fawzi Zamri¹, Syh Kai Lim¹ and Ahmad Razlan Yusoff¹

¹Faculty of Manufacturing, Universiti Malaysia Pahang, Malaysia

ABSTRACT

Due to the demand for reduction in gas emissions, energy saving and producing safer vehicles has driven the development of Ultra High Strength Steel (UHSS) material. To strengthen UHSS material such as boron steel, it needed to undergo a process of hot stamping for heating at certain temperature and time. In this paper, Taguchi method is applied to determine the appropriate parameter of thickness, heating temperature and heating time to achieve optimum strength of boron steel. The experiment is conducted by using flat square shape of hot stamping tool with tensile dog bone as a blank product. Then, the value of tensile strength and hardness is measured as response. The results showed that the lower thickness, higher heating temperature and heating time give the higher strength and hardness for the final product. In conclusion, boron steel blank are able to achieve up to 1200 MPa tensile strength and 650 HV of hardness.